GEOSCIENCE AUSTRALIA

Australian Government
Geoscience Australia

Government of South Australia
Primary Industries and Resources SA

The 2003 Gawler Craton Seismic Survey:

Notes from the Seismic Workshop held at Gawler Craton State of play 2004

Compiled and edited by P. Lyons & B.R. Goleby

Record
2005/19

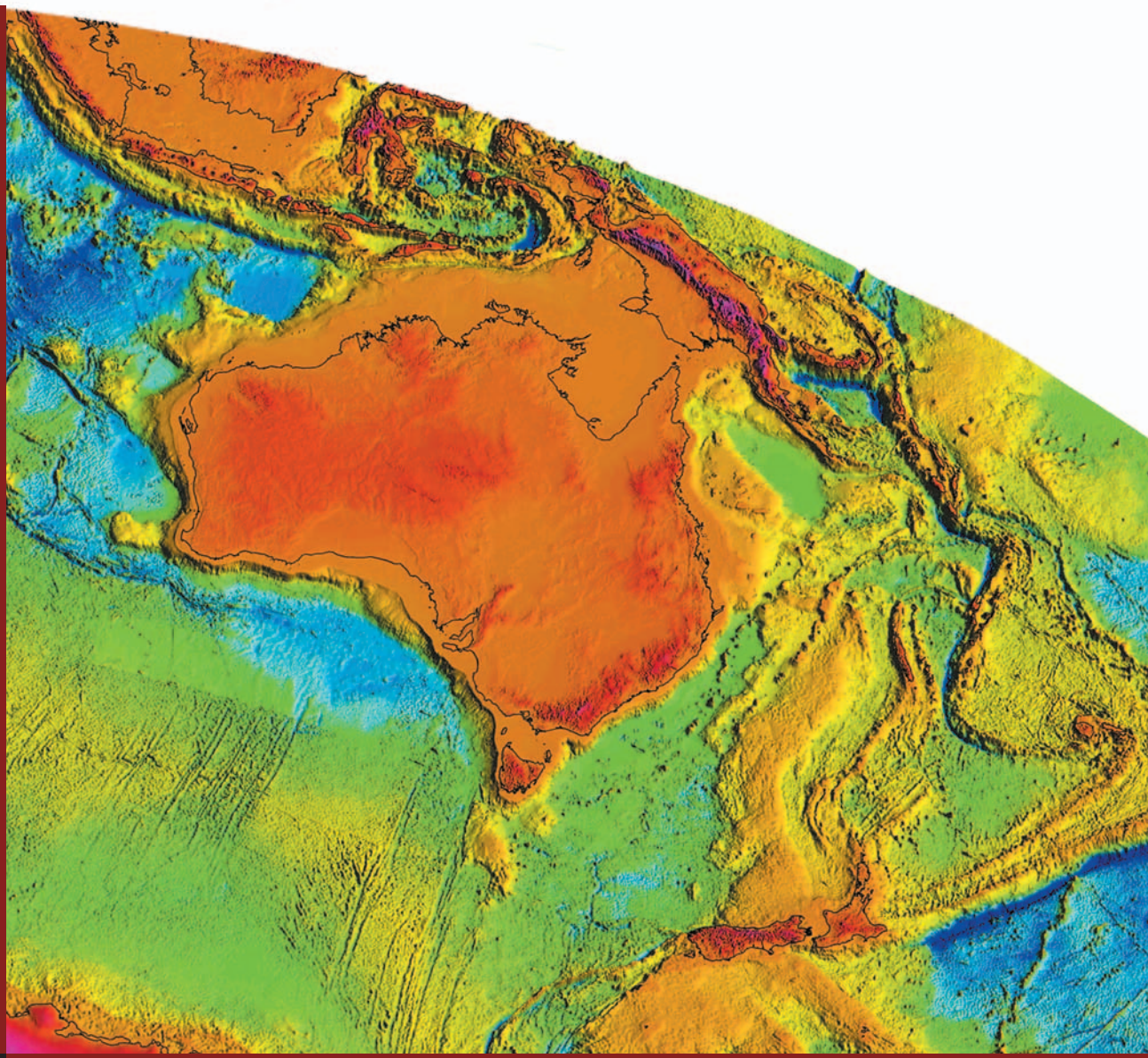

SPATIAL INFORMATION FOR THE NATION

THE 2003 GAWLER CRATON SEISMIC SURVEY:

NOTES FROM THE SEISMIC WORKSHOP HELD AT GAWLER CRATON STATE OF PLAY 2004

GEOSCIENCE AUSTRALIA
RECORD 2005/19

Compiled and edited by

P. Lyons & B.R. Goleby

Australian Government
Geoscience Australia

Government of South Australia
Primary Industries and Resources SA

Department of Industry, Tourism & Resources

Minister for Industry, Tourism & Resources: The Hon. Ian Macfarlane, MP
Parliamentary Secretary: The Hon. Warren Entsch, MP
Secretary: Mark Paterson

Geoscience Australia

Chief Executive Officer: Dr Neil Williams

ISSN 1448-2177
ISBN 1 920871 59 4

GeoCat No. 63538

Suggested Bibliographic Citations

Whole volume:
Lyons, P & Goleby, B.R. 2005. The 2003 Gawler Craton seismic survey: Notes from the Seismic Workshop. Geoscience Australia, Record 2005/19**,** 81 pp.

Individual papers:
Preiss, W., Korsch, R. and Totterdell, J. 2005. Gawler Craton cover-successions: Stuart Shelf to Adelaide Geosyncline transition. In: Lyons, P. & Goleby, B.R. (eds) The 2003 Gawler Craton seismic survey: Notes from the Seismic Workshop. Geoscience Australia, Record 2005/19, pp 68-72.

The Seismic Workshop was held at the Australian Mineral Foundation Building, Adelaide on the 6th August, 2004 as part of the 2004 Gawler Craton State of Play.

Contents

EXECUTIVE SUMMARY

Iron oxide-copper-gold (IOCG) systems, and their related magnetite-apatite systems, are suggested to form in orogenic belts (e.g., Cloncurry, Andean magmatic arc, Urals) and extensional settings (e.g., St François Terrane, Missouri). Even so, the tectonic setting of arguably the most important of the IOCG class of the deposits, the giant world-class Olympic Dam deposit in South Australia, has been uncertain to date. It has previously been used as an example of the IOCG in an anorogenic intracontinental setting. The region has no outcrop as it is covered by Neoproterozoic sedimentary successions exceeding 5 km thick, in places. Given its economic significance and importance in defining the IOCG mineral deposit class, resolving the tectonic setting of Olympic Dam is crucially important. To address this, two orthogonal deep seismic reflection traverses, centred on the Olympic Dam deposit, were recorded to 18 s TWT.

The nearly north-south line, 193 km long, oriented as near to regional dip-direction, defined by potential-field data, as land access would allow, sounded units of the Archaean-Proterozoic Gawler Craton and a possible allochthanous Proterozoic terrane. The shorter east-west cross-line (57 km) provides control on the three dimensional geometry of the major structures and gives information about some out-of-plane structures imaged by the north-south traverse.

The seismic data show that the Olympic Dam deposit occurs in a fold- and thrust-belt, formed over a number of periods of orogeny, which was probably subject to compressional tectonics at the time of IOCG mineralisation. In the north of the study area, the upper crust, of the crystalline basement, shows south-dipping reflectors, interpreted as shear zones that cut through crust of sub-horizontal reflections. To the south, the upper crust and lower crust have reflectivity indicating thrusting to the south and, or, southwest, toward the interior of the Gawler Craton. However, the upper crustal deformation is decoupled from lower crustal deformation at a layer of sub-horizontal reflectors interpreted, by their reflection-amplitudes, to contain more mafic rocks than the regions above and below. This layer is up to 5 km thick and mostly un-deformed, except where it is duplexed. The duplexes appear to form the loci of strain partitioning in the upper crust. The lower crust of the centre of the study area contains fewer reflections, and appears anomalous but homogenised compared with the crust to the north and south.

Imaging of the cover-successions shows a previously unknown Adelaidean rift, which has been partially inverted.

PREFACE

This record contains abstracts and explanatory notes from the presentations given at the Seismic Workshop and Data Release held as part of the Gawler Craton State of Play 2004 conference, held at Adelaide in August 2004. The workshop was the first public display and discussion of data and results of the 2003 Gawler seismic survey. Interpretation of the seismic data, at the time of the workshop had only been ongoing for about two months and was still at the preliminary stage. Normally, such a quantity of seismic data takes a minimum of six to twelve months to analyse and interpret, and must be done with regard to other available datasets. The complexity of the work requires much collaboration and does not just rely on the expertise of seismic interpreters. Data processing, sequence stratigraphy, structural geology, tectonics, mineral-systems analysis, geochronology, and local and regional geology must all be taken into account.

So, at the time of compiling and editing of these notes, ideas are still emerging and hypotheses are still being formed and tested, some of which have been written into papers currently in review for formal publication. We urge readers to view the Gawler project website, www.ga.gov.au/rural/projects/gawler.jsp, for more recent papers and presentations.

EASTERN GAWLER CRATON: DEEP SEISMIC PROPOSAL

N.G. Direen[1], B.R. Goleby[1], R.G. Skirrow[1], S.J. Daly[2], P. Lyons[1], and P. Heithersay[2]

[1]Geoscience Australia
[2]Office of Minerals and Energy Resources, S.A.

This is a copy of the proposal to conduct a seismic survey in the eastern Gawler Craton, written in May 2002. It was not presented at the Seismic Workshop.

SUMMARY

The proposed seismic work is to be carried out within the framework of an ongoing program of seismic data acquisition across southern Australia. This extensive transect will contribute to a tectonic framework for understanding the relationships between the Gawler Craton, Curnamona Province and surrounding terranes.

The Gawler Craton, South Australia, is one of the least understood and under-explored Archaean to Mesoproterozoic terranes of Australia. It is nevertheless an emerging major mineral province, underpinned by the world-class Olympic Dam Cu-Au-U deposit, and by recent discoveries of copper and gold (e.g., Prominent Hill). Remarkably little is known of the tectonic framework and crustal evolution of the Gawler Craton, or its tectono-stratigraphic relationships to the Curnamona Craton to the east, with which it shares many features. Similarly, the relationships with the proto-Yilgarn Craton to the west have remained obscure, due in part to extensive but relatively thin cover.

This is a proposal to address a key geological and exploration problem in the Gawler Craton: What was the crustal structure of the Olympic Dam region, and what specific tectonic features controlled the localisation of early Mesoproterozoic Cu-Au mineralisation within the Olympic Cu-Au province?

A workshop, held in Adelaide in July 2000, on proposed deep crustal seismic work in the Gawler Craton, attended by approximately 40 representatives from industry, government, and academia, concluded that the highest priority for seismic work in the Gawler Craton is the Olympic Dam region. The view was that seismic data could provide a quantum increase in understanding of the crustal setting of the Olympic Dam mineral system. Hence, this dataset would provide the foundation for new exploration models for Cu-Au deposits in the Gawler Craton.

OBJECTIVES

The objectives established for the Gawler Craton seismic project were:—

- A seismic reflection transect passing near the Olympic Dam deposit to test tectonic models advanced for the Olympic Dam region. As part of its Gawler Craton Project, Geoscience Australia has developed a first-generation 3D crustal model of the Olympic Dam region, based on interpretation of potential field data integrated with drill hole geological and geochronological data (Direen et al., 2002). The proposed transect will test and constrain this 3D model, and the results will lead to subsequent 3-D models.

- The profiling will test whether a large mafic/ultramafic intrusion exists beneath the Olympic Dam deposit, as implicated in some genetic models of Cu-Au-U mineralisation. Crustal underplating by mafic magmas has been proposed in the generation of the syn-mineralisation Hiltaba suite granites and Gawler Range Volcanics.

- In addition to imaging crustal structure near Olympic Dam, this line will provide new insights on Neoproterozoic basin formation in the Adelaide Geosyncline to the east of the Torrens Hinge Zone.

INTRODUCTION

Deep seismic reflection investigations form a major contribution to Geoscience Australia's regional mineral systems projects. In many cases, provision of these data and interpretations have resulted in an enhanced understanding of crustal architecture and tectonic history of many significant Australian mineral provinces.

This document contains details of a deep seismic reflection survey planned for the Gawler Craton, one of Australia's significant Archaean-Proterozoic provinces, and host to the world-class Olympic Dam Cu-U-Au deposit.

The deep seismic reflection survey will be arranged through collaboration between the South Australian Office of Minerals and Energy Resources (MER), within the Department of Primary Industry and Resources, South Australia (PIRSA) and Geoscience Australia (GA). MER and GA are joint collaborators in the Gawler Mineral Promotion Project, under the National Geoscience Accord.

This document is a summary of the views expressed by interested stakeholders at the Gawler Seismic Workshop, which was held in July 2001 in Adelaide. It also includes work from an initial internal planning document prepared by the Gawler Mineral Promotion Project (Direen, 2000).

BACKGROUND

The Gawler Mineral Promotion Project proposal was based on the following principles:—

- Application of a 'mineral systems' approach to investigations of mineralised provinces focuses geoscientific research concerning the essential components of the mineral systems under investigation (viz, driving energy, fluid/metal source, transport pathways, depositional trap, and preservation).

- Project objectives are targeted at specific problems addressing how each mineral system operated in time and space; a broader, region- to craton-scale view of the systems will advance exploration and genetic models.

- Integration of multidisciplinary and collaborative studies allows maximum opportunity for cross-disciplinary innovation and mutual benefit among stakeholders.

- Although significant datasets of geophysics, geology and geochemistry exist for the project area, there is great potential for major advancements in geological understanding to be made via focussed acquisition of new data and their synthesis.

These principles were used in developing the three modules within the Gawler Mineral Promotion project, with each module focussing on different mineral systems. These modules represent three important regions within the Gawler Craton (Skirrow, 1999):—

- Olympic Cu-Au province - Mesoproterozoic Cu-U-Au.
- Mulgathing Complex, Christie Domain - Archaean Au.
- Fowler Orogenic Belt, Fowler Domain - Palaeoproterozoic Ni.

These three regions were discussed in the July 2001 Gawler Seismic Workshop and the outcomes formed the basis for developing priorities for seismic traverses within the Gawler Craton.

The main distinguishing characteristics of each of the geological domains of the Gawler Craton (as described by Teasdale, 1997 and revised by Ferris et al., 2002; Table 1) in the three module areas of the Gawler Craton are summarised below. Inferences regarding lower crustal ages have been made using εNd model ages at 1590 Ma from Stewart and Foden (1997).

Table 1: Main distinguishing characteristics of geological domains of the Gawler Craton.

Sub-Domain Name	**Upper Crust composition**	**Upper Crust age**	**Middle Crust composition**	**Middle Crust age**	**Lower Crust age (inferred)**
Adelaide Fold Belt	Sediments, Minor volcanics	≤ 830 Ma Neoproterozoic - Phanerozoic	Sediments, Granitoids, Volcanics	?Mesoproterozoic	?Neoproterozoic rift / underplate
Stuart Shelf	Sediments, Granitoids	≤ 830 Ma 1590 Ma 1750-1710 Ma 1850 Ma	Sediments, Granitoids, Volcanics	Palaeoproterozoic	Archaean+ Palaeoproterozoic
Moonta	Mafic volcs, Metaseds Granitoids	1760 Ma 1720 Ma 1590 Ma			
Lincoln	Granitoids	1850 Ma			Archaean
Cleve	Metaseds	>2450 Ma			Archaean+ Palaeoproterozoic
Launch M *Coulta*	Metaseds Granitoids	2600 Ma			Archaean
GRV	Volcanics, Granitoids	1590 Ma	?Gabbro or Sediments, Granitoids	Archaean+ Palaeoproterozoic	Archaean+ Palaeoproterozoic
Nuyts	Granitoids, Volcanics	1620 Ma 1630 Ma	??	??Palaeoproterozoic	Palaeoproterozoic
Wilgena	Metaseds Metaseds Granitoids	>2600 Ma 1690 Ma 1590 Ma			Archaean+ Palaeoproterozoic
Fowler	Mafic volcs Metaseds	1730 Ma 1490 Ma			
Christie	Granulites, Granitoids	>2600 Ma 1670 Ma			
Coober Pedy	Granulites, Sediments	1700 Ma 2500 Ma			
Nawa	Granulites, Granitoids	1690 Ma ??			

SEISMIC WORKSHOP 2001: SUMMARY OF STAKEHOLDERS' VIEWS

At the Gawler Seismic Workshop held in July 2001, interested industry, government, and university stakeholders discussed the scientific benefits of seismic reflection surveying across the three key areas within the Gawler Craton. The seismic proposal was based on the following criteria:—

- The main objective in acquiring seismic data is to improve understanding and enhance knowledge of the region's mineral systems. Therefore, the seismic traverse should cross a known (ideally major) mineral system.

- Surface and/or drill hole geological knowledge should be available to link geology with the seismic interpretation.

- There should be good coverage of potential field data (gravity and magnetics).

- The seismic traverse should be seen as a means of stimulating area selection and exploration in the area chosen.

One area was clearly identified as the highest priority for seismic investigation is the Olympic Dam region of the Olympic Cu-Au province (Figures 1, 2 and 3).

The meeting recommended that any new seismic work should cross the Olympic Cu-Au province.

Three possible traverses were identified, Traverses A, B and C, as shown on Figures 1 and 2. Traverse A was accorded highest priority by the workshop. Traverse B was identified as it addressed many of the issues that Traverse A addressed but in an area where the geology crops out and is better understood. Traverse C is a short seismic traverse running orthogonal to Traverse A, intersecting near Olympic Dam. The key scientific objectives for each traverse discussed during the workshop are given below.

Traverses A, B and C: The Olympic Cu-Au Province

The world-class Cu-U-Au deposit, Olympic Dam was discovered in 1975 by WMC, in Mesoproterozoic basement concealed by ~300 m of sedimentary rocks of the Stuart Shelf. Since that time there has been a large effort to advance the understanding of basement, mainly through potential field data acquisition and drilling (though drilling has proved very costly). However, industry representatives at the workshop stated that exploration concepts for the Olympic Dam region have stagnated. Seismic is a new way to increase the understanding of fundamental crustal controls on location of mineralisation.

The principle objectives for a seismic reflection survey in the Olympic Dam region, together with an estimate of the relative importance of the objective in understanding the region's mineral systems is shown in Table 2. Several possible traverse locations are shown in Figure 3 that meet all of these objectives. The final traverse position will be determined through liaison with ANSIR representatives.

Table 2: Principle objectives for a seismic reflection survey in Olympic Dam region.

	Scientific Objective	Ranking
1	Architectural setting of Olympic Dam deposit	High
2	Architectural setting of Acropolis, Wirdda Well and other Cu-Au occurrences	Medium
3	Nature of the Torrens Hinge Zone (THZ)	Low
4	Thickness of Stuart Shelf cover over prospective Mesoproterozoic basement	High
5	Lithospheric origins, linkage of fluid pathways, and role of mafic magmatism (faults, shear zones, aquifer packages; mafic intrusions)	High
6	Proterozoic tectonic style and history of the Olympic Cu-Au province	High
7	Architecture of Mesoproterozoic GRV and Hiltaba intrusive systems	High

The traverse location as shown cuts several major gradients in long-wavelength gravity data (Figure 3). These major gravity gradients are interpreted to represent fundamental changes in crustal properties and architecture at depth.

The Olympic Dam deposit and Acropolis and Wirrda Well prospects are located near one of the major gravity gradients, which is sub-parallel to parts of the Neoproterozoic Torrens Hinge Zone in this region.

Traverse A

- A NE-SW traverse across the basement to the Stuart Shelf in the region of Olympic Dam. Major structures run NE and NW so traverse A runs roughly perpendicular and parallel to these structures.
- Commences east of the Gawler Craton margin and extends to Gawler Range Volcanics in the west, providing information along an NE–SW corridor across the Olympic Cu-Au province.
- Start in the western region of the Adelaide Fold Belt, in the vicinity of the 'Northwest Fault'.
- Crosses the Neoproterozoic Torrens Hinge Zone.
- Crosses the 'G2' lineament.
- Crosses the footprint of a major Proterozoic Cu-Au mineral system.
- Makes use of available potential field data.
- Costly to explore the basement regions under the sedimentary cover and hence seismic is crucial in imaging the basement architecture.
- Mesoproterozoic and older basement to the Stuart Shelf does not crop out in the area and hence drill hole data will be vital.

Traverse B

- An east-west traverse of the Palaeoproterozoic and Mesoproterozoic basement to the west of Port Augusta.
- Makes use of relatively good basement outcrop geological information along the traverse.
- Crosses several lithostratigraphic domains.
- Olympic, Spencer (previously Lincoln), Moonta and Cleve Domain boundaries are all mapped within this area and are relatively closely spaced.
- Provide some 3D information (if recorded in conjunction with Traverse A) on one or two structures as they extend northwards beneath the Gawler Range Volcanics (GRV) and Stuart Shelf sedimentary cover.
- Crosses the Neoproterozoic Torrens Hinge Zone.
- Traverses Cu-Au mineral systems in the Roopena region of the Olympic Cu-Au province.

Traverse C

- A short NW-SE traverse (orthogonal to Traverse A, Figures 1 & 2) across the basement to the Stuart Shelf in the region of the Olympic Dam deposit.
- Crosses the footprint of a major Proterozoic Cu-Au mineral system.
- Investigate NW-SE structures possibly related to the Olympic Dam Cu-U-Au deposit.
- Makes use of available potential field data.
- Costly to explore the basement regions under the sedimentary cover and hence seismic is crucial in imaging the basement architecture.
- Mesoproterozoic and older basement to the Stuart Shelf does not crop out in the area and hence drill hole data will be vital.

Additional Experiments

Two additional seismic activities were raised and discussed at the workshop. These activities have the advantage of bringing new researchers into the project, and would provide additional information on the crustal structure of the region:

- Teleseismic Survey / Receiver Function Survey (broadband seismometer survey) east-west across the Stuart Shelf, and well into the Adelaide Fold Belt (to the east) and across the Gawler Range Volcanics, west to the Nuyts domain (Figure 1).
- Crustal-scale seismic refraction survey (using short period seismic recorders) coincident with the deep seismic reflection survey, extending from the Adelaide Fold Belt in the east to the Gawler Range Volcanics in the west.

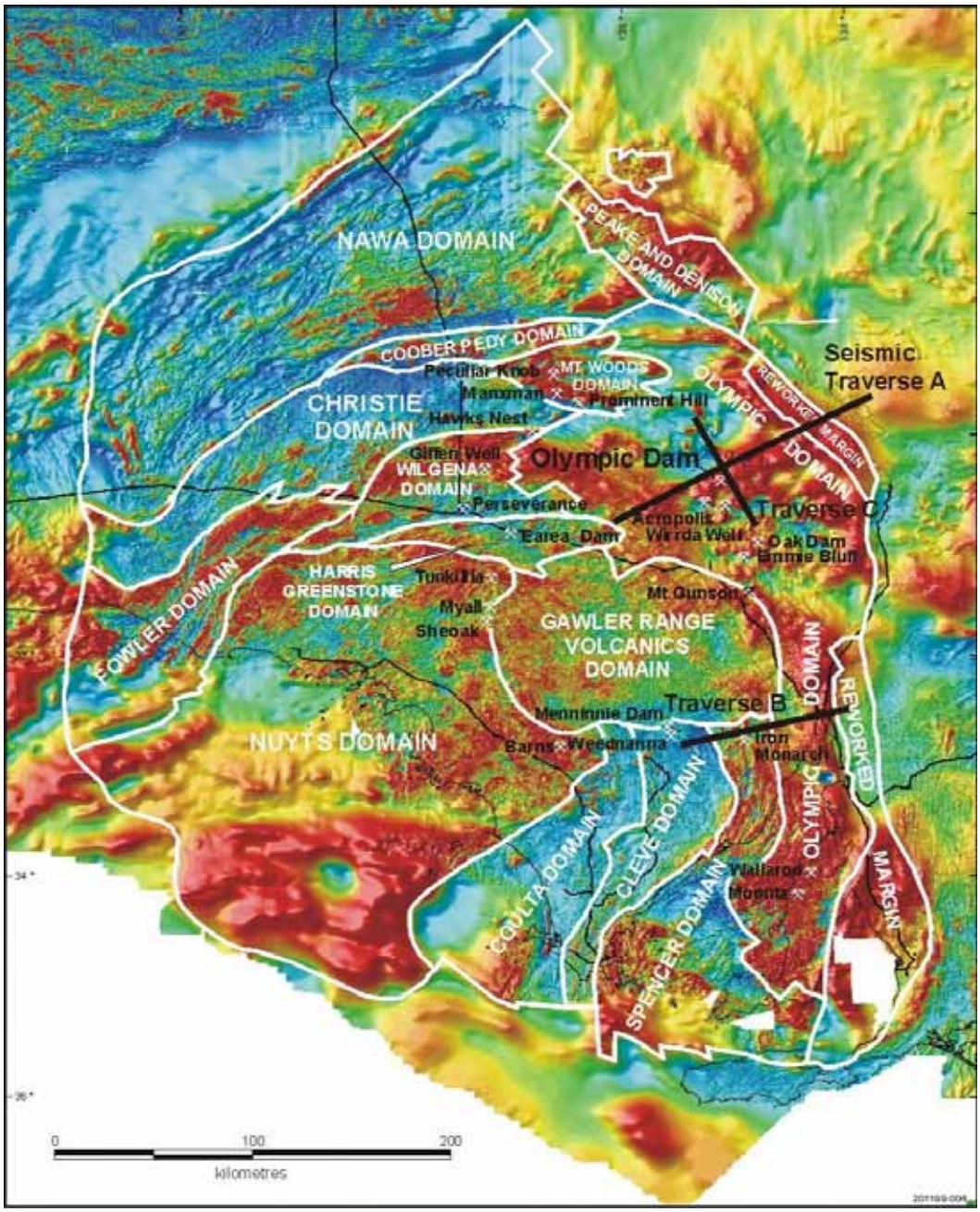

Figure 1: *Domains of the Gawler Craton (as described by Ferris et al. 2002) in white on the aeromagnetic image of the Gawler Craton. The three deep seismic reflection traverses proposed in 2000, Traverses A, B and C are shown in black. Major mineral deposits are also shown in black.*

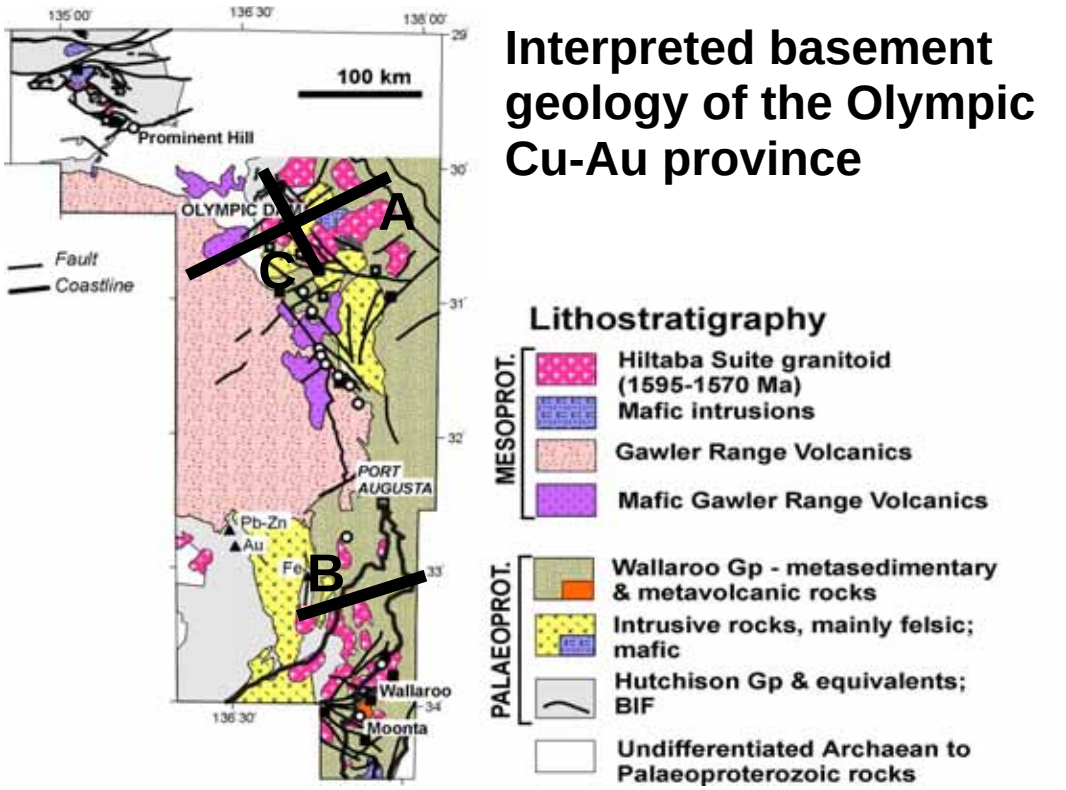

Figure 2: *Domains Interpreted basement geology (pre-Pandurra Fm) of the Olympic Cu-Au province in the eastern Gawler Craton (from Skirrow et al., 2002). Major Cu-Au±U mineralisation occurs in the Olympic Dam, Moonta-Wallaroo and Prominent Hill (Mt Woods Inlier) areas. The three deep seismic reflection traverses proposed in 2000, Traverses A, B and C are shown as thick black lines. Open circles and black squares represent drill holes with low-temperature and high-temperature hydrothermal alteration, respectively.*

FINAL POSITIONING OF SEISMIC TRAVERSES

Final traverse positions will be determined by liaison with ANSIR (Australian National Seismic Imaging Resource) representatives. However, several aspects of traverse positioning need to be flagged in the early planning stages. These are the need to:—

- Integrate the proposed seismic reflection work into work being undertaken by GA and MER Gawler research projects.
- Image key structures at near-orthogonal angles to their strike.
- Avoid areas where sideswipe and/or aliasing of subsidiary structures may reduce data quality.
- Avoid areas of Cambrian limestone outcrop/subcrop that may reduce data quality.
- Avoid sensitive land use areas e.g., National Parks, conservation/wilderness areas, heritage sites, mine leases, and seismically noisy built up areas.
- Minimise land clearance, both in order to reduce environmental impacts and cost.

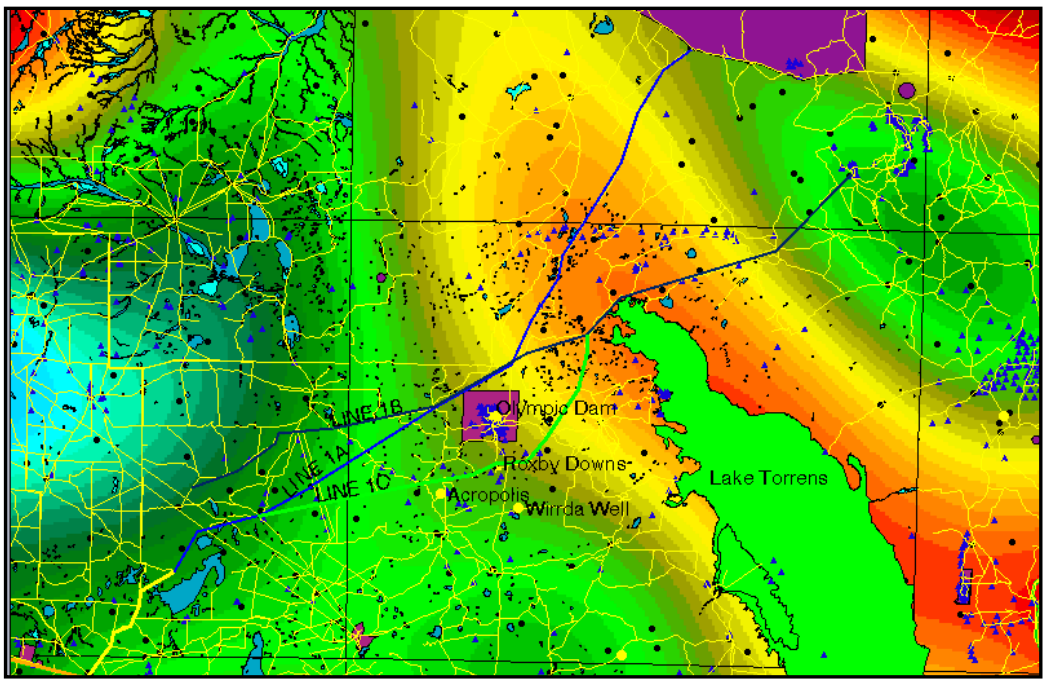

Figure 3: *Alternative line positions proposed in 2000 for the highest priority seismic Traverse A across the Olympic Cu-Au province. Background coloured image is upward-continued Bouguer gravity (50km window), representing long-wavelength gravity anomalies. Roads and tracks shown as thin yellow lines. Drainage networks shown in blue. Restricted areas shown in purple. Conservation areas shown in green. Black filled circles = localities; Blue filled triangles = exploration drill holes; Yellow filled circles = ore deposit/occurrence. Thin black lines = 1:250k sheet area boundaries. From Direen (2000).*

Participants at the Seismic Workshop identified several logistical issues that will need to be addressed during the final planning of the traverse location. These are:—

- Lake Torrens (and the Torrens Hinge Zone)
  - Two areas to the Torrens Hinge Zone
    - North end of Lake Torrens, or
    - North of Port Augusta
- Adelaide Fold Belt (rugged Flinders Ranges)
- Rugged region in Gawler Range Volcanics

SUMMARY

The Seismic Workshop participants recommended that the seismic traverse should cross the Stuart Shelf region within the Olympic Cu-Au province in the vicinity of Olympic Dam.

The traverse locations described above are intended to form the basis for further planning. It is likely that alternatives or modifications to these proposals will be made after consultation with the relevant stakeholders. These include ANSIR; PIRSA (including PIRSA Office of Minerals & Energy Petroleum Group); minerals industry representatives (e.g., WMC, Dominion Mining, Resolute, Gunson Resources, Minotaur Resources, etc.); petroleum industry representatives (e.g.,

Hemley Exploration); the academic community (e.g., Adelaide University, CODES, ANU); local landowners; and local Aboriginal community groups.

REFERENCES

Direen, N G, 2000, Recommendations for joint AGSO-PIRSA-ANSIR deep seismic reflection-refraction program in the Gawler Craton, 2001-2002 Financial Year. Unpublished AGSO report.

Ferris, G.M, Schwarz, M.P. and Heithersay, P., 2002. The Geological Framework, Distribution and Controls of Fe-Oxide Cu-Au Mineralisation in the Gawler Craton, South Australia. *In* Porter, T.M. (Ed.). *Hydrothermal Iron Oxide Copper-Gold and Related Deposits: A Global Perspective, Volume 2*. PGC Publishing, Adelaide, 380p.

Skirrow, R.G., 1999, Geoscientific framework of the Gawler Craton, Unpublished Geoscience Australia report.

Skirrow, R.G., Bastrakov, E., Davidson, G, Raymond, O. and Heithersay, P., 2002. Geological framework, distribution and controls of Fe-oxide Cu-Au deposits in the Gawler Craton. Part II. Alteration and mineralisation. *In*: Porter, T.M. (Ed.). *Hydrothermal iron oxide copper-gold and related deposits, Volume 2*. PGC Publishing, Adelaide, 33-47.

Stewart, K. and Foden, J., 1997, Mesoproterozoic granitoids of South Australia, Department of Geology and Geophysics, University of Adelaide, Unpublished Report.

Teasdale, J., 1997, Methods for understanding poorly exposed terranes: The interpretive geology and tectonothermal evolution of the western Gawler Craton, Unpublished Ph.D thesis, University of Adelaide.

CHOOSING THE LINES

B.R. Goleby[1], D. W. Johnstone[1], L.E.A. Jones[1], B.J. Drummond[2] and T. Barton[1]

[1] Australian National Seismic Imaging Resource, Geoscience Australia, GPO Box 378, Canberra, ACT 2601, Australia
[2] Geoscience Australia, GPO Box 378, Canberra, ACT 2601, Australia

INTRODUCTION

In choosing the location of a seismic line, there are four main considerations. The location of the survey must allow:—

- The scientific objectives to be met.
- Avoidance of geological problem areas.
- Logistical feasibility of recording seismic data, given the topographical constraints.
- Avoidance of sensitive areas.

In meeting these constraints, it is important to understand how the seismic method works.

The seismic reflection method requires an energy source and a series of receivers. On most seismic systems, the receivers are all connected by cable to create a seismic spread. For deep seismic surveys, this spread can be 10 km or more. The cables must connect to a recording truck that stores the data after each shot. The receivers are continuously recovered from the back of the seismic spread and redployed at the front of the spread. In this way the seismic spread moves along across the ground, along with its energy source, the recording truck, the crew, and support vehicles.

The first requirement is to have a continuous track along which to work. Ideally, it must meet the following conditions:—

- It can be driven along, or if there are obstacles, it is possible to drive around them and get back to almost the same spot.
- It can be negotiated at a reasonable safe speed. A 20 km/hr track takes too long to move from the front of the spread to the back and visa versa.
- It is wide enough to allow other vehicles to pass safely, especially the bigger trucks.
- It does not damage or delay the vehicles, through punctures, sliding, or bogging.

MEETING SCIENTIFIC OBJECTIVES

The objectives of the Gawler seismic are to:—

- Image the crustal structure of Palaeo- and Mesoproterozoic basement near the Olympic Dam Cu-Au-U deposit.
- Use the crustal structure to define tectonic controls on Cu-Au mineralisation.
- Test whether a large mafic/ultramafic intrusion exists beneath the Olympic Dam deposit, as implicated in some genetic models of Cu-Au-U mineralization.

- Determine the geometry and geodynamic significance of the Torrens Hinge Zone at the eastern margin of the Gawler Craton, with a view to ultimately understanding the relationship with the Curnamona Province.
- Provide new insights on Neoproterozoic basin formation in the Adelaide Geosyncline to the east of the Torrens Hinge Zone.

To achieve these objectives, the seismic line had to go close to the Olympic Dam deposit, cover enough distance to image the regional crustal structure, cross the Torrens Hinge Zone, and cross part of the Neoproterozoic basins (Figure 4).

Which way should the eastern Gawler Craton be crossed – north-south or east west or somewhere in between?

In the eastern Gawler Craton, there is a significant cover of younger material. For this survey, using the available potential field images assisted in determining the regional grain to the geology and associated structures. Analysis of regional geology and regional gravity and magnetic data, ensured that the seismic lines crossed the main geophysical features and dominant strike at high angles.

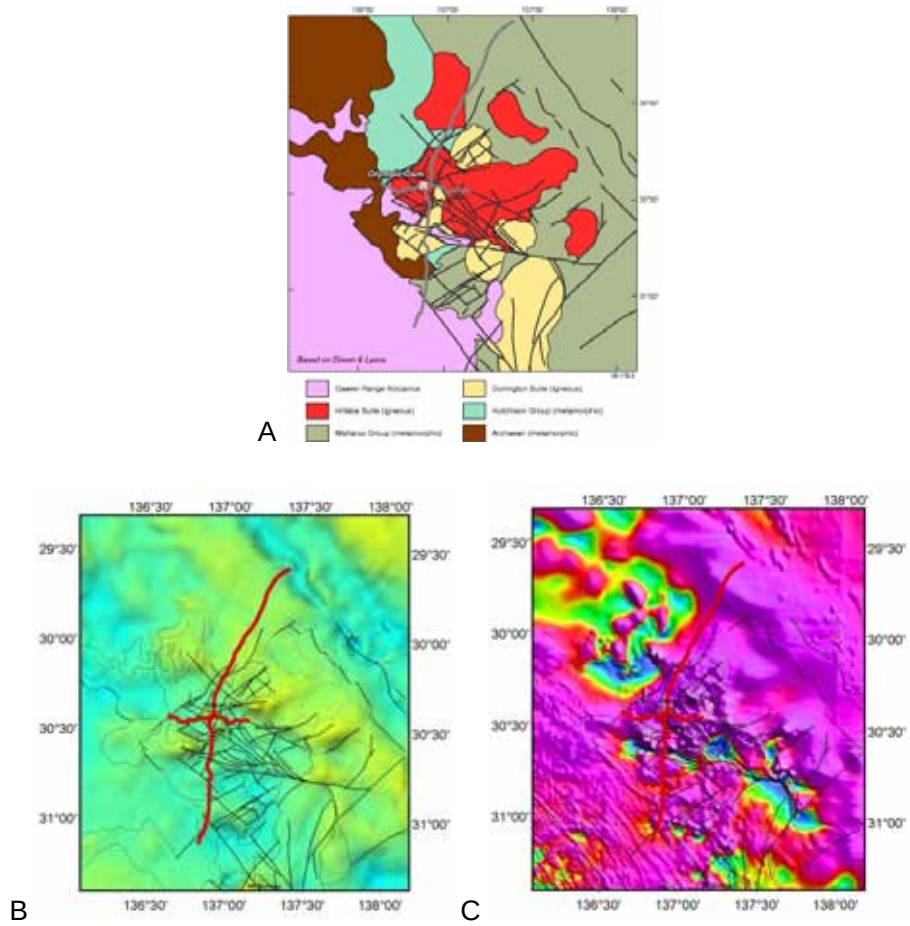

Figure 4: *Location of the 2003 Gawler Craton deep seismic reflection lines on (A) regional geological map, (B) gravity data from the National Gravity Data Set, and (C) aeromagnetic from the National Aeromagnetic Data Set. In all cases the seismic lines cross the main geophysical features interested in.*

Figure 4 shows the eastern Gawler Craton seismic traverse on the interpreted basement geology, on the regional gravity coverage, and on the regional magnetic coverage. It shows that the seismic lines were recorded at high angles to the tectonic grain, and even where deviation from orthogonal approach thirty or forty degrees, the apparent dip in section was no more than about ten degrees from true.

AVOIDING GEOLOGICAL PROBLEM AREAS

The seismic method will always work. However, for the seismic method to produce an interpretable image of the region, then there must be a reasonable density contrast between the rock units being imaged (Jones et al., these volume).

A massive sequence of sandstones will not produce any reflections, unless there are some thin shale bands or similar or some structuring within the sandstone. Equally a homogenous granite body will produce no reflections unless there is some structuring within the granitic body.

Equally, some rock units are not conducive to the seismic method. For example, extreme variations in unconsolidated regolith, basalt sills within a sedimentary succession, cavernous limestones near or at the surface, karst units or brecciated fault zones all either absorb the seismic energy or prevent it returning to the recorders. These geological environments inhibit recording of good quality seismic data.

The optimal orientation of seismic lines, with respect to basement structures, is northeast-southwest. However, this has a major disadvantage in that such a line, passing close to the Olympic Dam minesite, would also cross large areas of near-surface limestone and along to the surface trace of one of a major fault; two serious geological problems to be avoided because of the possible degradation of data quality.

The lines shown in Figure 4 did not pose any significant geological problems that might cause data degradation. The only concern was the thickening Neoproterozoic cover-successions, at the northern end of the traverse, and the mass of Gawler Range Volcanics, to the south, but inspection of some old seismic reflection data near these areas suggested that data could be obtained beneath both the sedimentary cover and volcanics.

TOPOGRAPHIC CONSTRAINTS

Topographical features like mountain ranges, rivers, salt lakes and towns all can restrict the location of seismic lines (e.g., Figure 5).

Where possible, it is best to use existing roads, tracks or fence lines. However this is not always practical as the seismic line must be orientated at a high angle to regional strike and the roads do not always run that way. In such cases you must clear a track and topographical issues must be considered very carefully as clearing of new tracks significantly add to the cost of the survey. Figure 6 shows some topographical features in northeastern South Australia that would cause concern for planning a seismic line.

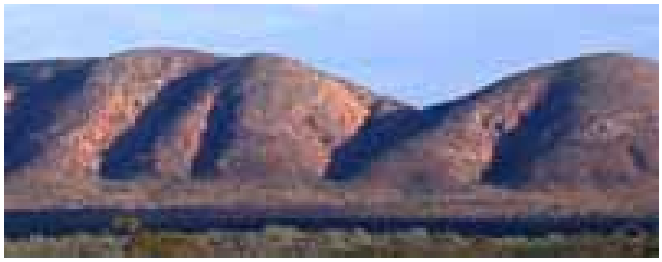

Figure 5: *Photograph of the Gawler Ranges. This is not a trivial range to cross. If the seismic had to cross this range, considerable effort would be needed in either finding an existing route across the range or devising a new route. The later would add significantly to the cost of the seismic survey.*

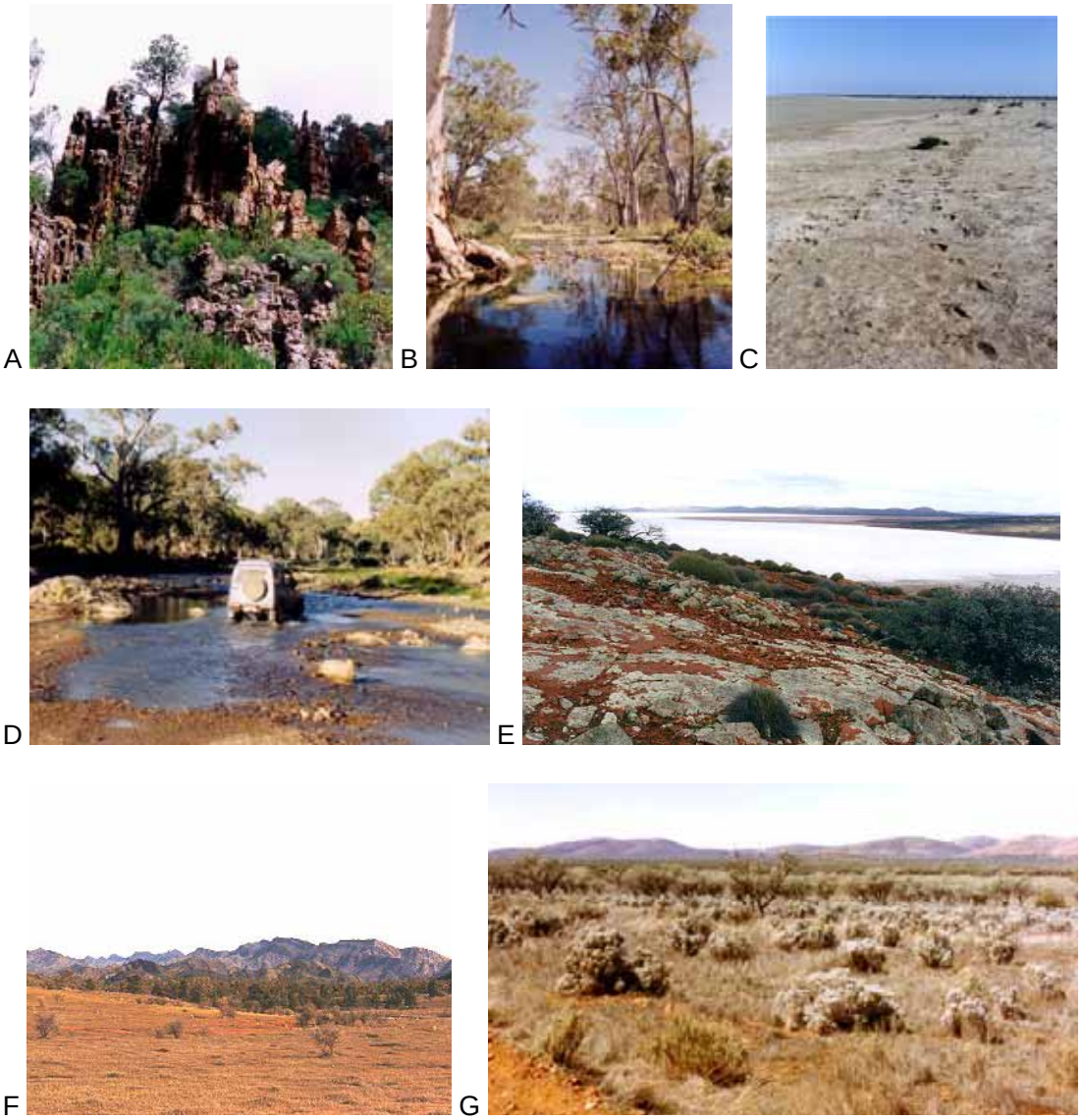

Figure 6: *Collage of photographs of the northern region of South Australia. These show some of the topographical features you must consider when planning a seismic traverse. (These photographs have been downloaded from http://homepages.picknowl.com.au/anne_brown. Images from top left are A) extremely rough country, B) billabongs, swamps or lakes, C) fragile and boggy areas, D) creeks or water bodies, E) salt lakes, F) mountain range and G) more mountain ranges.*

CULTURAL CONSTRAINTS

Cultural constraints include mines, cities or towns, main roads, national parks, exclusion areas, etc. Figure 7 shows some of these in northern South Australia.

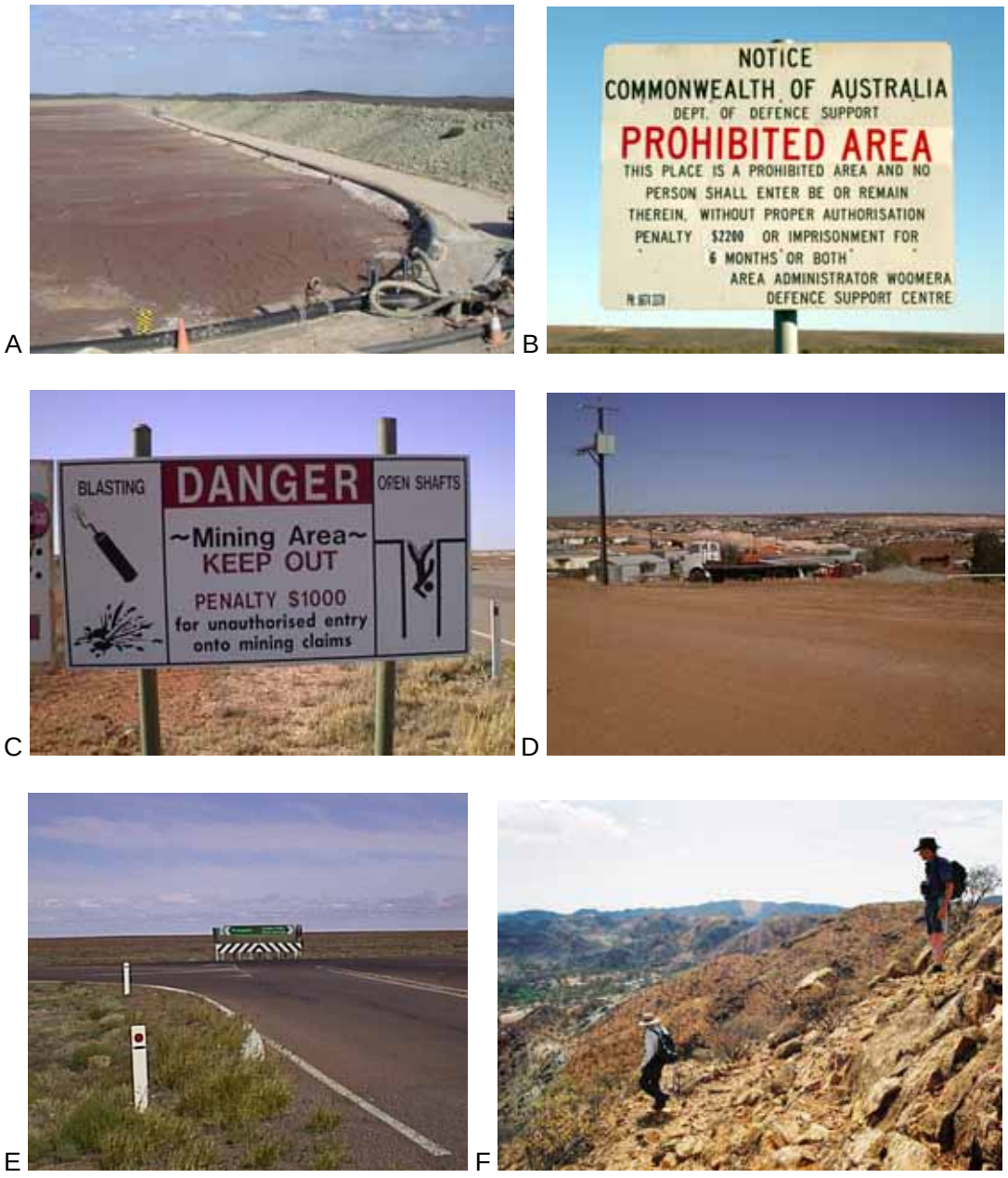

Figure 7: *Collage of photographs from the northern region of South Australia. These show examples of man-made features to be consider when planning a seismic traverse. From top left are: A) mine tailings dam, B) legislated prohibited areas, C) mine sites, D) towns, E) bitumen roads and F) national parks.*

In some ways, cultural features are often harder to negotiate than topographical features because they may provide sources of seismic or electromagnetic noise that degrades the quality of the data. Contamination of the data aside, the option of bulldozing a track through a cultural feature is not always open to us.

AVOIDING SENSITIVE AREAS

The positions of seismic lines may need to be adjusted to avoid culturally or environmentally sensitive areas, including Aboriginal heritage areas or sites of significance, early settler heritage areas.

Figure 8 shows some examples of such sensitive areas. Aboriginal heritage sites can be identified through consultation with anthropologists and archaeologists. Environmental sites can be identified through discussion with the local government environmental department.

A  B 

C  D 

Figure 8: *Collage of photographs illustrating sensitive areas that may be encountered during planning a seismic survey. From top left: A) an early setters house, B) aboriginal carvings on outcrop, C) fragile dunes with limited vegetation and D) stand of Mulga (Acacia aneura).*

SUMMARY

At the end of this process of elimination, you will end up with a continuous track along which to work (or the survey will be cancelled). This track will be located to best solve the projects scientific objectives, but modified for local geological problems, topographical features, and sensitive areas. At all times, the most important aspect of locating the seismic lines is to meet the scientific objectives, which add to our understanding of the geology of the Australian continent.

GEOLOGICAL FRAMEWORK OF THE GAWLER CRATON AND THE OLYMPIC DOMAIN

Michael Schwarz[1]

[1] Primary Industries and Resources South Australia, Minerals, Petroleum and Energy, GPO Box 1671, Adelaide, South Australia, 5001, Australia

INTRODUCTION

The Gawler Craton is an Archaean to Mesoproterozoic crystalline shield that has been tectonically stable, with the exception of minor epeirogenic movements, since ~1450 Ma (Thomson, 1975; Parker, 1990, 1993).

The boundaries of the eastern Gawler Craton have been interpreted from potential-field data. Outcrop information and drill hole data are used to determine the limit of rock units known to be of Gawler Craton affinity. The eastern limit of the craton is relatively well defined by the Torrens Hinge Zone, marking Neoproterozoic rifting initiated during the development of the Adelaide Geosyncline. Later deformation, during the Delamerian Orogeny, reworked the eastern Gawler Craton.

The Olympic Domain (incorporating the Moonta Domain of Parker, 1993) is an arcuate zone of Archaean gneisses variously intruded and overlain by Palaeoproterozoic sedimentary successions and felsic igneous rocks and Mesoproterozoic granite, volcanics, quartz-rich sedimentary rocks and conglomerates.

The oldest known rocks of the Olympic Domain are of the Archaean Mulgathing Complex. It comprises aluminous metasedimentary rocks (Christie Gneiss), felsic igneous rocks (Kenella Gneiss), mafic and ultramafic extrusives, felsic intrusives and metasediments (Harris Greenstone Domain), felsic volcanics (Devil's Playground Volcanics), and syn-tectonic felsic intrusives (Glenloth Granite) (Daly and Fanning, 1993; Daly et al., 1998; Ferris et al., 2002).

In the region of Olympic Dam, equivalents of the Hutchison Group are a schistose unit occurring as enclaves in deformed granites (Creaser, 1989). These rocks are strongly deformed, containing at least one foliation. The Hutchison Group is an extensive sequence of shallow clastic and chemical marine sediments, with minor felsic and mafic volcanics (Parker, 1993). Parker and Lemon (1982) subdivided the Hutchison Group into three main sequences; a basal quartzite sequence (Warrow Quartzite); a mixed chemical and clastic sequence (Middleback Subgroup); and an upper pelitic unit (Yadnarie Schist).

Numerous drill holes have intersected coarse-grained, deformed granite. U-Pb SHRIMP analysis of zircons from these give a crystallisation age of 1845 Ma, which is considered to be part of the Donington Suite (Creaser, 1995). The Donington Suite is defined from the southern Gawler Craton, where it crops out on the eastern coast of the Eyre Peninsula and the west coast of the Yorke Peninsula. In the Olympic Dam region, the suite varies from quartz gabbronorite to ultrafractionated granite (Parker et al., 1988), with small volumes of mafic to intermediate

magmas, voluminous felsic, megacrystic granite and gneiss and smaller volumes of late, ultrafractionated, fine-, even-grained granite. Distinct units within the Donington Suite exhibit abundant co-magmatic relationships, suggesting evolution from a common magmatic source (Schwarz, 2003). Numerous U-Pb zircon dates from different units have all returned crystallisation ages, within error, of 1850 Ma (Fanning, 1997)

The Kalinjala Mylonite Zone separates the Donington Suite in the south from similar rock types in the Cowell-Cleve region, northern Eyre Peninsula. The Kalinjala Mylonite Zone is interpreted to continue north, as a series of anastomosing mylonite zones, into the Olympic Dam region, probably passing to the west of the Burgoyne batholith.

Within the Olympic Dam region, overlying the Donington Suite, there is a sequence of intercalated, deformed felsic volcanics and schists (Creaser, 1989). This unit has not been dated, but possibly correlates with the Myola Volcanics (~1791 Ma), the Moonta Porphyry (~1760 Ma), or the Tidnamurkuna Volcanics (~1780 Ma).

Overlying the older granites of the Olympic Domain is a widespread sequence of finely laminated metasiltstone, feldspathic sandstones, calc-silicates and amphibolites. This sequence is unconformably overlain by Gawler Range Volcanics, hence Creaser (1989) correlated this unit with the Wandearah Metasiltstone. Cowley et al. (2003) redefined the Wallaroo Group to include all meta-sedimentary and meta-igneous units older than the Mesoproterozoic Hiltaba Suite (Tickera and Arthurton Granites) and the Oorlano Metasomatite. The Wallaroo Group includes the Wandearah Formation, Weetulta Formation and Matta Formation. The age of the sequence has been determined from the interbedded volcanics, dated by U-Pb zircon analyses at between 1763±14 Ma and 1737±5 Ma (Cowley et al., 2003)

The last major magmatic event observed in the area is that of the Hiltaba Suite/Gawler Range Volcanic magmatic event (1595-1575 Ma). The Gawler Range Volcanics cover an area of approximately 25 000 km^2. They are the dominant Proterozoic unit cropping out in the Gawler Craton. They comprise a series of felsic and minor mafic volcanics. The Hiltaba Suite, which intruded its co-magmatic Gawler Range Volcanics in places, comprises mostly oxidised, K-feldspar dominant granite. The Olympic Dam Cu-U-Au ore body is hosted within the Roxby Downs Granite, a member of the Hiltaba Suite.

The Pandurra Formation unconformably overlying the basement, is a thick sequence of undeformed arenaceous redbeds that extend over a greater part of the Olympic Domain (Cowley, 1991). Fanning et al. (1983) reports that the Pandurra Formation has a minimum depositional age of 1424±51 Ma based on Rb-Sr geochronology. Unconformably overlying the Pandurra Formation in the Cultana area are subaerial basalts of the Beda Volcanics and intercalated coarse fluvial clastics of the Backy Point Formation.

REFERENCES

Conor, C.H.H., 1995. Moonta–Wallaroo region: an interpretation of the geology of the Maitland and Wallaroo 1:100 000 sheet areas. South Australia. Department of Primary Industries and Resources. Open file Envelope, 8886 (unpublished).

Cowley, W.M., 1991. The Pandurra Formation. South Australia. Department of Mines and Energy. Report Book, 91/7.

Cowley, W.M., Connor, C.H.H. and Zang, W., 2003. New and revised Proterozoic stratigraphic units on northern Yorke Peninsula. *MESA Journal*, **29**, 46-58.

Creaser, R.A., 1989. The geology and petrology of middle Proterozoic felsic magmatism of the Stuart Shelf, South Australia. Latrobe University. Ph.D. thesis (unpublished).

Daly, S.J. and Fanning, C.M., 1993. Archaean. *In*: Drexel, J.F., Preiss, W.V. and Parker, A.J. (Eds.). *The Geology of South Australia. Volume. 1, The Precambrian*. South Australia. Geological Survey. Bulletin, **54**, 32-49.

Daly, S.J., Fanning, C.M. and Fairclough, M.C., 1998. Tectonic evolution and exploration potential of the Gawler Craton, South Australia. *AGSO Journal of Australian Geology and Geophysics*, **17**, 145-168.

Fanning, C.M., 1997. Geochronological synthesis of South Australia. Part II: The Gawler Craton. Australian National University. Research School of Earth Sciences. PRISE Report (unpublished).

Ferris, G.M., Schwarz, M.P. and Heithersay, P., 2002. The geological framework, distribution and controls of Fe-oxide and related alteration, and Cu–Au mineralisation in the Gawler Craton, South Australia. Part 1: geological and tectonic framework. *In:* Porter, T.M. (Ed.). *Hydrothermal iron oxide copper–gold and related deposits: a global perspective. Volume 2*. PGC Publishing, Adelaide.

Parker, A.J., 1990. Gawler Craton and Stuart Shelf — regional geology and mineralisation. *In*: Hughes, F.E. (Ed.). *Geology of the mineral deposits of Australia and Papua New Guinea.* Australasian Institute of Mining and Metallurgy. Monograph Series, **14**, 999-1008.

Parker, A.J., 1993. Palaeoproterozoic. *In*: Drexel, J.F., Preiss, W.V. and Parker, A.J. (Eds.). *The Geology of South Australia. Volume 1*, The Precambrian. South Australia. Geological Survey. Bulletin, **54**, 51-105.

Parker, A.J. and Lemon, N.M., 1982. Reconstruction of the Palaeoproterozoic stratigraphy of the Gawler Craton, South Australia. *Journal Geological Society of Australia*, **29**, 221-238.

Schwarz, M.P. 2003. LINCOLN, South Australia, sheet SI53-11. South Australia, Geological Survey. 1:250 000 Series — Explanatory Notes.

Thomson, B.P., 1975. Gawler Craton, SA. *In*: Knight, C.L. (Ed.) *Economic Geology of Australia and Papau New Guinea, 1, Metals*. Australasian Institute of Mining and Metallurgy. Monograph Series, **5**, 461-466.

CAPABILITIES AND LIMITATIONS OF THE SEISMIC REFLECTION METHOD IN HARD ROCK TERRANES

L.E.A. Jones[1,2], B.R. Goleby[1,2], and B.J. Drummond[2]

[1] Australian National Seismic Imaging Resource, Geoscience Australia, GPO Box 378, Canberra ACT 2601, Australia
[2] Geoscience Australia, GPO Box 378, Canberra ACT 2601, Australia

INTRODUCTION

The seismic reflection method was developed for petroleum exploration in sedimentary basins, where its accuracy, resolution, and depth penetration result in detailed pictures of structure and stratigraphy. The reflection method uses a controlled source which generates seismic waves that are reflected from interfaces between different rock units, as shown in Figure 9. An explosive or vibratory source is used. Continuous 2D coverage is achieved by moving sources and receivers along a seismic traverse.

The Earth is not homogeneous or isotropic, but a good approximation in seismology is a system of layers, individually homogeneous and isotropic, which is why the seismic method works so well in sedimentary basins. In hard rock areas too, reflections are indisputably produced. The salient questions are: What causes reflections? What can't we see? What are the pitfalls?

Some of the key features of hard rocks are steep dips associated with folds and faults, and high seismic velocities. Steeply dipping events can be difficult to image. High velocities affect resolution, but also make it easier to stack reflections since there is less move-out. In hard rock terranes, there may also be more problems correcting for delays in the weathered zone and in getting sufficient energy through it. However, a counteracting factor is that hard rock should have lower intrinsic attenuation of seismic energy, resulting in greater depth penetration of the higher frequencies.

Much of the material covered here can be found in geophysics texts. However, we have selected and developed those aspects relevant to seismic imaging in hard rock.

BASIC CONCEPTS

Seismic waves

A seismic (elastic) wave is a propagating oscillatory disturbance that travels as a series of wavefronts (equal amplitude of disturbance). Usually ray paths (path travelled by a point on a wavefront) are drawn, as in Figure 9. The distance between successive peaks (or troughs) is the wavelength (λ). The frequency of the wave (f) is the number of cycles per second, so that the velocity of the wave is $V = \lambda f$.

Two types of seismic body waves can travel within the Earth, namely P (compressional) and S (shear). In reflection surveys, P waves predominate, being preferentially generated by the

commonly used sources. Surface waves (ground roll) can be a source of noise in reflection surveys, travelling along the surface at low velocity and arriving at the same time as reflections from depth.

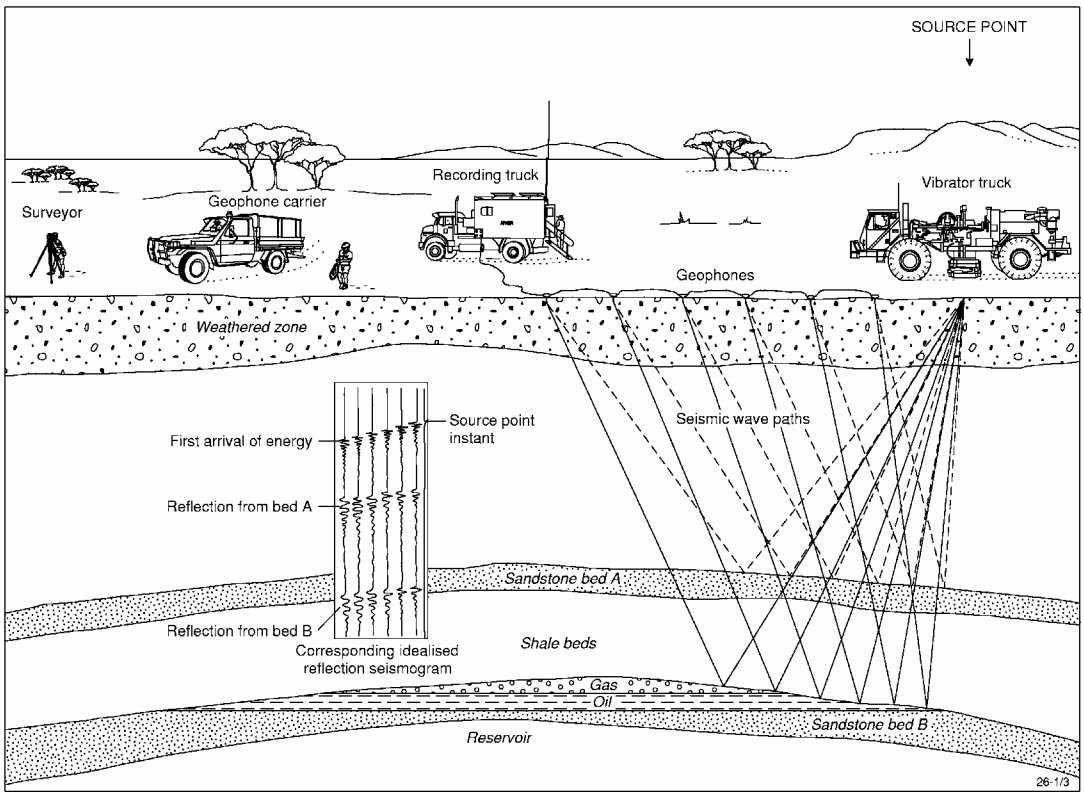

Figure 9: *Schematic representation of a seismic reflection survey.*

Factors influencing P wave velocity in rocks include mineralogy, porosity (and cracks), pore fluid content, cementation and texture. For igneous and metamorphic rocks, the dominant factor is mineralogy, although micro-cracks in low concentrations can significantly reduce velocity. Empirical laws for such rocks show that the velocity is approximately proportional to density. In sedimentary rocks, the most important factors are porosity, pore fluid content and cementation. As a general statement, velocities are high in igneous and metamorphic rocks and lower in sedimentary rocks, particularly young sedimentary rocks.

Generation of reflections

When a seismic wave encounters a boundary where there is an abrupt change in elastic properties, some of the energy is reflected depending on the size of the reflection coefficient, but most is transmitted into the second medium, as shown in Figure 10. Some energy will also be critically refracted along the boundary, and forms the basis of the seismic refraction method. The reflection coefficient RC is the ratio of the reflected wave amplitude A_r to the incident wave amplitude A_i and for near normal incidence (up to 20°) can be expressed as

$$RC = \frac{A_r}{A_i} = \frac{\rho_2 V_2 - \rho_1 V_1}{\rho_2 V_2 + \rho_1 V_1} = \frac{Z_2 - Z_1}{Z_2 + Z_1} \ .$$

The product ρV (=Z) is the acoustic impedance, where ρ is the density and V is the P-wave velocity. The larger the contrast in acoustic impedance, the larger will be the reflection coefficient. An impedance decrease causes a negative reflection coefficient, i.e., the reflected wave is reversed in polarity compared with the incident wave. Typically reflection coefficients are small, generally less than 0.05, but in hard rock terranes could reach 0.075 for a felsic-mafic contact (ρ = 2.7 t m^{-3} and V = 6000 m s^{-1} overlying ρ = 2.9 t m^{-3} and V = 6500 m s^{-1}).

Thus the density contrast governs whether reflections occur at boundaries between different rock types (since velocity is proportional to density for igneous, metamorphic and well-lithified rocks). It is not likely that reflections will result from a foliated fabric within a rock, unless this is strongly developed into alternating bands of material on a macroscopic scale, such as in shear zones.

As a seismic pulse (wavelet) travels down into the Earth, energy will be reflected back at each interface, with amplitude governed by the reflection coefficient, and an extra time delay corresponding to the extra time down to and back from the interface. Thus a seismic reflection trace consists of a succession of 'echoes' of seismic energy, as shown in the reflection seismogram in Figure 9.

Figure 9 also illustrates that the travel time for a reflection increases with increasing offset between source and receiver. It can be shown that the time (T), along a reflection ray path emerging at offset (X), from the source follows a hyperbolic relationship,

$$T^2 = T_0^{\,2} + X^2/V^2 \;;$$

where V is the velocity of the layer, and T_0 is the two way travel time for vertical incidence. The difference between T and T_0, known as normal moveout, decreases with both increasing T_0 and increasing V. The high velocities typical of hard rock areas mean that moveout is generally small, so that uncertainties in moveout velocity are not so problematical for stacking the data. However, a corollary is that velocities for depth conversion are very poorly constrained.

For dipping reflectors, the above relationship is modified with V replaced by V/cos α, where α is the angle of dip, thus increasing the stacking (moveout) velocity.

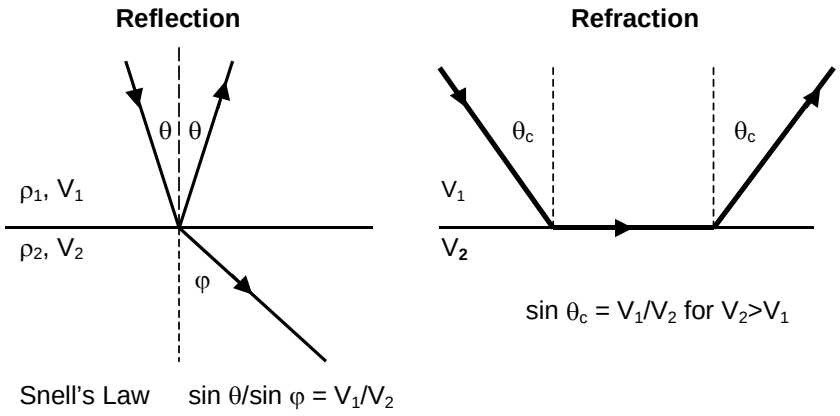

Figure 10: *Reflection and refraction of a seismic wave at a boundary between two media with velocity V_1 and V_2 and density ρ_1 and ρ_2, respectively. The angle of incidence equals the angle of reflection. The wave is transmitted into the second medium with angle of refraction φ. For $\varphi = 90°$, the refracted ray follows the boundary (critical refraction).*

SEISMIC RESOLUTION

Seismic resolution deals with the question: How thick and how wide do features have to be to produce recognisable reflections on a seismic section?

Vertical Resolution

The concept of vertical resolution can be illustrated by considering waves reflected from a layer of thickness H and velocity V_1 embedded in a medium of velocity V_0, as shown in Figure 11. The reflection from the bottom will be reversed in polarity (reflection coefficient has opposite sign) and will lag behind the reflection from the top by a time ΔT, as shown in Figure 11. If the layer is

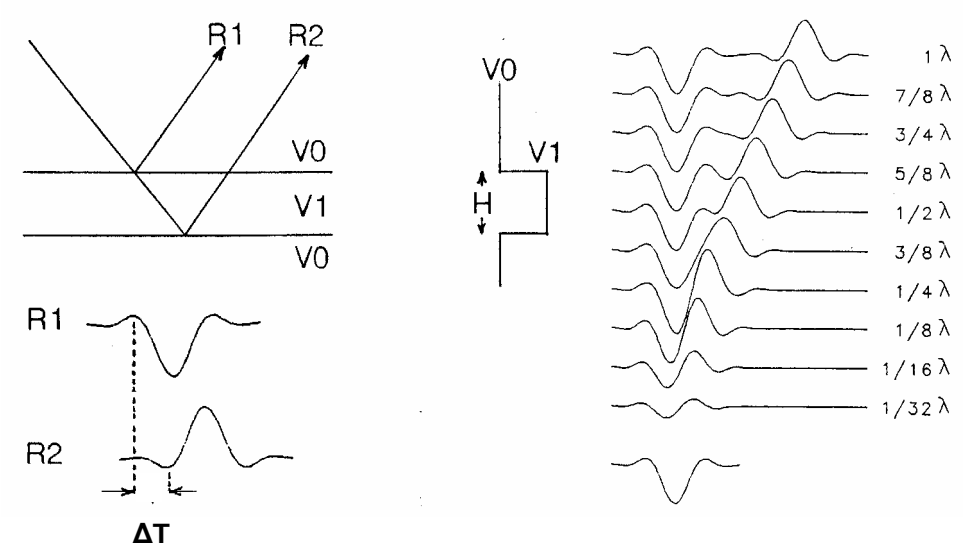

Figure 11: *Vertical resolution (identification of an embedded layer) is determined by the superposition of reflections from the top and bottom of the layer. Because the two reflections are of opposite polarity they cancel for thin layers and reinforce for thicker layers.*

thick, ΔT will be large and the two wavelets will appear as separate events. If the layer is thin, ΔT will be small and the two wavelets will almost cancel. A commonly used criterion for resolution is that interference effects are maximised when the wavelets are separated by half a cycle, which corresponds to a layer thickness of $\lambda/4$ (λ being the dominant wavelength for the wavelet).

The seismic response of layers of different thickness is illustrated on the right hand side of Figure 11. Thickness is parameterised in terms of λ. A maximum response occurs for $\lambda/4$, but the top and bottom of the layer are not resolvable and it thus appears as a single interface. In practice, the layer can still be detected as it becomes thinner, but becomes progressively harder to see. Layers thinner than $\lambda/32$ would not be detectable. It is not until the layer thickness exceeds $\lambda/2$ that reflections from the top and bottom of the layer can just be seen as two events.

What are typical values of λ in hard rock areas? The range of frequencies (band width) contained in a seismic pulse is narrow, normally from 5 Hz to 100 Hz. Because the amplitude loss with depth depends on frequency, the highest frequencies are rare at depth. Typically, the dominant frequency would be 40 Hz or less, corresponding to a wavelength of 150 m for a typical velocity of 6000 m s^{-1}. Layers would need to be greater than 75 m thick to be identified as such. However, a layer of about 37.5 m will produce a strong response, even if it cannot be differentiated from an interface. It would not be possible to detect layers less than 5 m thick (and probably not even less than 10 m). Thus the vertical resolution in hard rock is not as good as in sedimentary basins.

Shear Zones

Shear zones are often very strong reflectors of seismic energy, due to their layered nature on a macroscopic scale. Bands of alternating low and high velocity (density) material can explain the seismic response as shown in Figure 12. Tuning of the interference between reflections from tops and bottoms of the layers can result in a much larger seismic response than for a homogeneous layer of the same total thickness (compare Figure 12(a) and (b)). Zones in which layer thickness is variable and less than $\lambda/4$ can still produce strong reflections as illustrated in Figure 12(c) and (d). Typically shear zones exhibit a strong amplitude response, which is spatially variable. If the amplitude response is due to constructive interference of reflections from many layers, then lateral change in layer thickness could explain the variability from trace to trace.

Horizontal resolution

Horizontal resolution is concerned with the minimum lateral extent of features that can be detected. Consider the case of vertical incidence for a reflecting point P as shown in Figure 5. Geometrical ray theory would predict that only point P contributes to the reflection recorded vertically above on the surface at S. Wave theory shows that not only P, but surrounding points within a certain radius also contribute to the reflection amplitude.

For down-going wavefronts from source S, zones on the reflector can be constructed such that the difference in path lengths from S is $\lambda/4$ as shown in Figure 13 (a). For two-way travel, the difference in path length will be $\lambda/2$. It can be shown that the innermost zone (known as the first Fresnel zone) makes the dominant contribution to the wave amplitude observed at S.

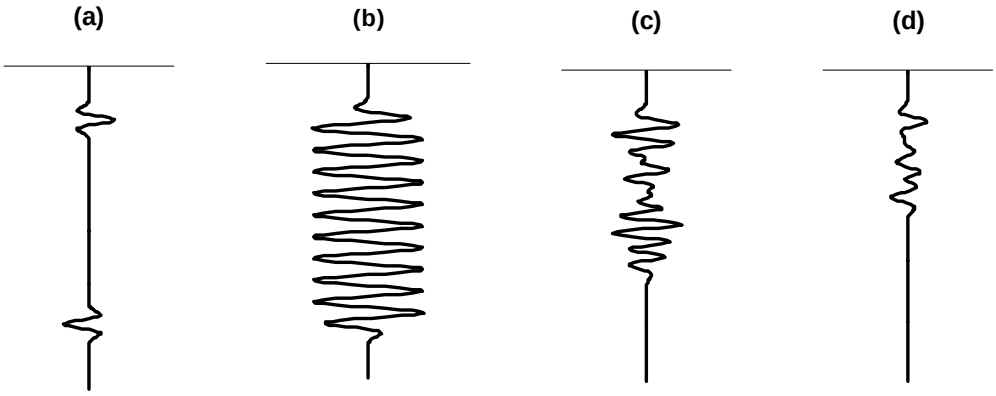

Figure 12: *Modelled seismic response for (a) Single layer 4.75 λ thick. (b) 19 layers each of thickness λ/4 with the same absolute reflection coefficient as in (a) alternating in sign. (c) 19 layers as in (b) but with random thickness between λ/16 and λ/4. (d) 19 layers as in (b) but with random thickness between λ/40 and λ/10. Wavelength λ modelled as 120 m.*

The first Fresnel zone has a radius equal to $(\lambda d/2)^{1/2}$ where d is the depth to the reflector. Thus, the width of the zone increases (resolution decreases) as both depth (two-way time) and dominant wavelength increase. In practice, features smaller than the Fresnel zone will not be resolved, since the reflected wave amplitude depends on the average properties over the width of the Fresnel zone.

Diffractions

When a seismic wave encounters a feature whose dimensions are comparable to, or smaller than the wavelength, the wave is diffracted, rather than reflected or refracted. Since the seismic wavelength in hard rock is typically 150 m, there will be many instances where geological features are smaller than this. Diffractions are commonly produced from very small geological structures or where continuous reflectors suddenly stop. Examples such as tight bends on folds, ends of fault-truncated layers, and tips of dykes are illustrated in Figure 14a.

The generation of diffractions can be explained by treating the feature as a point from which secondary waves radiate after excitation by the incident wave. An incident wave spreading out from a source at P1 in Figure 14b will generate a returning wave that will travel back along the same path; similarly for point P2. On a seismic section, the returning wave is assumed to come from vertically below P1 and P2, and will lie along a hyperbolic curve as shown in Figure 14c.

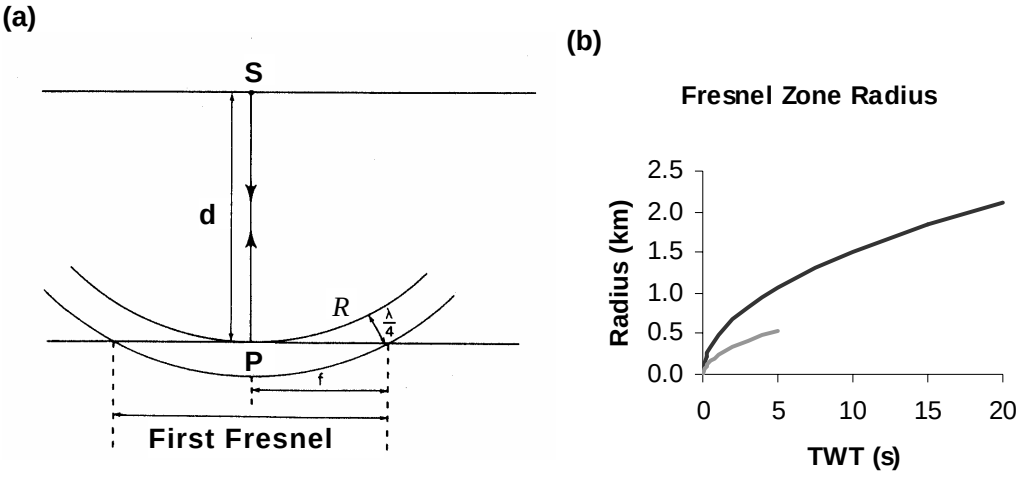

Figure 13: *(a) Representation of the reflector zone (first Fresnel zone) contributing to the amplitude of a wave reflected back to S. (b) Radius of the first Fresnel zone for typical hard rock areas (black) and sedimentary basins (grey) versus two-way time (TWT).*

In Figure 13b, two-way time (s) for the hard rock areas can be converted to depth (km) by multiplying by 3, using a typical velocity of 6000 m s^{-1}. For mid-crustal depths of ~24 km (TWT = 8 s), reflecting bodies must extend over a kilometre or two to be visible. As shown in Figure 13b, horizontal resolution is poorer than it would be for a typical sedimentary basin, i.e. the Fresnel zone is larger for hard rock areas, because of the greater wavelength (~150 m). However, because of the mathematical formulation above, the Fresnel zone radius increases by a factor of only 1.4 for a doubling of the wavelength, for features at the same depth.

The crest of the diffraction locates the diffracting point (in time and space). In practice, amplitude is stronger towards the crest of the diffraction curve. The curvature of the diffraction depends on the depth to and the velocity above the diffracting point, but standard overlay curves can be produced to differentiate diffractions from structure. Migration will collapse diffractions as described later. Diffracted waves will also fill in gaps in reflectors, thus making the seismic event appear continuous when the physical interface is not (another way of visualising the concept of horizontal resolution).

Dipping Reflectors

In hard rock areas, rocks are commonly highly deformed, resulting in steeply dipping rock units within folds, as well as faults of varying dips. Since the seismic method was originally developed for sub-horizontal layering within sedimentary basins, a critical issue is the greatest dip that can be imaged by the method in hard rock terranes.

The maximum dip is constrained by two parameters, the length of the seismic line and the duration of the seismic record. The general picture is illustrated in Figure 15. For near coincident source and receiver at P, a reflection will return along a path that is perpendicular to the reflector. To be imaged from P, sub-horizontal reflectors must lie below P, but steeply dipping reflectors will lie off to the side by a considerable distance. Thus a seismic line must be long enough to encompass both the reflecting surface and the seismic reflection system. In addition, recording time must be long enough to record reflections from the offset reflectors.

Figure 16 shows this relationship for a typical deep crustal seismic survey in hard rock. Note that a recording time of 20 seconds would be necessary to record reflections from a distance of 60 km, assuming a velocity of 6000 m s^{-1}. A semi-circular region in the Earth, centred on the observation point, is divided into equiangular segments. Each segment shows the zone within the Earth where a particular range of dips will be imaged, out to a distance of 60 km. For example, in the segments labelled 70° to 80°, only reflectors with dips in this range towards the observation point will be imaged. In the 0° to 10° segments, only shallow dips will be imaged.

(a)

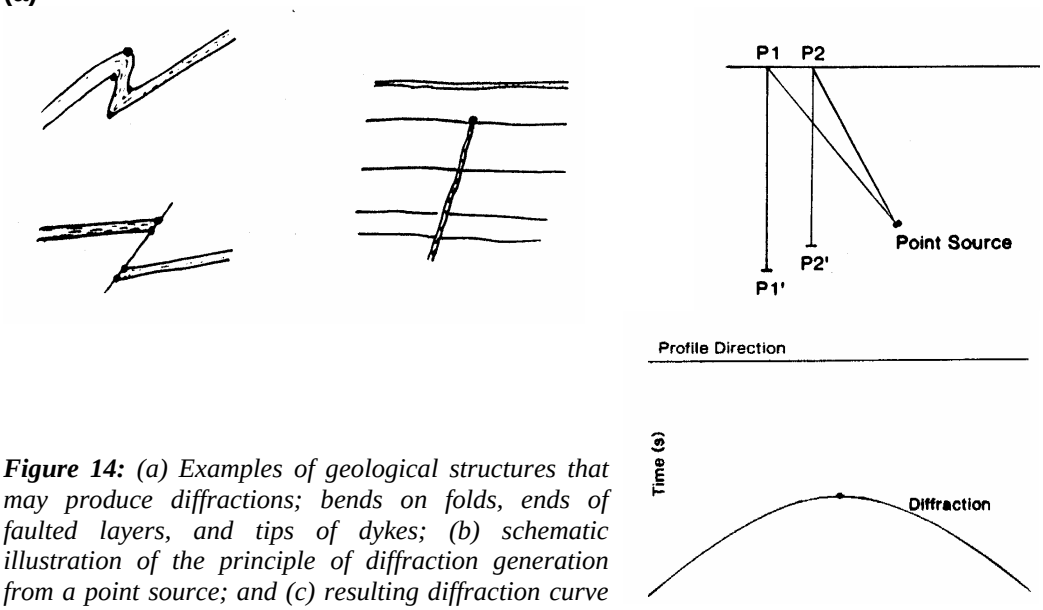

Figure 14: *(a) Examples of geological structures that may produce diffractions; bends on folds, ends of faulted layers, and tips of dykes; (b) schematic illustration of the principle of diffraction generation from a point source; and (c) resulting diffraction curve from the point source shown in (b).*

Consequently, shallowly dipping structures are imaged when the observation point is directly above, and continuous coverage will be obtained as the point moves along the line. Very steep dips near the surface can be imaged from the side. For lines of approximately 100 km length, it could reasonably be expected that dips as high as 50° in the middle crust may be seen.

A further consideration concerns the survey acquisition parameters - whether these discriminate against steep dips at any frequencies of interest. In the field, geophone arrays are used to attenuate coherent noise and random noise, by summing the individual geophone responses. A source array is also used with typically three vibrators in line with moveup between sweeps. Arrays will pass vertically travelling energy, but will discriminate against horizontally travelling energy with wavelengths shorter than the effective length of the combined source and receiver array.

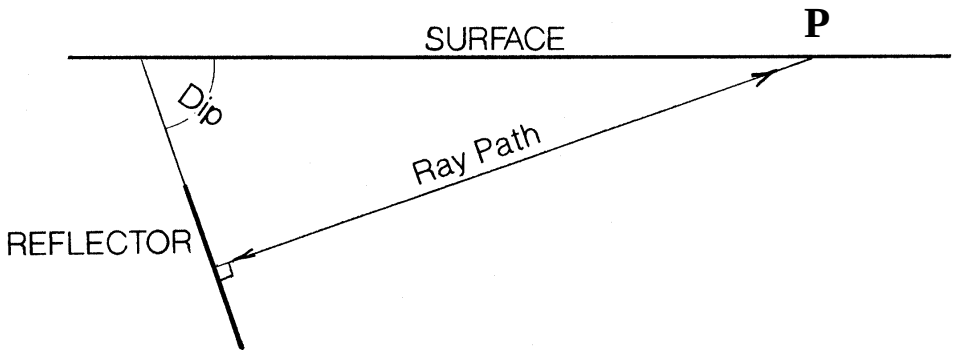

Figure 15: *The length of the seismic line and the recording time determine the maximum dip that is imaged. For steep dips, the observation point must be off to the side, and the recording time must be long for energy to travel out to and back from the reflector.*

For a ray incident at the surface at angle α (to the normal) the apparent velocity across the array is $V_a = V / \sin \alpha$ with corresponding apparent wavelength $\lambda a = \lambda / \sin \alpha$. For the ray path in Figure 15, α equals the dip angle. Thus, apparent wavelengths will range from infinite for reflections from horizontal reflectors to the true wavelength for reflectors with a dip of 90°. For frequencies from 40-100 Hz, the true wavelength λ will range from 150 m to 60 m. Thus dip filtering by the array is not likely to occur for the typical combined array effective length of approximately 60 m.

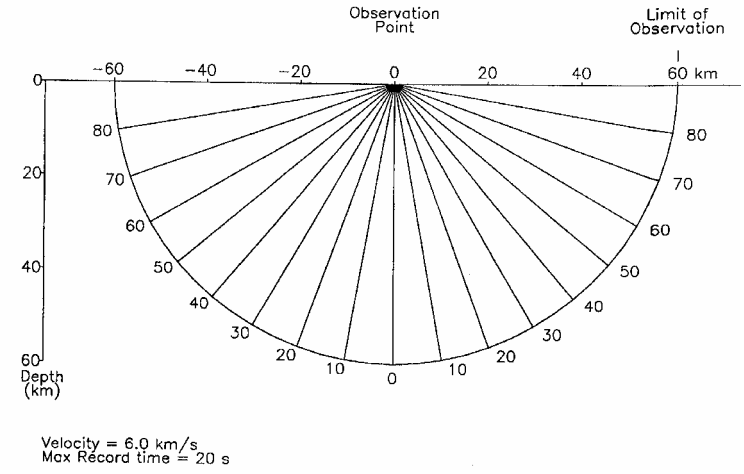

Figure 16: *Each segment shows where dipping reflectors must be located, in order to be imaged from the observation point, for the dip range annotated on the segment edges.*

A further consideration in imaging steeply dipping reflectors is that dipping reflectors require higher stacking velocities than horizontal reflectors. For example, where a horizontal reflector has a stacking velocity of 6000 m s^{-1}, a reflector in the same material dipping at 60° would stack at 12000 m s^{-1} ($V/\cos \alpha$). The difficulty of simultaneously stacking reflectors of different dips is more pronounced at shallow depth (and TWT), since normal moveout is greater. Dip moveout

(DMO) processing is required, but can be difficult to apply correctly for crooked lines where the fold may be low and the offset distribution irregular.

Migration

Migration is the process of moving reflectors to their correct positions and is essential in areas of steep dip and complicated structure. Because of the way seismic data are displayed, dipping reflectors are not correctly imaged, as shown in Figure 17. The ray paths for coincident source and receiver at points P1, P2, and P3 must be perpendicular to the reflector at the corresponding reflecting points. However, on the seismic section, these reflecting points appear to be vertically below points P1, P2, and P3. Thus the reflector segment is shifted downwards and its apparent dip, β, is less than the true dip, α, such that $\tan \beta = \sin \alpha$. Dipping reflectors, such as faults, and the flanks of synclines and anticlines, will not appear in their correct positions. Moreover, such features will appear to have lower dip as illustrated in Figure 18. A consequence of the relationship between true dip and apparent dip is that dips will never appear to be greater than 45° on an unmigrated section.

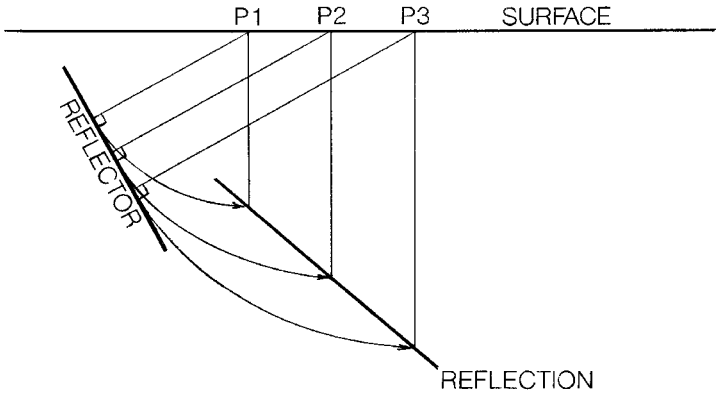

Figure 17: *On a stacked seismic section, reflecting points will appear vertically below the coincident source-receiver points on the surface. Thus dipping reflectors will appear deeper than their true position, with a lower apparent dip. The process of moving reflectors to their correct positions is known as migration.*

The effect of lack of migration is shown in Figure 19a for the southern end of line 03GA-OD1. Arcuate features and dipping events can be seen throughout, crossing one another to give a 'basket-weave' pattern. Some of these are diffractions emanating from lithological discontinuities. Dipping features appear shifted downwards from their true position, and anticlinal features appear to be broad.

Conceptually, migration is a simple procedure. In principle, the position of the reflector shown in Figure 17 just needs to be swung back through an arc equal to the true dip angle. In actual implementation, migration is a complicated process, not only because of velocity variations, but also because of out of plane energy. Because most of the migration algorithms use the wave equation, diffractions will also collapse to a point, thus improving horizontal resolution. It is important to note that 2D migration can only be carried out in the presence of dip. Thus strike lines with apparently horizontal reflectors cannot be migrated. Migration works best for seismic data with strong lateral continuity. However, in hard rock terranes, lateral continuity of reflections is often poor, making it difficult to implement migration successfully.

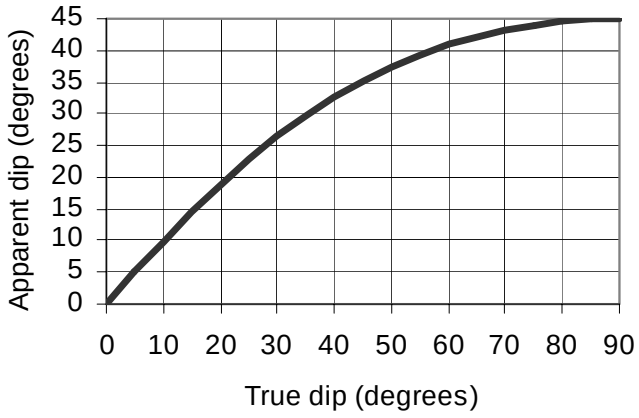

Figure 18: *Apparent dip of a dipping reflector on an unmigrated section versus true dip.*

The result of migration is shown in Figure 19b. Migration has collapsed the diffractions, cleaning up the image and leaving only reflections from continuous surfaces, which are shifted back to their correct position. Dipping parts of reflectors have moved up and become steeper and anticlines have thus become narrower in the process. More steeply dipping events have been migrated greater distances. For example, the steeply dipping reflectors on the left hand side of the section have been moved up to the left, off the end of the section. Note that care must be exercised in interpreting events on the ends of migrated lines. If events are dipping towards the end of the line, they will be moved up dip, but no more data exists to be migrated to fill in the gap.

Several criteria can be used to decide whether the sections are under-migrated or over-migrated. Since migration moves reflectors upwards and steepens them, the termination of reflectors against another surface can be used as a guide to the correctness of migration (see also Figure 21). On under-migrated sections, the diffractions still look like diffractions, whereas on over-migrated sections, the diffractions turn into 'smiles'. Figure 20 shows a diffraction hyperbola in the vicinity of Olympic Dam which is collapsed by migration. If this diffraction is associated with the ore body, then in this case it would be useful to interpret both the stack and migrated sections.

EXAMPLES OF FEATURES IMAGED IN THE GAWLER CRATON

In the Gawler Craton, the seismic reflection survey was able to image features with a range of dips, including shallow to moderately dipping lithology and moderately dipping thrusts and faults. In places, the presence of steeply dipping surfaces could be inferred from the progressive upturn of more shallowly dipping surfaces.

Dipping features

The migrated seismic section for line 03GA-OD1 is characterised by prominent, northerly dipping features at the southern end of the line (see Figure 19). These are among the steepest features imaged on the line, but are still of moderate dip. More steeply dipping features on the extreme edge of the line migrate off the end of the section and cannot be interpreted.

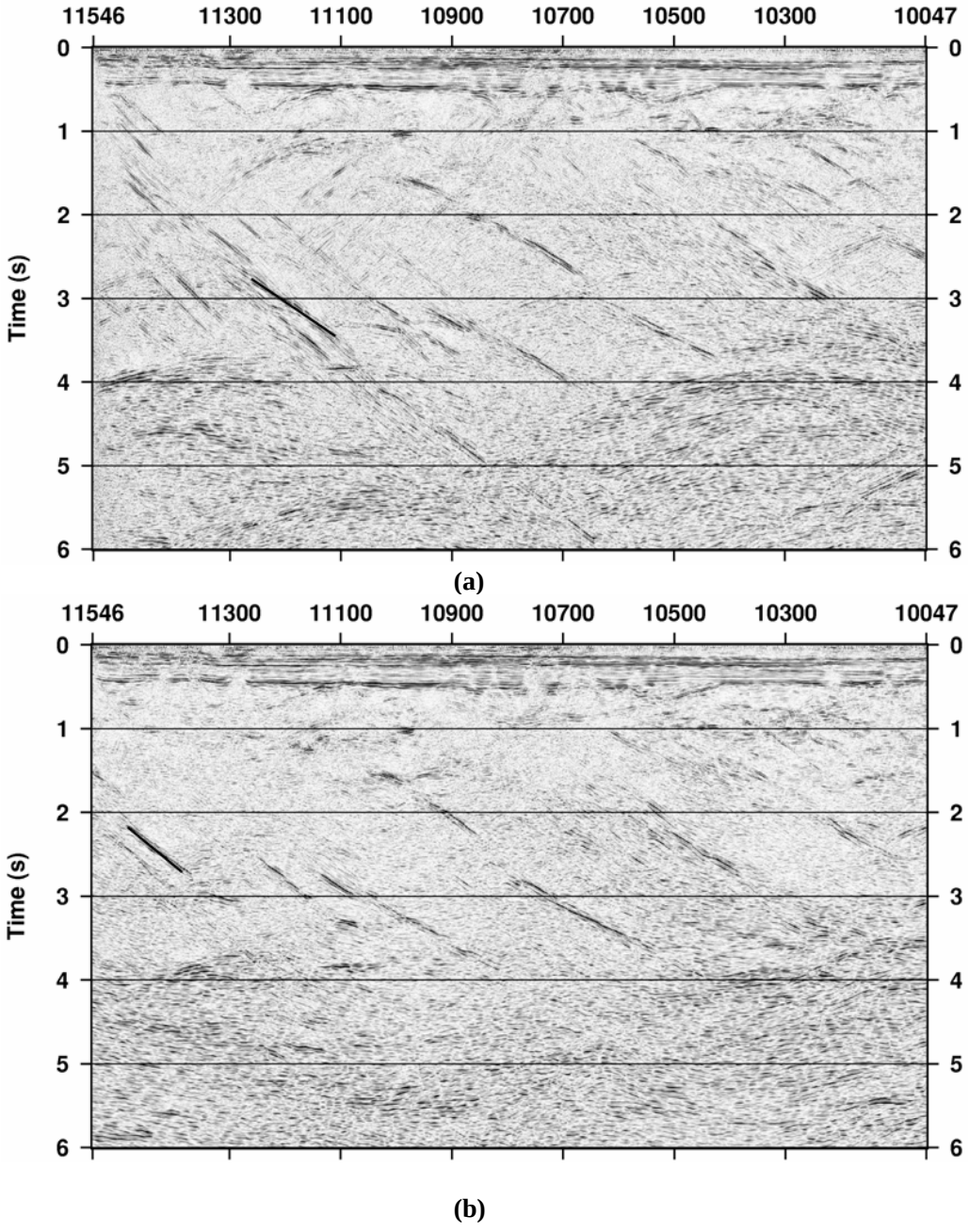

Figure 19: *Seismic sections for line 03GA-OD1 from CDP 10047 to 11546 and 0-6 s TWT. V/H ~ 1. 100 CDP = 2 km. 1 s = 3 km. (a) Final stack. (b) Migrated section. The black line shows the position of a single dipping reflector before and after migration.*

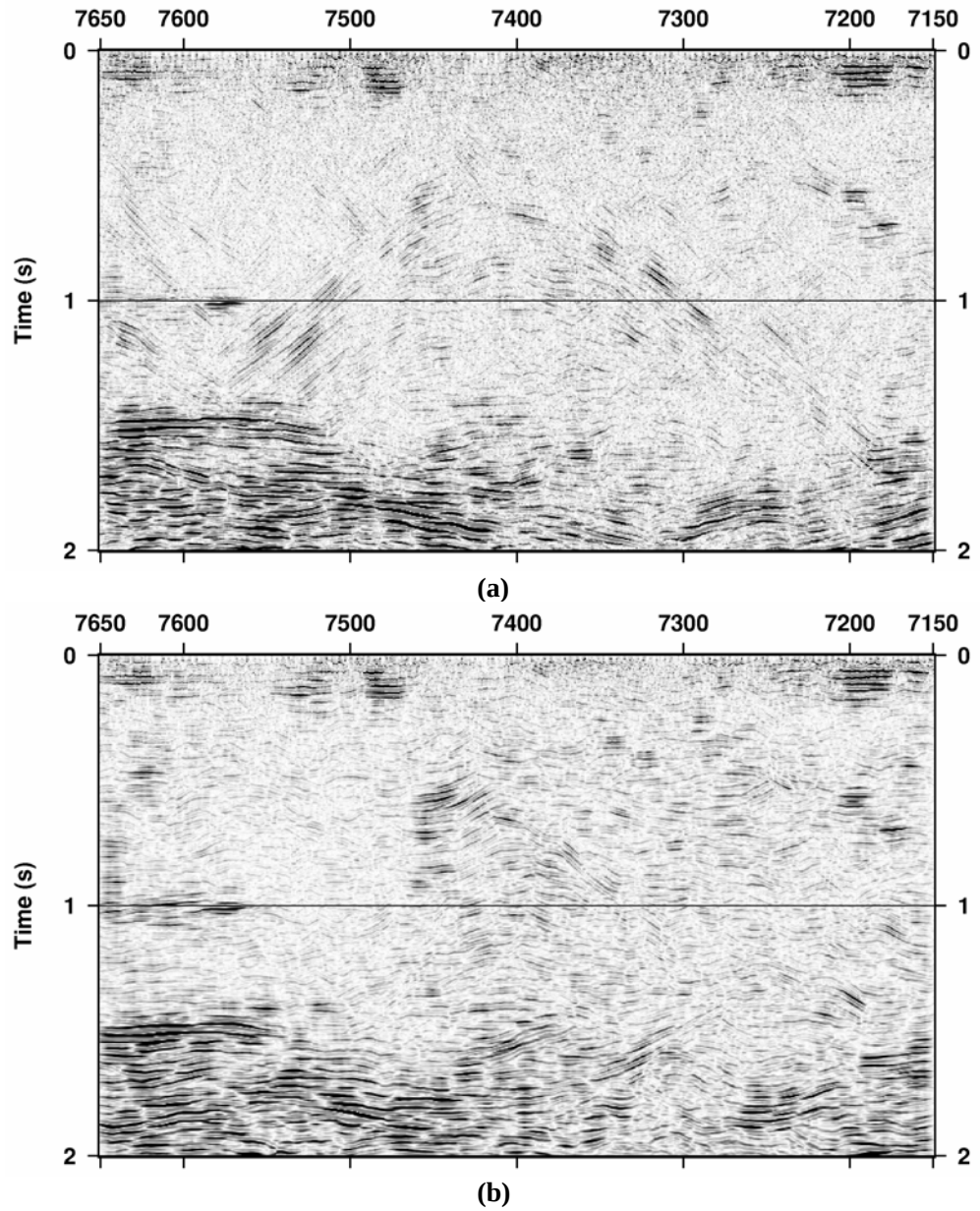

Figure 20: *Seismic sections for line 03GA-OD1 in the vicinity of Olympic Dam from CDP 7150 to 7650 and 0-6 s TWT. V/H ~ 1. 100 CDP = 2 km. 1 s = 3 km. (a) Final stack. (b) Migrated section.*

An issue still to be resolved is whether steep near-surface reflectors of limited extent can be satisfactorily imaged, in view of the vertical and horizontal resolution obtainable. Horizontal resolution would be no better than 250 m on an un-migrated section, even at the highest frequencies, for steeply-dipping shallow features. Thus small scale folding will not be seen, but enveloping surfaces may be imaged. In some cases, steep dips may be inferred from a progressive up-turning of layers before entering a reflection-free zone, as can be seen in Figure 21. Resolving these issues needs further research, using seismic modelling and pre-stack migration.

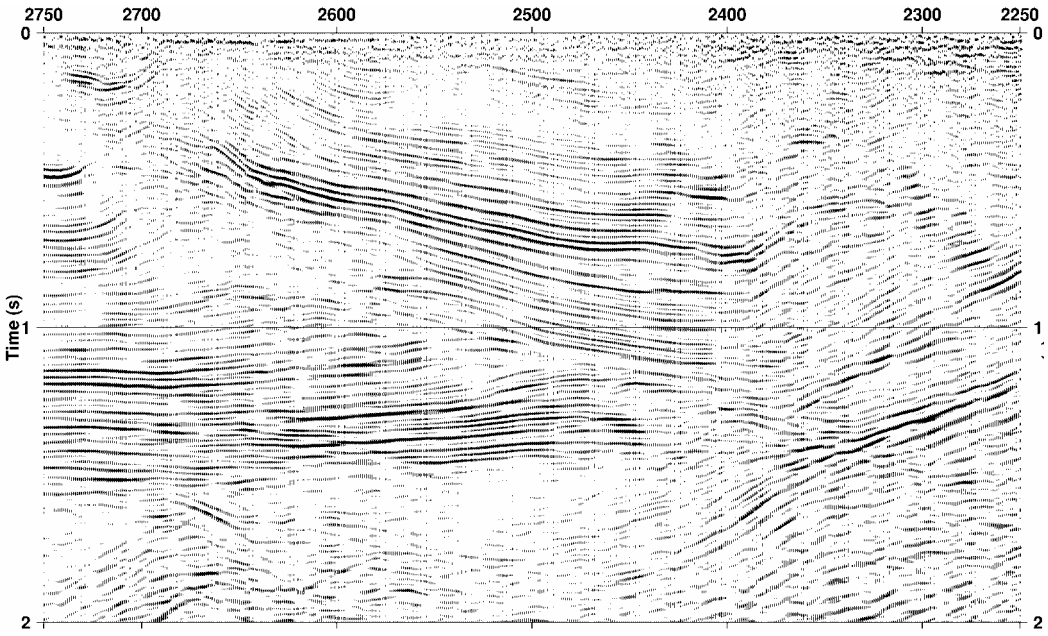

Figure 21: *Migrated seismic section at the northern end of line 03GA-OD1 from CDP 2250 to 2750 and 0-2 s TWT. V/H ~ 1. 100 CDP = 2 km. 1 s = 3 km.*

Faults and dykes

Faults can be recognised by the way they disrupt layering, with similar criteria to those used for identifying faults in sedimentary basins. These include offset of layers, abrupt change in reflection character or layer thickness, change in dip and the presence of diffractions from truncated layers. Note that vertical faults can be identified in this way, because the fault is imaged by its effects and not by reflections from it. Similarly disruption of bedding and a lack of reflectivity can indicate the possible presence of vertical dykes, as can be seen in several places in Figure 19 at approximately 0.5 s TWT.

Figure 21 illustrates a thrust surface which can be identified by the truncation of layers above and below, the change in the dip of the strata and by the occurrence of anticlinal structures in the hanging wall. Note also that after migration, the reflectors correctly truncate against the thrust surface.

SUMMARY

The seismic reflection method was originally designed for use in sedimentary basins where the sub-horizontal and continuous layers correspond to primary bedding. Reflections are generated by acoustic impedance contrasts at the boundaries between layers. In hard rock areas, too, reflections are indisputably produced at boundaries between rocks with different densities (and hence velocities). These boundaries may follow bedding, or be fault surfaces and shear zones.

Some of the key differences between hard rock terranes and soft rock are steep dips associated with folds and faults, and high velocities. High velocities affect resolution, since both vertical and horizontal resolution depends on the seismic wavelength. Compared with sedimentary basins, vertical resolution is probably only half as good, with the situation being slightly more favourable

for horizontal resolution. The high velocities make it easier to stack reflections since there is less move-out, but more difficult to use the stacking velocity analysis to determine accurate velocities for depth conversion and migration.

Steep dips can affect the ability to image successfully. The seismic line must be long enough to encompass both steeply-dipping reflectors and the seismic acquisition system. Recording times must also be long enough for energy to travel to and from steeply dipping reflectors. Migration is essential in areas of complicated structure in order to move dipping reflectors to their correct positions and to collapse diffractions emanating from discontinuities in the layers. Unless migration is carried out, dips on the seismic section will never appear greater than 45°.

Examples from the 2003 Gawler seismic survey show that shallow to moderate dips are routinely imaged, with more steeply dipping faults inferred from discontinuities. The migrated sections provide a spectacular set of images that underpin interpretations of the geological structure of the eastern Gawler Craton.

SEISMIC ACQUISITION AND PROCESSING – 2003 GAWLER CRATON SEISMIC REFLECTION SURVEY (L163)

L.E.A. Jones[1], D. W. Johnstone[1] and B.R. Goleby[1]

[1] Australian National Seismic Imaging Resource, Geoscience Australia, GPO Box 378, Canberra ACT 2601, Australia

INTRODUCTION

The 2003 Gawler Craton Seismic Survey (L163), consisting of 2 lines 03GA-OD1 and 03GA-OD2, was conducted in July/August 2003 for Geoscience Australia in conjunction with the Department of Primary Industries and Resources South Australia (PIRSA). The Australian National Seismic Imaging Resource (ANSIR) was responsible for seismic data acquisition, as well as for field QC and preliminary in-field processing.

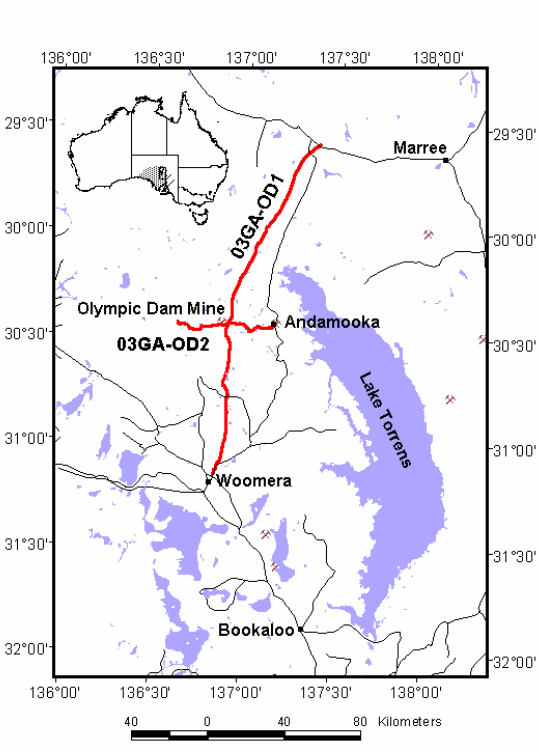

Figure 22: *Location of 2003 Gawler seismic lines in the eastern Gawler Craton, South Australia. Salt lakes shown in blue. Inset shows Gawler Craton position within Australia.*

The 193 km line 03GA-OD1 started approximately 120 km north of Roxby Downs and stopped just short of Woomera (Figure 22). The shorter 57 km line 03GA-OD2 ran from west to east just south of the Olympic Dam mine site.

ACQUISITION

The seismic reflection data were acquired along the edge of roads. Station coordinates were surveyed using differential GPS by Dynamic Satellite Surveys (2003). A split-spread geometry was used with the source nominally at the centre of the spread. Receiver groups were centred between station pegs, while the source array was centred on the peg.

Three IVI Hemi-60 (60,000 lb) vibrators were used in-line, with moveup between each of three varisweeps. Sweep parameters were chosen from experiments conducted at the beginning of the survey. An ARAM 24-bit 240 channel recording system was used to record and correlate the seismic data.

A summary of acquisition parameters is

given in Table 3 and in Appendix 1. Further details are provided in the Operations Report (Trace Energy Services, 2003).

Table 3: Summary of acquisition parameters for lines 03GA-OD1 and 03GA-OD2

LINE	03GA-OD1	03GA-OD2
AREA	Roxby Downs – Olympic Dam (SA)	Roxby Downs – Olympic Dam (SA)
DIRECTION	N to S	W to E
LENGTH	193.36 km	57.44 km
STATIONS	1000 – 5834	1000 – 2436
CDP RANGE	2000 – 11546	2001 – 4658
GROUP INTERVAL	40 m	40 m
GROUP PATTERN	12 in-line @ 3.33 m	12 in-line @ 3.33 m
# VIBRATION POINTS	2446	718
VP INTERVAL	80 m	80 m
SOURCE TYPE	3 x IVI Hemi-60	3 x IVI Hemi-60
SWEEP TYPE	3 x 12 s: 7-56, 12-80, & 8-72 Hz	3 x 12 s: 7-56, 12-80, & 8-72 Hz
SOURCE PAD-PAD	15 m	15 m
SOURCE MOVE-UP	15 m	15 m
# CHANNELS	240 (<240 on roll off)	240 (351 on roll off)
FOLD (NOMINAL)	60	60
RECORD LENGTH	18 s @ 2 ms	18 s @ 2 ms

PROCESSING

Production processing utilised the Disco software package, while the interactive version Focus was used for parameter tests, first break picking and QC. Table 4 shows the final processing flow, including migration, for the 6 s data for line 03GA-OD1. For adequate resolution, only 4 ms sampling was required. The 18 s processing stream was similar, except that dip moveout correction (DMO) was not applied pre-stack and a run mix equivalent to combining two CDP gathers was used pre-migration.

The processing flow was designed with the aim of enhancing reflections, while avoiding processes that could potentially degrade data, particularly in the shallow section. Parameter testing was done on shot records, CDP gathers or stack panels for the processing modules that were used. The key processing steps are discussed in the following sections, with particular emphasis on those that resulted in the most improvement in data quality.

Crooked line definition and CMP/CDP sort

The geometry for each line (i.e., receiver and shot locations) was entered into an internal seismic database prior to actual seismic data processing. Since the receiver groups were centred between the surveyed stations, the receiver station coordinates for processing were defined to be half-way between surveyed stations (i.e. station 1000 for processing is located at 1000.5 as surveyed).

CDP (common-depth-point) locations were also defined. Ideally, for a horizontal reflector, the midpoint between a source and receiver pair lies vertically above the depth point (or reflecting point) for that pair, so that the CDP location is the same as the common midpoint (CMP) location. For dipping reflectors, this correspondence no longer holds, but the CDP terminology is so entrenched in seismic processing that it is used in place of the more correct term “common midpoint”. Note that the midpoint spacing along a straight line is half the receiver group interval.

Table 4: Final processing flow for 6 s data for line 03GA-OD1

[1]	line geometry and crooked line definition (fixed CDP interval)
[2]	field segy to 'disco' data format; resample to 8 s at 4 ms
[3]	quality control displays and trace edits
[4]	spectral equalization (with 1000 ms gate AGC)
[5]	common mid point sort (bin wide open)
[6]	gain recovery (spherical divergence option)
[7]	application of refraction statics, datum 0 m (AHD)
[8]	application of automatic residual statics
[9]	bandpass filter
[10]	stacking velocity analysis using velex, 1st pass after refraction statics, 2nd pass after automatic residual statics, 3rd pass after DMO correction
[11]	normal moveout correction
[12]	stretch mute used as front end mute
[13]	dip moveout correction (DMO)
[14]	common mid-point stack
[15]	trace amplitude balance
[16]	f-x migration with migration velocities
[17]	signal enhancement (digistack 0.8)
[18]	run mix, trace amplitude scaling and resample to 6 s for display

Crooked line processing was used for both 03GA-OD1 and 03GA-OD2, and was essential for the latter due to bends in the existing roads. In the crooked line case, the midpoints do not always lie along the line defined by the surveyed stations. The CDP line is defined as a smoother representation that follows the highest density of midpoints, while keeping as close as possible to the original line (Figure 23). Note that the CDP bins extend perpendicular to the CDP line as shown in Figure 23. For both lines, the CDP line was defined with a constant CDP interval of 20 m. Since the CDP line is shorter than the line of stations, the CDP number will be less than twice the station number.

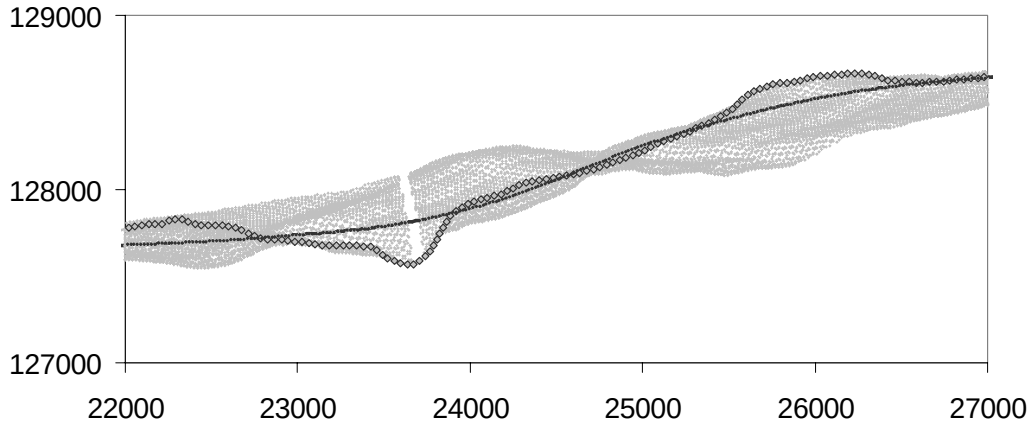

Figure 23: *Crooked line geometry, with X and Y coordinates in m. A series of triangles indicates the surveyed station line, with the smoother CDP line in black. Shaded area shows midpoints. Unshaded strip perpendicular to the CDP line is a diagrammatic representation of a CDP bin, showing location of midpoints assigned to a particular CDP. (Actual bins 20 m wide).*

The CDP line was calculated automatically as a least-squares fit to the shot-receiver midpoints, with an inclusion radius of 600 m. To ensure that the CDP line kept close to the original line of stations, a dummy line with a shorter spread length (half the actual) was used for the calculations. Typically the CDP line lay within 250 m of the surveyed line for 03GA-OD1 and 300 m for 03GA-OD2. The final choice of CDP line was confirmed by assessing the distribution of midpoints into CDP bins and examining the quality of the brute stack.

During processing, a seismic trace was assigned a CDP number according to the CDP bin in which its midpoint was located. A common midpoint (or CDP) sort gathered the data into ensembles of traces with the same CDP. The term fold is used for the number of traces in this CDP gather. These traces would later be stacked (added together) after correction for travel time differences for different source-receiver offsets. The stacked seismic data was displayed as a section along the CDP line, the annotated stations being merely those closest to the CDP locations. The CDP line should be used for geological interpretation, not the original line of surveyed stations.

Edits

During seismic data acquisition, problems occurred, such as void shot records and occasional recording equipment malfunctions. Affected traces were removed by manual edits of whole records or individual traces. In addition, the two shortest offset traces were omitted during processing, due to near source noise contamination.

Random noise trains also occurred, mainly due to crew vehicle movement along the line and other traffic. An automatic edit was designed to zero such traces, based on anomalously high amplitudes prior to the first arrival of seismic energy. This was used successfully to eliminate noisy traces from the automatic first break picking routine. However, a judgement was made not to use automatic editing of vehicle noise in the final processing flow because the noise trains are not vertical and at later times good data would be removed instead of noise. Other processes such as spectral equalisation and high fold stack would be more effective.

Refraction statics and datums

Statics corrections are needed to remove variability in seismic travel times due to variations in surface topography and regolith thickness and velocity. The travel times of refracted waves, recorded as the first arrivals in seismic reflection data, are analysed to obtain a model of the main refracting interface, that is, the boundary between low velocity and high velocity material, usually the regolith/bedrock boundary. The first breaks (first arrivals) were picked on 2 s subsets of the original 2 ms shot records, using a combination of manual and supervised automatic picking. Apart from amplitude balance and automatic edits, no pre-processing was done. The first strong peak was interpreted as the first arrival, since the correlated traces should be zero phase.

The method of Taner et al. (1998) was used to separate the refraction statics into a long wavelength component due to gradual change in surface and refractor topography and a short wavelength component attributed to more rapid near surface variations in seismic velocity. The smoothing radius chosen to separate the statics was 160 m (4 times the receiver group interval). A one-refractor model was used, since with a group interval of 40 m, there were too few picks to robustly define an additional near surface layer in areas of thinner regolith. Geological variability along the line made it difficult to adequately define the seismic velocity in the regolith which was taken as a nominal constant value for calculation of the long wavelength statics.

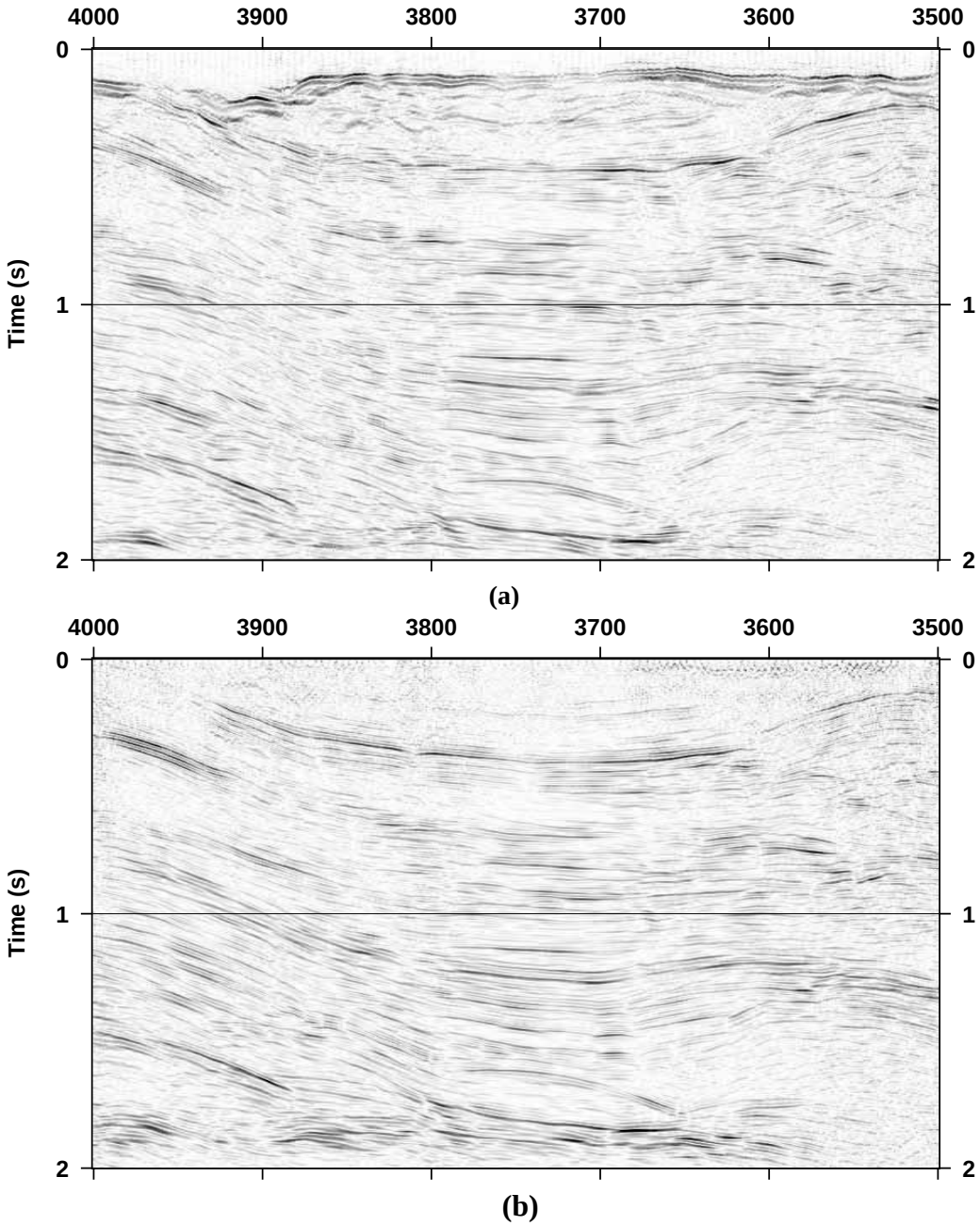

Figure 24: *Stacked seismic section for line 03GA-OD1 for CDP 3500 to 4000 and 0 to 2 s Two Way Time (TWT). (a) Stack with no statics. (b) Stack with refraction statics.*

Refraction statics are calculated by subtracting the vertical travel time calculated for the lower velocity regolith, and adding the vertical travel time calculated from datum to bedrock at a higher replacement velocity. A datum of 0 m and replacement velocity of 5000 m s^{-1} were used. Thus 0 s on the processed seismic data corresponds to the 0 m datum. Generally the one-way static value ranged from -75 ms to -10 ms for line 03GA-OD1 and from -60 ms to -15 ms for line 03GA-OD2.

The necessity for statics corrections is shown in Figure 24 for a stacked seismic section through the thick Adelaidean sequence. Figure 24(a) shows a section with no statics applied Processing

parameters such as stacking velocity were determined without statics. Poor continuity and low amplitudes result from the misalignment of reflections due to variable time delays in the regolith, which can be seen at the top of the section.

Figure 24(b) shows the same data after application of refraction statics, using stacking velocities determined after refraction statics. The section is shifted upwards to the 0 m datum. Statics corrections also result in much better definition of reflectors, particularly in the shallow section.

Spectral equalisation

Spectral equalisation is a key processing step which minimises contamination by low-frequency source-generated noise, such as ground roll and direct waves, plus random noise such as traffic noise. This step is particularly critical at shallow depths where the fold is lower and where source generated noise interferes with reflections. Spectral equalisation employs a zero-phase deconvolution operator to perform spectrum balancing or whitening across the range of signal bandwidth, as shown in Figure 25.

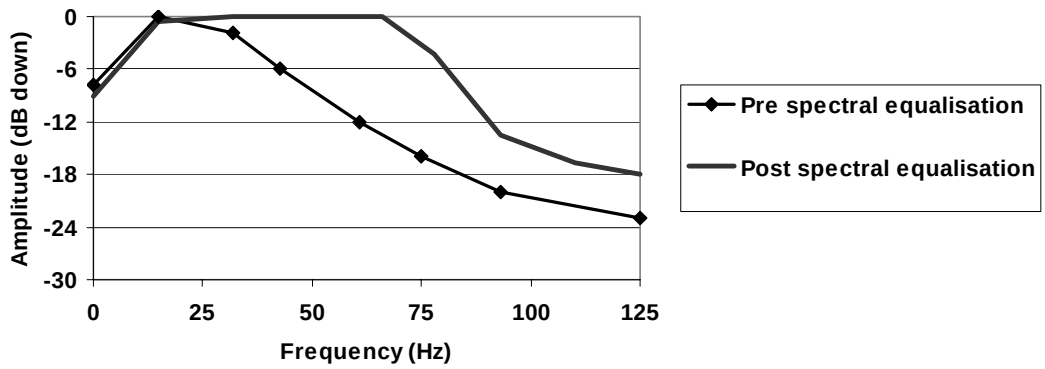

Figure 25: *Frequency spectrum for shot 2149 on line 03GA-OD1 from 0 to 2 s, prior to and after spectral equalisation.*

The spectrum balancing is carried out using a number of user designed frequency gates. The final spectral equalisation parameters consisted of overlapping gates of the form (8-12-16-20) Hz, with 5 subsequent repeats (outer gate values are 50% and inner gate values 100% amplitude).

The record for shot 2149 on line 03GA-OD1 is a typical example of a raw shot record (Figure 26a). Linear dipping bands of coherent low-frequency source-generated noise mask shallow reflections, although there are hints of reflection hyperbolas between 0 and 1 s TWT (two-way time). The corresponding spectrum (Figure 25) is dominated by energy in the range 20-25 Hz. Application of spectral equalisation successfully enhances the high frequencies relative to the lower frequencies (Figure 25). On the processed shot record (Figure 26b); several reflection hyperbolas are now visible above 1 s, even above 0.5 s. The several offset hyperbolas, indicative of dipping reflectors, are now very obvious, between approximately 1 and 1.5 s.

The same reflection events can be seen in the middle of the sections in Figure 27, demonstrating the effect of spectral equalisation on stack data. All other processing is identical. Spectral equalisation suppresses low frequency noise that would survive the stacking process and results in much better vertical resolution and continuity of shallow reflections.

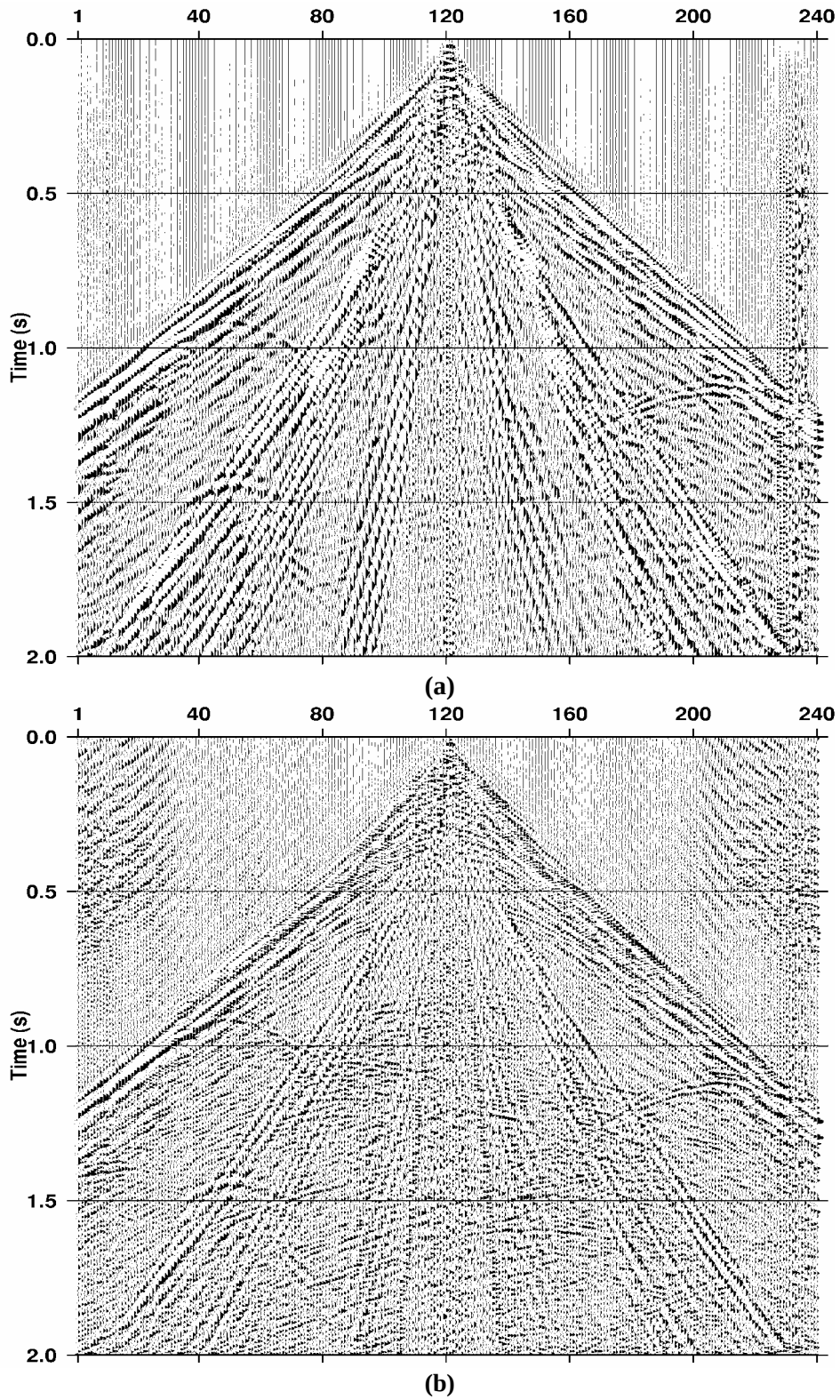

Figure 26: *Record for shot 2149 on line 03GA-OD1 displayed from 0 to 2 s. An AGC has been applied for display purposes. (a) Shot record with no spectral equalisation. (b) Shot record with spectral equalisation.*

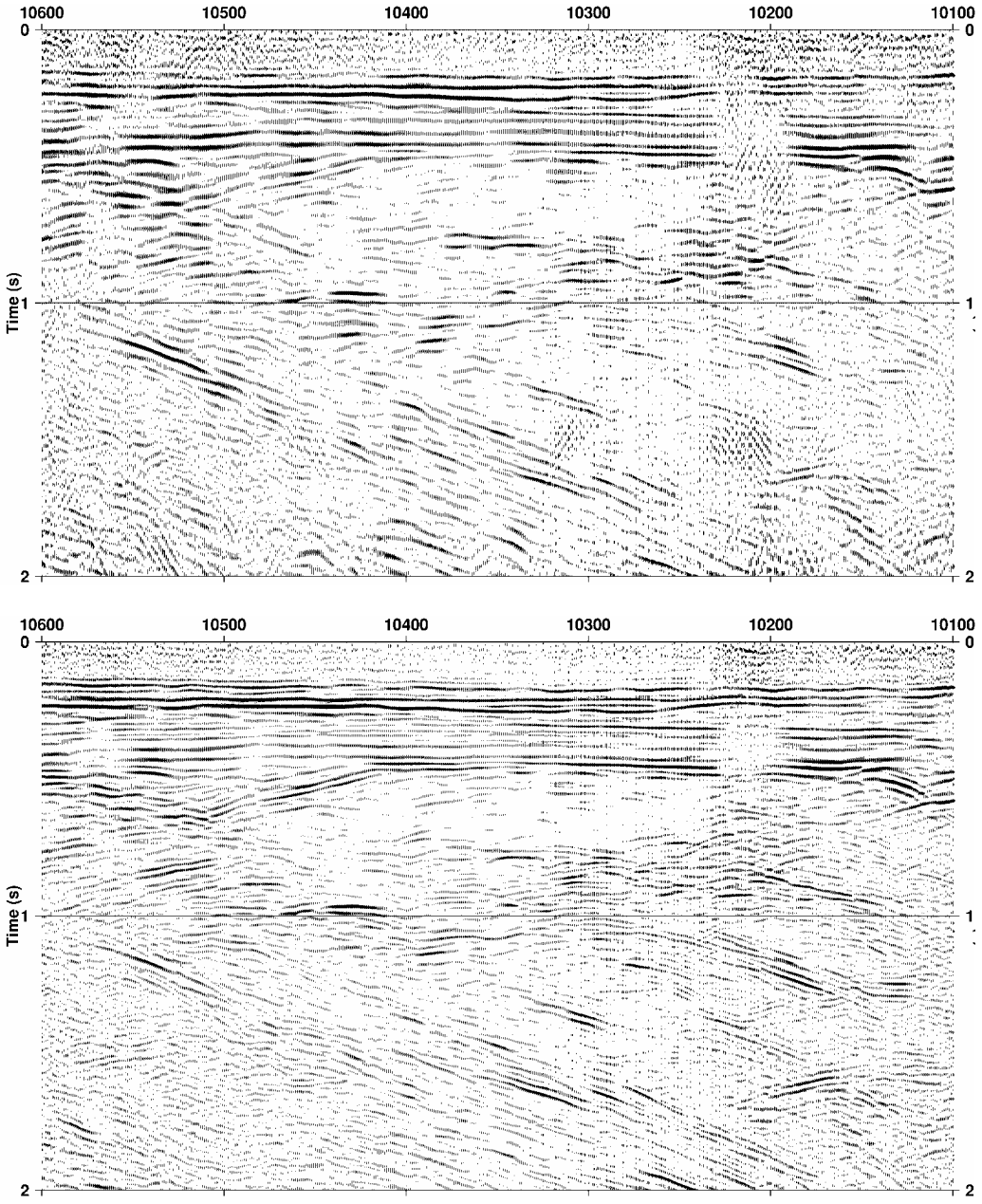

Figure 27: *Stack for line 03GA-OD1 from CDP 10100 to 10600 and 0 to 2 s TWT at V/H=1. (a) Stack with no spectral equalisation. (b) Stack with spectral equalisation applied. Shot 2149 (shown in Figure 26) is located at approximately CDP 10370.*

In practice, even worse results would be obtained without spectral equalisation, because spectral equalisation was used prior to fine tuning parameters such as automatic statics and stacking velocity, which depend on stack quality for evaluation.

Stacking velocity analysis and dip moveout correction

Another critical processing step is the correction of seismic data for the offset dependence of travel time, the normal moveout (NMO) correction, which depends (inversely) on seismic velocity and two-way travel time. With the appropriate choice of velocity for NMO correction, a

reflection event will add constructively when the traces of a common-midpoint gather are stacked. In the shallow section (less than 1 to 2 s TWT), the quality of the stack is quite sensitive to changes in the stacking velocity, but becomes progressively less so for the deeper data. For example, for a reflection event at 750 ms TWT with stacking velocity 5900 m s^{-1}, varying the velocity by ± 200 m s^{-1} results in an obvious degradation of the stack.

Dipping reflectors cause additional complications, particularly in the shallow section. For the traces in a CDP gather, the reflecting point moves up dip with increasing offset, thereby reducing the travel time at larger offsets and resulting in an apparent higher moveout velocity. Thus horizontal and dipping events will not stack with the same stacking velocity, unless the dip effect is corrected. Dip moveout (DMO) correction is a partial pre-stack migration process applied to the data after NMO correction.

Stacking velocity analysis was carried out using a velocity estimation and plotting module that applied a series of normal moveout corrections to designated CDP gathers according to user specified velocity functions. Velocity picks for reflections were made on the basis of maxima in coherency, flattening across the CDP gather and the quality of narrow stack panels. Several passes were made, including initial estimates of velocity, plus more detailed analysis after application of refraction statics and again after application of automatic residual statics. A further analysis was carried out after DMO (dip moveout correction) was applied. For the last two passes, velocity analyses were made on average every 4 km.

The dip corrected stacking velocities are shown in Figure 28. Below 2 s TWT, control on stacking velocity is poor, but in the shallow section velocities are indicative of the different reflector packages. For example, the sedimentary sequences towards the north have higher stacking velocities (generally >5000 m s^{-1}) than those towards the south, even though both are characteristic of well indurated sedimentary rocks. In the vicinity of Olympic Dam (~CDP 7400), stacking velocities are higher, indicating the lack of thick sedimentary cover over the granite.

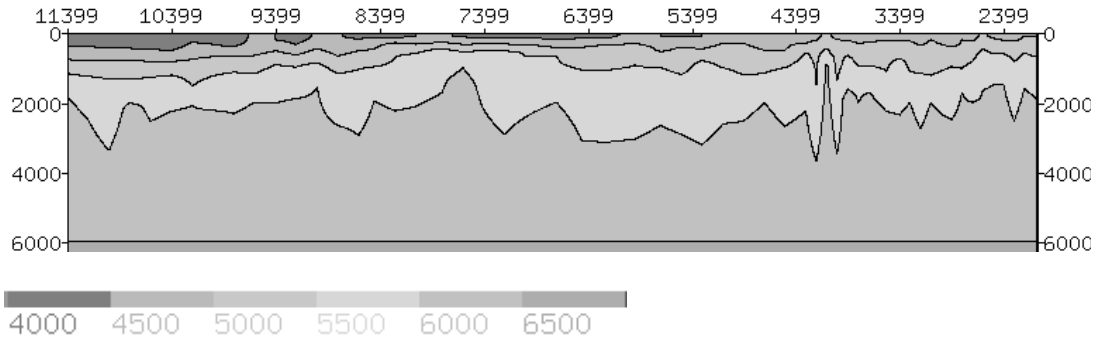

Figure 28: *Dip-corrected stacking velocities for line 03GA-OD1. Display is from 0 to 6 s. Contours are every 500 m s-1from 4000 to 6500 m* s^{-1}*. N is on the right.*

Stack and stretch mute

A stretch mute was used instead of a specific front end mute, as it satisfactorily removed most of the first arrival energy train from the stack, as well as zeroing those parts of traces distorted by the NMO correction process. The stretch mute is velocity dependent and is more severe for lower

stacking velocities. A spatially invariant high velocity function with a maximum stretch of 20% was used to avoid eliminating reflection data along with the first arrivals.

Stacking seismic traces after NMO correction improves the signal to random noise ratio by √n, where n is the fold.

Automatic residual statics

Automatic residual statics were calculated in order to fine-tune the stack. This process operates on unstacked CDP gathers with normal moveout and refraction statics applied and calculates the additional time shifts (residual statics) necessary to maximise correlation across the gather in a selected time gate, such that shot and receiver surface consistency is maintained. An iterative technique is used to apply the static before the next calculation, with the number of iterations specified by the user.

A single broad gate was used for the entire length of line 03GA-OD1. It was chosen from 0.25 s to 4.5 s TWT to include all the zones of good reflector strength and continuity. For line 03GA-OD2 the gate encompassed the good reflectivity between 1 s and 5 s. A maximum time shift of 10 ms was allowed, being half the period of a 50 Hz wavelet. Automatic residual statics generally lay within ± 5 ms for both lines.

The effect of automatic statics on the stack is shown in Figure 8, again in the thick sedimentary sequence shown in Figure 24. There is a very marked improvement compared with using refraction statics only.

Migration

On an unmigrated final stack section with V/H=1, the apparent dip of reflectors will not exceed 45°. Migration is the process of moving the recorded reflections into their true spatial locations. Thus dipping reflectors will be steepened, shortened and moved up dip. Diffractions from discontinuities, such as reflector terminations at faults, are collapsed in the process.

An f-x migration algorithm (using finite difference approximation to the wave equation) was used because it allows a spatially varying velocity function and gives the user the capacity to handle steep dips. A layer thickness of 32 ms TWT was used for migration with the dip option for handling dips up to 70°. In order to prevent migration artefacts, the 18 s data was padded with zeroes to 20 s and a bottom mute applied below 17.5 s.

A reference migration velocity model was constructed with the dip moveout (DMO) corrected stacking velocities as an initial model, with some of the anomalous velocity functions omitted. Then the velocity values were manually adjusted in the top 2 s, so that interval velocities did not exceed 6000 ± 200 m s^{-1}, resulting in more smoothly varying interval velocities along the line. The deep crustal interval velocities were constrained by the Shackleford and Sutton (1981) model (V_{int}= 5900 m s^{-1} between 2 s and 6 s TWT, V_{int}=6450 m s^{-1} between 6 s and 13 s TWT and V_{int}=8000 m s^{-1} below 13 s TWT). Finally, migration tests were carried out with different velocity models scaled at different percentages of the reference migration velocity model. Final migration velocities were 90% of the reference model.

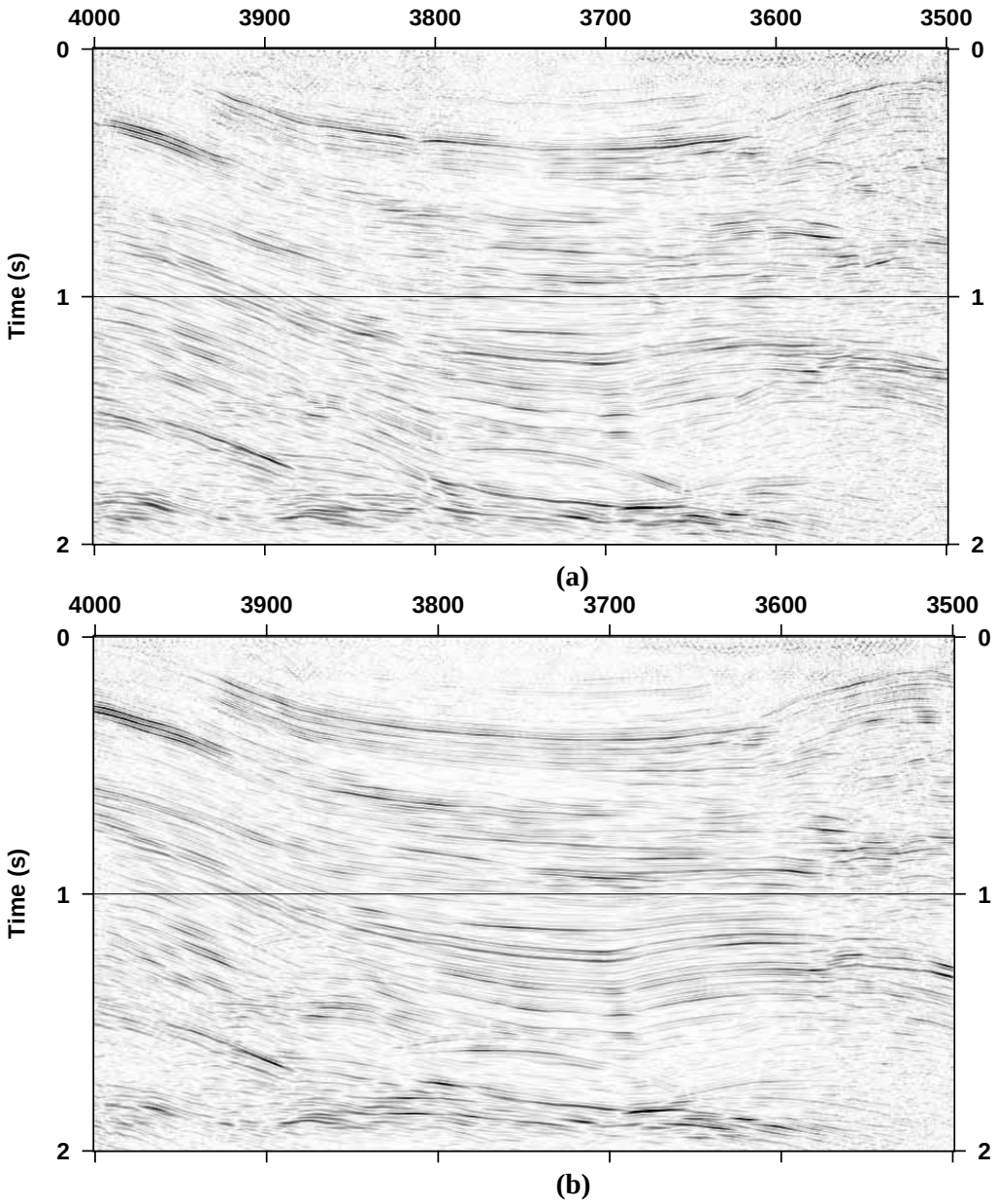

Figure 29: *Stack for line 03GA-OD1 from CDP 3500 to 4000 and 0 to 2 s TWT at V/H=1. (a) Stack with refraction statics only. (b) Stack with both refraction and automatic statics.*

Migrated sections (hard copy and digital) are the end product of the processing stream. The successful application of migration is attributed to the continuity of reflectors resulting from earlier stages of processing and the detailed velocity analysis. Figure 30 shows the results of migration in the thick deformed sedimentary sequence at the northern end of the line. Migration tightens the anticline and sharpens the image of the faults.

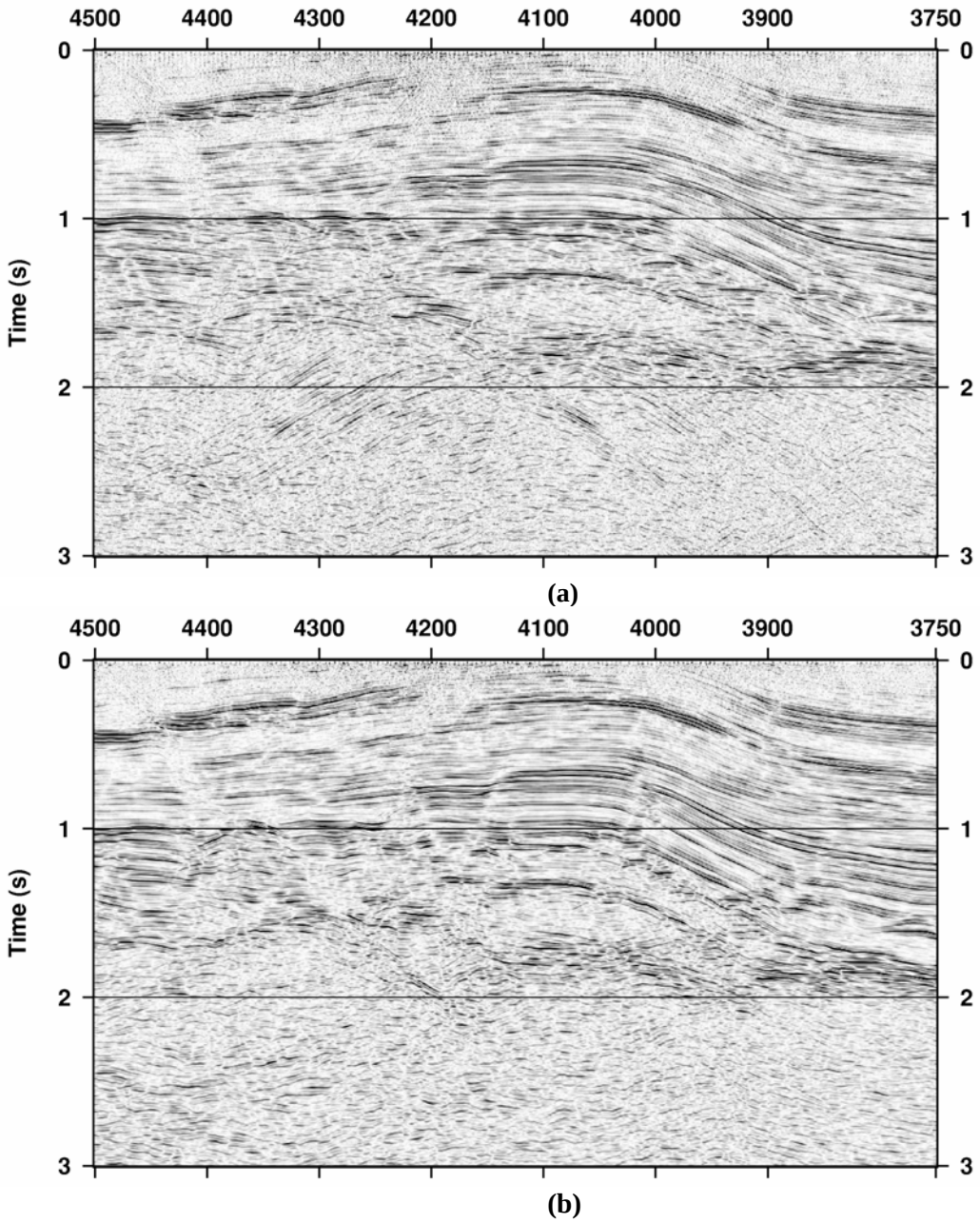

Figure 30: *Line 03GA-OD1 from CDP 3750 to 4500 and 0 to 3 s TWT at V/H~1. (a) DMO stack. (b) f-x migration of DMO stack.*

Coherency enhancement

A signal enhancement algorithm (digistack) was applied for final display only to the stacked or migrated data. Digistack enhances events that are coherent across several traces, thus making reflections stand out better against background noise.

This process determines the coherency of linear events for all dips within a specified range and outputs a second set of seismic traces that is essentially a coherency section. A weighted sum is

then made of the coherency section and the actual seismic section, such that a weight of zero reproduces the input seismic data and a weight of one gives the coherency section. For final display, weights of 0.8 or 0.85 were used. For the stack data, dips up to 50° were enhanced, while for the migrated data the range was extended to 70°.

Display parameters

Trace amplitude scaling was applied using an AGC where the scale factor was calculated with either 25 or 50% contribution from amplitude in the gate and 75 or 50% from the whole trace amplitude. A gate length of 1000 ms was used. For the 18 s data, the lower value of 25% was used in order to preserve some amplitude standout to delineate the Moho. In addition a running mix of two traces was used for display for the 6 s data.

The digital versions of the data in SEG-Y format have had coherency enhancement and trace amplitude scaling applied.

CONCLUSION

A total of 250 km of 60-fold seismic reflection data was acquired to 18 s TWT along two intersecting lines in the eastern Gawler Craton, using three 60,000 lb peak force vibrators. Key processing steps included calculation of refraction and automatic residual statics, spectral equalisation, stacking velocity analysis, DMO and migration. The resulting seismic sections successfully image the crust from the base of regolith to the Moho, facilitating detailed interpretation of geological structure.

REFERENCES

Dynamic Satellite Surveys, 2003. Final Operations Report on the 2003 Gawler Seismic Survey for Trace Energy Services Pty, Ltd and Geoscience Australia, July/August 2003. *DSS Report* **DSS03034(a)**

Shackleford, P. R. J. and Sutton, D. J., 1981. A first interpretation of structure in the Adelaide Geosyncline in South Australia using quarry blasts. *Journal of the Geological Society of Australia*, **28**, 491-500.

Taner, M. T., Wagner, D.E., Baysal, E. and Lee, L., 1998. A unified method for 2-D and 3-D refraction statics. *Geophysics*, **63**, 260-274.

Trace Energy Services, 2003. 2003 Gawler Seismic Survey – Field Acquisition & Operations Report. *Geoscience Australia, Record*, **2003/27**

GENERAL BASEMENT INTERPRETATION (18 s DATA)

B.R. Goleby[1], P. Lyons[1], B.J. Drummond[1], M. Schwarz[2], A.J. Shearer[2], M.C. Fairclough[2], R.J. Korsch[1] and R.G. Skirrow[1]

[1] Geoscience Australia, GPO Box 378, Canberra, ACT, 2601, Australia.
[2] Primary Industries and Resources South Australia (PIRSA), GPO Box 1671, Adelaide, South Australia, 5001, Australia.

INTRODUCTION

The Olympic Cu-Au province of the Gawler Craton is South Australia's major mineral province and contains the world-class Olympic Dam Cu-Au-U deposit, Mt Gunson, and the recently discovered Prominent Hill Cu-Au deposit. However, little was known of the crustal architecture of the region, its evolution, or its tectono-stratigraphic relationship with other Proterozoic terranes within Australia.

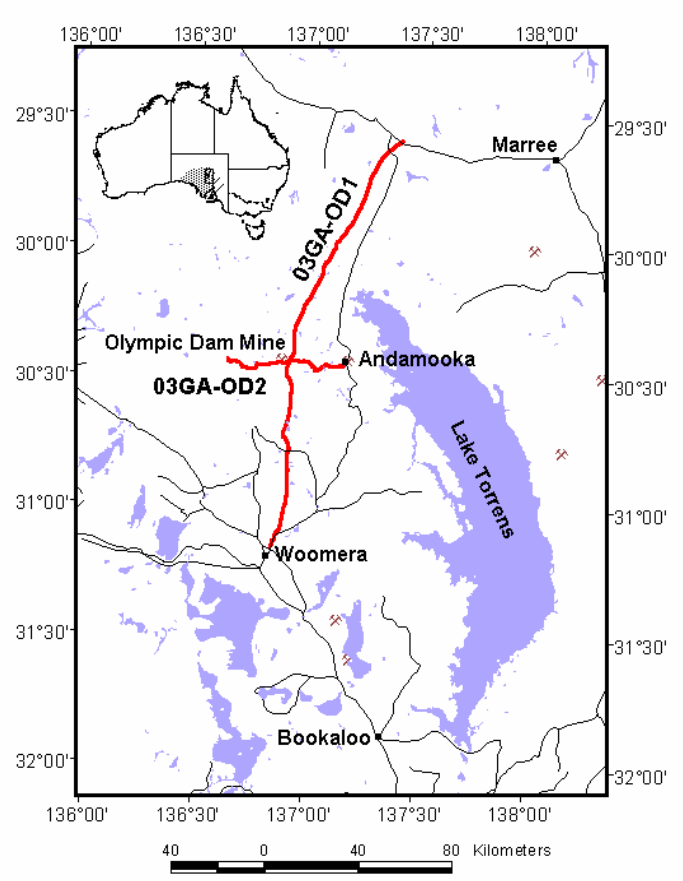

Figure 31: *Location of the 2003 Gawler Craton deep seismic reflection traverses.*

The results from the 2003 Gawler Seismic Survey have gone a long way towards answering these questions. The Gawler Seismic Survey consisted of two deep seismic reflection traverses (Figure 31): a regional north-south traverse, 193 km long, that extended from Woomera in the south, through Olympic Dam to the Oodnadatta Track and a 57 km-long east-west traverse that crossed the regional line near the Olympic Dam minesite.

The traverses crossed several major gradients in long-wavelength gravity data. These major gravity gradients are interpreted to represent fundamental changes in crustal properties and architecture at depth.

The main objectives of the Gawler seismic survey were to investigate the tectonic

architecture of the regional Fe oxide Cu-Au mineralisation, investigate the nature of the Torrens Hinge Zone (THZ), determine the architecture of the Gawler Range Volcanics (GRV) and Hiltaba Suite, map the thickness of Neoproterozoic cover-successions, and identify potential fluid pathways.

These results have been used to define tectonic controls on the evolution of the craton as well as on Cu-Au mineralization (Skirrow *et al*., this volume), to test the presence or absence of large mafic and/or ultramafic intrusions beneath the Olympic Dam deposit (Lyons *et al*., this volume), as well as to provide new insights on Neoproterozoic basin formation in the Adelaide Geosyncline to the east of the Torrens Hinge Zone (Priess *et al*., this volume).

The results are being used to develop fluid flow models to explain the mineral system operating during the emplacement of the Olympic Dam Cu-U-Au deposit and to develop theories as to why Olympic Dam is where it is and not somewhere else (Drummond *et al*., this volume).

INTERPRETATION METHOD

The method used to interpret the deep seismic reflection data was as follows:—

- Identify prominent trends in the seismic reflectivity by highlighting the main trends defined by the stronger reflections.
- Identify angular relationships between different reflective packages that indicate an inferred discontinuity in geology.
- Draw boundaries around regions of similar reflectivity,or between regions of different reflectivity, or both, to create packages or domains of consistent reflectivity. To be consistent, the tops of highly reflective zones were used to define the domain boundaries (we used similarities in the amplitude, coherency and dip of the seismic reflections to define the regions).
- Identify major regional-scale trends in reflectivity, such as reflectivity extending over large distances, either as dipping bands or sub-horizontal bands (e.g., the Moho).
- Using the known surface geology, project the mapped faults and geological units to depth along previously defined reflective zones.
- Identify any kinematic indicators that suggest movement directions or sense of displacement.
- Link the surface information projected to depth to the major large-scale trends and package or domain boundaries to create a crustal structure consistent with the geology and the seismic data.
- Add interpretations to the section for those features identified in the geological mapping but not imaged by the seismic data. It is assumed that these structures or units are non-reflective.
- Add interpretations to the section to account for areas of strong reflectivity that do not correlate to known geological structures of units.
- The seismic interpretation was then cross-checked against the geology, and the results discussed by the project team, and evaluated against all known geological and geophysical data.
- The seismic interpretation was forward-modelled using both gravity and magnetic data to test for consistency.
- The seismic interpretation is presented to geoscientists for further feedback and improvement.

SCALES

Choosing a suitable scale for interpretation is very important. Bigger features are often more obvious when you reduce scale, whereas you need high resolution displays to interpret the details

of a package of material. All sections were plotted at a V:H equal to 1, with an assumed average crustal velocity of 6 kms^{-1}.

Detailed seismic sections (plotted to 3 s TWT or ~10 km depth) displayed at 1:25 000 scale were used to interpret the Neoproterozoic northern basins. The upper crustal sections were interpreted at 1:50 000 scale. This scale was used to identify details within the basement and investigate boundaries or changes in the seismic data that would relate to the known surface geology. A 1:100 000 scale was used to interpret the 18 s (54 km depth) deep seismic sections. These were used to interpret the larger structures and check continuity of reflectivity through the entire crust. Smaller-scaled sections (1:250 000 and 1:500 000 horizontally compressed section) were used to investigate the deeper structure.

Because the two seismic traverses are orthogonal, it is possible to build a three-dimensional view of the crust.

GAWLER CRATON SEISMIC CHARACTERISTICS

The Gawler Craton seismic data quality is very good. The recorded frequencies were high, indicating that seismic wave attenuation within the basement is low. The coherency of the returned seismic signal was variable. This has been interpreted to represent changes in geological conditions rather than seismic acquisition variations. On average, the continuity of reflections is over several kilometres, or more, within the basement. Complex deformation has partially destroyed reflection continuity, in places, which can make interpretation more ambiguous.

The major cause of the reflectivity throughout the section is interpreted to represent both lithological variations, and faults and shear zones.

Finally readers should be reminded that the seismic method tends to image the horizontal and straighter structures over the folded or deformed structures. There is also a preference to image the latest deformation over the older more deformed surfaces, hence late structures are imaged better because they cut across and deform earlier structures.

MAIN SEISMIC FEATURES OF THE GAWLER CRATON SEISMIC DATA

The main features interpreted from the eastern Gawler Craton deep seismic reflection data are shown on Figure 32. In summary these are:—

- The crust is approximately 40 km thick.
- The seismic characteristics of the crust in the south differ from those of the crust in the north.
- The southern half of the traverse is dominated by a series of north-dipping reflections, both within the upper crust and the lower crust; with some of these north-dipping reflections within the upper crust spatially correlating with interpreted faults at the surface.
- In middle and lower crust at the southern end of the traverse, there is a north-dipping zone of reflectivity that extends to the Moho.
- The northern half of the traverse contains (less pronounced) south-dipping reflections.
- In the middle of the profile, there is an anomalous region, possibly extending below the Moho, within the middle and lower crust marked by a general reduction in amplitude of reflections.
- There is a major basement unconformity with the overlying cover-successions up to 6 km thick.

- The Burgoyne batholith, host to the Olympic Dam Cu-U-Au deposit, is imaged as a region of very weak reflections.
- The Olympic Dam area lies between two regions of different structural signature.

The following descriptions are based on our preliminary interpretation of the seismic data. The interpretations are consistent with known geological data. The seismic interpretation has been modelled using the regional gravity and magnetic data (Direen et al., these workshop notes) and the recent magnetotelluric results (Heinson et al., these workshop notes) collected along the seismic traverse. In some places, however, several interpretations that are plausible and further information is required before these can be reconciled and a final interpretation presented.

Traverse 03GA-OD1

The seismic characteristics of the crust change in both the north-south and the east-west directions. Figure 32 shows traverse 03GA-OD1 with schematic interpretation of the main features as well as an un-interpreted seismic section. Figure 33 shows 03GA-OD1 with complete interpretation line-work.

In the south, the deep seismic data imaged three distinct layers within the crust, excluding the overlying Neoproterozoic basins (Figure 32a). The upper layer is up to 12 km (4 sec) thick, characterised by a series of high-amplitude north-dipping to sub-horizontal reflections against a low amplitude background signal. The north-dipping reflections are interpreted to be thrusts because they reverse-offset the sub-horizontal to shallowly dipping reflections interpreted to be lithological marker horizons. Some of these north-dipping reflections within this upper layer correlate spatially with surface faults interpreted from potential-field data.

The middle layer is up to 15-18 km (5-6 sec) thick and consists of a band strong high-amplitude shallow to sub-horizontal reflections (Figure 32a). This layer contains a series of north-dipping reflections that extend from the top of this layer and extend downwards towards the Moho. These north-dipping reflections are interpreted to be a series of shear zones within the middle crust. The upper part of this middle layer could be detached from the upper layer. The lowest layer is a thin layer (6-9 km, 2-3 sec) devoid of reflections (Figure 32a). We interpret this layer to represent ductile material lying above the Moho.This north-dipping zone of reflectivity that occurs in middle and lower crust extends to the Moho (Figure 32a; red lines Figure 32b), and probably transects it.

In the north, the deep seismic data imaged two distinct layers within the crust, excluding the overlying Neoproterozoic to Palaeozoic basins (Figure 32a). The upper layer is up to 18 km (6 sec) thick and is characterised by a series of less pronounced low-amplitude south-dipping to sub-horizontal reflections. The south-dipping reflections are interpreted to be shear zones. The lower layer is up to 18 km (6 sec) thick and consists of a stronger amplitude shallow south-dipping to sub-horizontal reflections (Figure 32a). These south-dipping reflections are interpreted as a series of shear zones within the middle crust. There is no evidence for a non-reflective, ductile layer lying above the Moho.

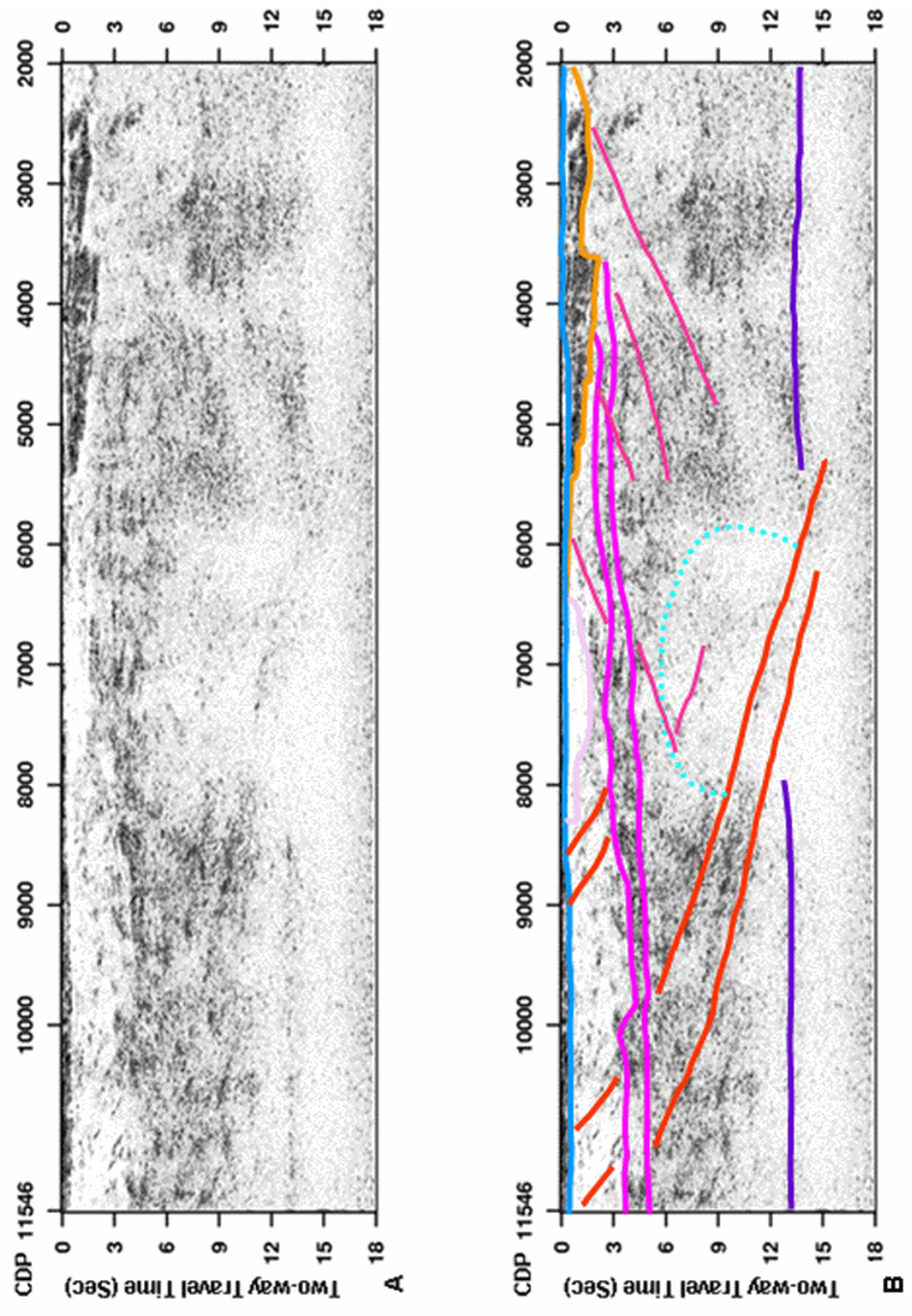

Figure 32: *The 2003 Gawler Craton deep seismic reflection data for traverse 03GA-OD1. Top) Uninterrupted seismic data. Bottom) Interpreted seismic section. North is to the right. V/H~1 at 6 km/s.*

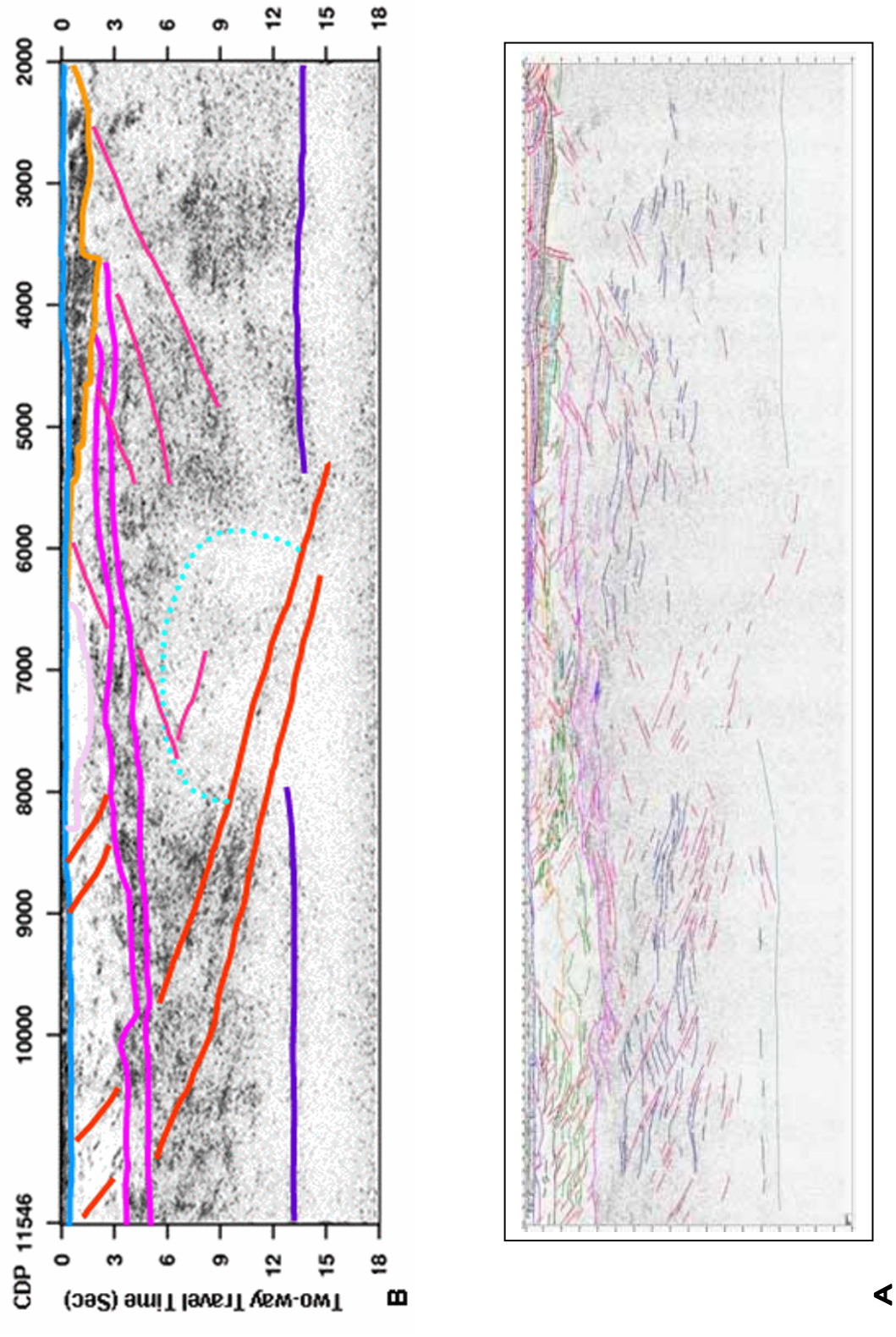

Figure 33: *A) The 2003 Gawler Craton deep seismic reflection data for traverse 03GA-OD1 showing all interpretation line work. B) Repeat of Figure 32B. North is to the right. V/H~1 at 6 km/s TWT.*

Refraction data collected between the 1970s and the 1980s (Finlayson et al., 1974; Greenhaulgh *et al*., 1989) indicated that the crust in the Gawler Craton is up to 40 km thick.

The Gawler Craton deep seismic reflection data imaged the Moho very well in the south. In this area, it appears as a highly-reflective, thin band of reflections at approximately 40 km (13 sec) depth. This highly reflective style of Moho is very similar to that imaged in the much older Yilgarn Craton to the west. In the north, the Moho is very different. It appears as a sub-horizontal zone where the strength and the number of reflections suddenly decreases to something similar to that seen beneath the Moho in the south. This change occurs at approximately 42 km (14 sec) depth. This style of Moho is similar to that imaged in the Mt Isa Inlier to the northeast and, to a lesser extent, the Broken Hill Block to the east.

Between the northern and southern crust, there is an anomalous region within the middle and lower crust in the middle of the traverse (6-12 sec between CDP's 6000-8000, Figure 32a; dotted aqua line Figure 32b).

The Burgoyne batholith, host to the Olympic Dam Cu-U-Au deposit, is imaged as a region of non-reflectivity when viewed at small scales (Figure 32a; pink line Figure 32b). There is considerable amplitude difference between reflections recorded from within the batholith to those reflection recorded outside. Special amplitude scaling applied within the batholith shows there is considerable structure within the batholith. Lyons *et al*. (this volume) discusses, in more detail, the Burgoyne batholith and the Olympic Dam deposit.

In the near surface, the seismic survey shows the unconformity below the Stuart Shelf that extends across this part of the Gawler Craton (Figure 32a; blue and orange lines Figure 32b). Successions above this unconformity are up to 6 km thick. Preiss *et al*. (this volume) describes these in detail.

Traverse 03GA-OD2

The seismic characteristics of the crust change in both the north-south and the east-west directions. Figure 34 shows traverse 03GA-OD2 with schematic interpretation of the main features as well as an un-interpreted seismic section. Figure 35 shows 03GA-OD2 with complete interpretation line work.

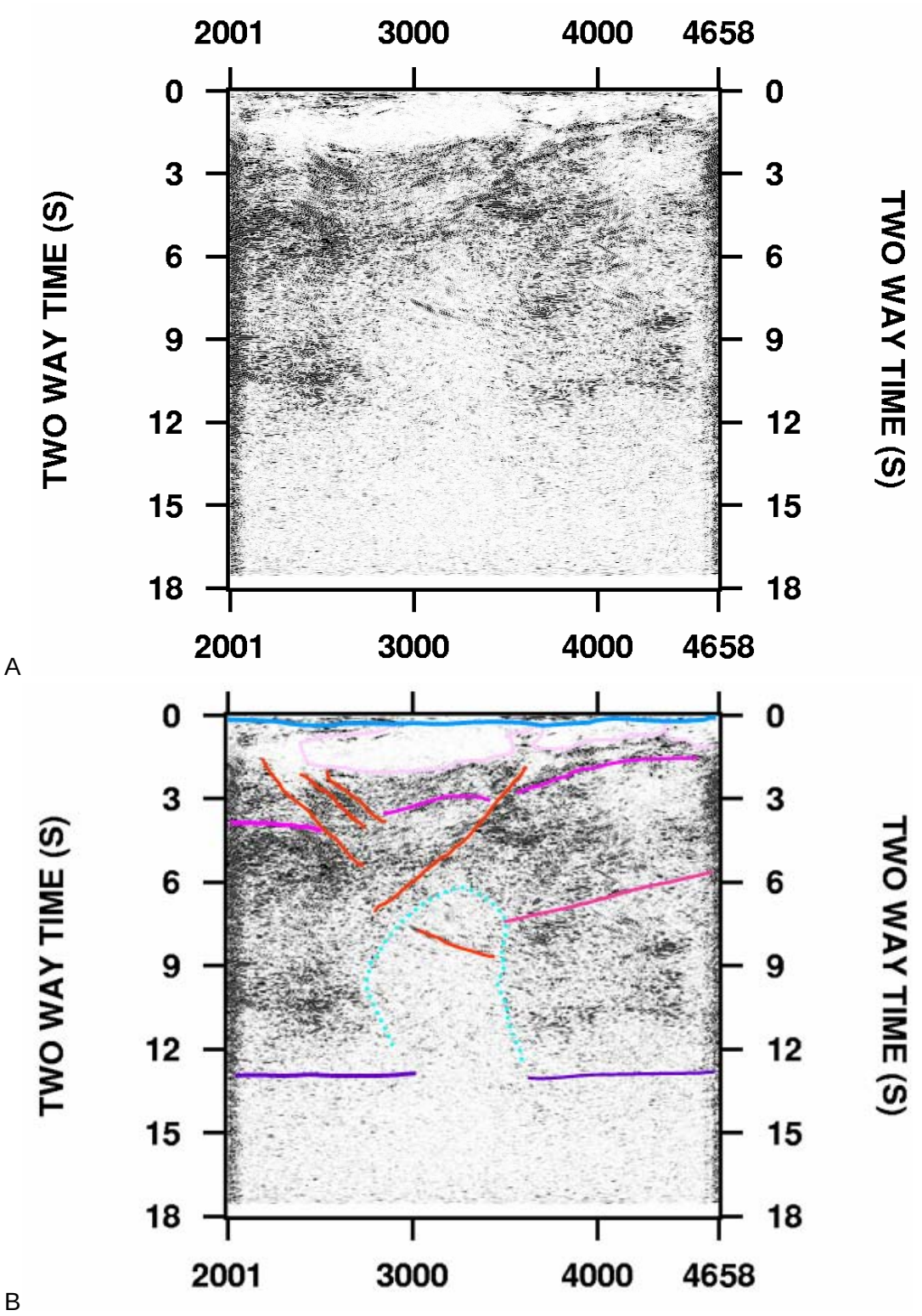

Figure 34: *The 2003 Gawler Craton deep seismic reflection data for traverse 03GA-OD2. A) Uninterrupted seismic data. B) Interpreted seismic section. East is to the right. V/H~1 at 6 km/s.*

In the west, the deep seismic data images a similar crust to that imaged in the southern portion of 03GA-OD1. There are three less distinct layers (Figure 34a). The upper layer is characterised by a series of high-amplitude east-dipping to sub-horizontal reflections against a lower amplitude background.

The middle layer is up to 9-12 km (3-4 sec) thick and consists of a band of high-amplitude shallow to sub-horizontal reflections (Figure 34a). This layer contains a series of east-dipping reflections that extend from the top of this layer and extend eastwards. The lowest layer is a thin layer (6-9 km, 2-3 sec) devoid of reflections as imaged on 03GA-OD1 (Figure 34a). We interpret this layer as ductile material lying above the Moho.

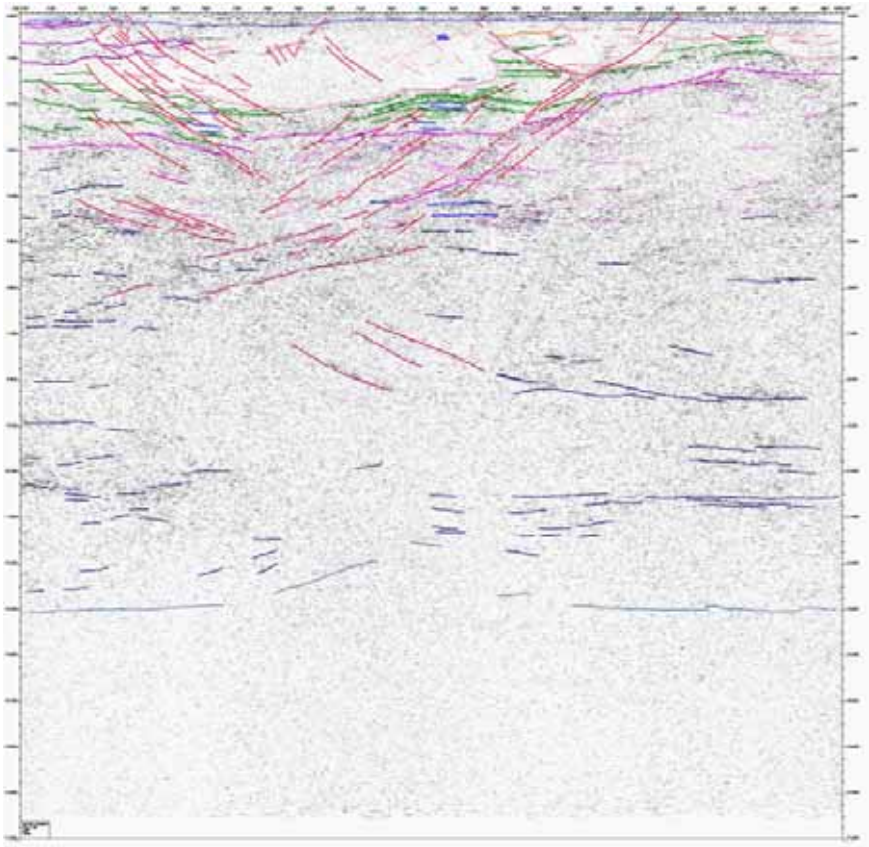

Figure 35: *The 2003 Gawler Craton deep seismic reflection data for traverse 03GA-OD4 showing all interpretation line work. East is to the right. V/H~1 at 6 km/s.*

In the east, the deep seismic data imaged two layers within the crust; the upper layer is characterised by a series of dipping, less pronounced, low-amplitude reflections. In the upper portion of the section, these reflections are sub-horizontal to west-dipping and deeper down they are sub-horizontal. Above the Moho reflectivity is poor. The Moho is well imaged at both ends of traverse 03GA-OD2. At both ends it lies at approximately 40 km (13 sec) depth. In the central part, the Moho is not well imaged where there is a suggestion of the presence of the anomalous region imaged on 03GA-OD1. This region lies at a similar depth within the middle and lower crust (6-12 sec, Figure 34a).

The Burgoyne batholith is again imaged as a region of non-reflectivity, similar to that described on 03GA-OD1 (Figure 34a; pink line Figure 34b). Lyons et al. this volume) discusses, in more detail, the Burgoyne batholith and the Olympic Dam deposit.

The major near surface unconformity, imaged by the seismic data, extends along the seismic traverse. (Figure 34a; blue and orange lines Figure 34b). The cover sequence above this unconformity is up to 6 km thick and is interpreted as Neoproterozoic successions.

SUMMARY

The two seismic traverses, 03GA-OD1 and 03GA-OD1, collected as part of the Gawler Craton seismic survey have successfully imaged the crustal structure of the Gawler Craton basement, including the crustal structure below the Olympic Dam Cu-U-Au deposit as well as the geometry of the surrounding crust.

The structures imaged in the seismic traverses show that the region is a fold-thrust belt. It was subject to compressional tectonics at least during the *ca*1720 Ma Kimban Orogeny and, mildly, during the *ca*1590 Ma Fe oxide Cu-Au mineralisation.

REFERENCES

Finlayson, D.M., Cull, J.P. and Drummond, B.J., 1974. Upper Mantle Structure from the Trans-Australia Seismic Refraction Data. *Journal of the Geological Society of Australia*, **21**, 447-458.

Greenhaulgh, S.A., von der Borch, C.C. and Tapley, D., 1989. Explosion seismic determination of crustal structure beneath the Adelaide Geosyncline, South Australia. *Physics of the Earth and Planetary Interiors*, **58**, 323-343.

NOTES ON DETAILED BASEMENT INTERPRETATION OF TRAVERSE 03GA-OD1– 6 s DATA

P. Lyons[1], B.J. Drummond[1], B.R. Goleby[1], N.G. Direen[3] M. Schwarz[2], A.J. Shearer[2], M.C. Fairclough[2] and R.G. Skirrow[1]

[1] Geoscience Australia
[2] Primary Industries and Resources South Australia (PIRSA
[3] University of Adelaide

These notes are a brief summary of the major features observed in the upper 6 s TWT of Traverse 03GA-OD1, the north-south traverse. Where possible, interpretation has been supported by information from potential field data and drilling. Only the Hutchison Group has not been intersected in the region of the seismic survey. Locations are referred to CDPs, common depth points. 100 CDPs is about 2 kilometres. A depth conversion of 1 s TWT to 3 km is used.

STRATIGRAPHY

1. Cover thickness. The Neoproterozoic successions overlying the basement comprise units of the Cariewerloo Basin, The Adelaide Rift, and the Wilpena Group. In the south the cover is ~1.2 km thick, comprising units of the Wilpena Group and the Cariewerloo Basin (Cowley, XXXX). The cover thins to 300-500 m over Burgoyne batholith, where it consists of the Wilpena Group. In the north, the thickness increases to over 5 km in graben of the Adelaide Rift, overlain by Wilpena Group. The Neoproterozic cover is overlain Early Cambrian Andamooka Limestone and Yarrawurta Shale, and parts of the Jurassic-Cretacous Eromanga Basin. The total thickness of this younger cover may not exceed 100 m, and is, in places, only about 20 m.

2. Gawler Range Volcanics. Between CDP 11546 and CDP 10400, the Gawler Range Volcanics are about a kilometre thick, with their base at ~2 km depth. They are characterised by 'festooned' reflections. Elsewhere, they are thin, only a few hundred metres, or less, and their presence is difficult to ascertain, except where they have been intersected in drilling or have a definite signal in magnetic data. In the seismic section, Gawler Range Volcanics have been interpreted to occur north of the Burgoyne batholith, although they are not 'seen' in magnetics—either because they are too deep to be detectable by magnetics or too thin and felsic to be sufficiently magnetised, or both.

3. Wallaroo Group. Wallaroo Group occurs from the CDP 11546 to about CDP 10200. It is characterised by low reflectivity and fairly flat-lying reflections. It is up to 3 km thick in the south with its base at about 4-5 km, in unconformable contact with the Hutchison Group.

4. Hutchison Group correlates. Inferred correlates of the Hutchison Group form a long wedge, thickest in the south, where it reaches a depth of ~12 km, tapering out at about CDP 4600. Its seismic character is similar to that of the Wallaroo Group, but with more reflective patches and horizons about 2 km to 4 km wide and 1 km thick. Beneath the Burgoyne batholith, the Hutchison Group may have a pronounced change in composition or it may be absent; replaced by more reflective rock packages, either of the underlying mid-crustal layer or an unknown unit.

5. Donington Granitoid Suite. The Hutchison Group was intruded by the Donington Granitoid Suite at about 1850 Ma. Bodies of Donington 'granite' are non reflective; but, as orthogneiss they may show some structure. A body of Donington granite with trapezoidal section occurs between CDP 9600 and CDP 8900, with a base at ~6 km. The trapezoid is bound on the south by the south-dipping Sandy Point Fault and on the north by a north-dipping fault of the Wirrda Fault Complex. More Donington granite is interpreted to occur between CDP 8400 and CDP 7800, in contact with the Burgoyne batholith. However, as both the Donington granite and the Burgoyne batholith have the low reflectivity expected of plutonic bodies, it is difficult to discern which is which. Also, the problem section may be sub parallel to the contact here.

6. Mid-crustal layer. At CDP 11546, at a depth of ~12 km, the crust becomes notably reflective. The reflective horizon extends to about CDP 4600, where it nears the Neoproterozoic unconformity. This is interpreted to be the top of a package of dense rock, possibly Archaean granulite or an unknown partly mafic unit (perhaps between 2500 Ma and 2000 Ma), some 4 km to 5 km thick.The layer is characterised by two prominent packages of duplexes. Internal packages are also apparent.

7. Burgoyne batholith. Typical of plutons, the Burgoyne batholith is identified by its general lack of reflectivity. It occurs between ~CDP 8300 and CDP 6400. Its margins are sill-like, especially at its northern end. The base of the batholith is at a depth of about 5 km. Some internal reflections are apparent and are possibly due to alteration, both on fault planes and diffusely distributed.

STRUCTURE

The overall structural character is of a fold-thrust belt. The crust is dominated by shallow to moderately dipping thrusts that cut the Palaeoproterozoic Hutchison Group correlates and Wallaroo Group detaching on the upper surface of the mid-crustal layer. In the Hutchison Group correlates and the Wallaroo Group, deformation is by thrusting and associated folding. Where thrust complexes occur, units are more folded. Away from thrust complexes, reflectors are sub-horizontal. The thrust complexes tend to be associated with brighter packages, suggesting either a rheological control on their location or that thrusting locally increased the acoustic impedance contrasts.

1. Between CDP 11546 and CDP 10550, north-dipping (~ 30 degrees) thrusts, the Elizabeth Creek Fault Complex, cut Hutchison Group and Wallaroo Group and possibly cut the Gawler Range Volcanics. Open folds in the Gawler Range Volcanics are possibly, in part, fault propagation folds.

2. At CDP 9600, a backthrust of the Elizabeth Creek Fault Complex marks the contact between the Hutchison Group correlates and the trapezoidal body of the Donington Granitoid Suite. The Donington body may have acted as a buttress for an up-thrust inverted wedge with its apex at ~7 km depth.

3. The northern contact of the Donington 'trapezoid' is marked by a north-dipping thrust which is part of a package of thrusts and folds, the Wirrda Fault Complex, part of a zone of intense deformation between CDP 8800 and CDP 8300. Less prominent south-dipping faults that cut the Burgoyne batholith are interpreted to be backthrusts of the Wirrda Fault Complex (In the east-west traverse, the north-dipping thrusts of the complex can be seen cutting the western end of the Burgoyne batholith as east dipping structures—therefore, they are actually northeast dipping thrusts—thus the Wirrda Fault Complex postdates intrusion of the Batholith. See below.).

4. On the northern side of the Burgoyne batholith, units are generally flat-lying and thrusts are usually south-dipping. These thrusts are less reflective and often picked by their termination of brighter patches. Some cut the Burgoyne batholith and interpreted Gawler Range Volcanics.

NOTES ON THE DETAILED BASEMENT INTERPRETATION OF 03GA-OD2 – 6 s DATA

Martin Fairclough[1], Bruce Goleby[2], Barry Drummond[2], Patrick Lyons[2] and A. Shearer[1]

[1] Primary Industries and Resources South Australia (PIRSA), GPO Box 1671, Adelaide, South Australia, 5001, Australia.
[2] Geoscience Australia, GPO Box 378, Canberra, ACT, 2601, Australia.

The east-west traverse, 03GA-OD2, confirms important observations from 03GA-OD1, and allows surfaces to be interpreted in a three-dimensional sense. Parts of the traverse are difficult to interpret without benefit of 3D viewing capability because the line contains some segments that deviate by about 45° from the general orientation; and its relative shortness means that end-effects, where migration is difficult, occupy a greater fraction of the data.

The cross-line confirms the interpreted depth (in TWT) of the Burgoyne batholith, the presence of Hutchison Group (or similar units: see notes for OD1 6 s data) beneath the batholith, and the mid-crustal layer.

Some unnamed plutons of the Hiltaba Suite (the Burgoyne batholith is also of the Hiltaba Suite) are well imaged to the east of the Burgoyne batholith. Their positions agree with interpretations of potential field data (Direen and Lyons 2002: solid geology). Separating these plutons from the batholith is an ‘inlier’ of Hutchison Group rocks with Donington granite resting over them.

The western end of the Burgoyne batholith is cut by apparent east-dipping thrusts which correspond to the apparent north-dipping thrusts of the Wirrda Fault Complex. Therefore, the Wirrda Fault Complex strikes northwest.

A distinct feature of the data from the cross-line is the apparent west-dipping package of reflections originating east of the Burgoyne batholith. However, the reflections are sub-horizontal to shallowly dipping, so the appearance of a west-dipping structure is due to an *echelon* of higher amplitudes.

REFERENCES

Direen, N.G and Lyons, P. 2002. Geophysical interpretation of the central Olympic Cu-Au Province, 1:500 000 scale map. Geoscience Australia.

Gow, P A. 1996. Geological evolution of the Stuart Shelf and Proterozoic iron oxide-associated mineralization: insights from regional geophysical data. PhD thesis. Monash University. .

.Swain, G., Hand, M., Rutherford, L. and Barovich, K. 2004. Timing of terrain-scale shear zones in the Gawler Craton. Abstracts: Gawler Craton State of Play 2004 PIRSA Report Book 2004/17.

GAWLER CRATON COVER-SUCCESSIONS: STUART SHELF TO ADELAIDE GEOSYNCLINE TRANSITION

Wolfgang Preiss[1], Russell Korsch[2] and Jennifer Totterdell[2]

[1] Primary Industries and Resources South Australia (PIRSA), GPO Box 1671, Adelaide, South Australia, 5001, Australia.
[2] Geoscience Australia, GPO Box 378, Canberra, ACT, 2601, Australia.

INTRODUCTION

As well as imaging the deep structure of the Gawler Craton, 03GA-OD1 crosses the northeastern transition from the craton, with its Adelaidean (Neoproterozoic) and Cambrian platform cover, the Stuart Shelf, through the transition of the Torrens Hinge Zone (THZ), into the rift complex of the Adelaide Geosyncline (Preiss, 1987, 2000), and thus provides new insights into the Neoproterozoic and Palaeozoic sedimentary and tectonic history of this region.

WHAT WAS KNOWN BEFORE THE SEISMIC DATA WERE COLLECTED

Tectonic Setting

The eastern margin of the Gawler Craton is defined by Neoproterozoic rifts, iniated at 827 Ma (Wingate et al., 1998). Successive rifts eventually led to the breakup of the supercontinent Rodinia (e.g., Dalziel, 1991). Rift and sag phases provided accommodation space for the deposition of very thick sediments of the Adelaide Geosyncline.

The THZ was a zone of active rifting during the early Adelaidean, a zone of gentle flexuring during the late Adelaidean and Cambrian, and a zone of gentle, open folding and reverse faulting in the Delamerian Orogeny (~500 Ma). The THZ is expected to show successive down-stepping extensional faults in the lower Adelaidean on seismic sections, while upper Adelaidean strata are expected to be flexured across the THZ.

The newly formed, sigmoidal continental margin may have extended from western Victoria to north-east of the Curnamona Province and beyond. An intra-cratonic rift extended northwest from this continental margin, between the Gawler Craton and the Curnamona Province, through the Flinders Ranges to the Willouran Ranges and thence to the Peake and Denison Ranges.

Stratigraphic Record

Sedimentation associated with the breakup of Rodinia produced an eastward thickening wedge of sediments, from a few hundred metres thick on the Stuart Shelf to 10-15 km in the Adelaide Geosyncline. The succession is divided into 14 subgroups (Table 5) bounded by major sequence boundaries (Preiss et al., 1997; Preiss and Cowley, 1998; Dyson, 1992). It is expected that evidence of these sequence boundaries (disconformities to low-angle unconformities) should be visible in seismic sections.

Table 5: Succession of Adelaidean (Neoproterozoic) and Cambrian platform cover on the Stuart Shelf and through the transition of the Torrens Hinge Zone (THZ).

PROTEROZOIC AND CAMBRIAN COVER STRATIGRAPHY				
Age	*Groups*	*Subgroups*	*Lithologies*	*Formations represented on seismic transect*
PALAEOZOIC Early Cambrian	UNNAMED	unnamed	Redbeds	*Yarrawurta Shale*
			?sequence boundary	
	HAWKER	unnamed	Limestone	*Andamooka Limestone*
			low-angle unconformity	
NEOPROTEROZOIC				
Marinoan	WILPENA	Upper Wilpena Group (incl. Pound Sgp)	Orthoquartzite, redbeds, limestone, siltstone	*not represented*
			red mudstone	*Yarloo Shale*
			sequence boundary	
		Sandison	Sandstone, siltstone, basal 'cap' dolomite	*Tent Hill Formation, Nuccaleena Formation*
			sequence boundary	
	UMBERATANA	Yerelina	Siltstone, sandstone, diamictite	*Whyalla Sandstone, Elatina Formation*
			sequence boundary	
		Upalinna	Siltstone, sandstone, redbeds, limestone, dolomite	*'Yudnapinna beds', Angepena Formation*
			sequence boundary	
Sturtian		Nepouie	Siltstone, limestone, basal shale and 'cap' dolomite	*Tapley Hill Formation, Woocalla Dolomite Member*
			sequence boundary	
		Yudnamutana	Diamictite, siltstone, sandstone, conglomerate	*Boila Bollana Tillite, Wilyerpa Formation*
			unconformity, locally angular	
	BURRA	Belair	Siltstone, sandstone, quartzite, arkose	*not represented*
			sequence boundary	
Torrensian		Bungarider	Siltstone, sandstone, dolomite	*Myrtle Springs Formation*
			sequence boundary	
		Mundallio	Shallow-water dolomite, magnesite, siltstone, sandstone	*Skillogalee Dolomite*
			sequence boundary	
		Emeroo	Sandstone, quartzite, siltstone, arkose	*Witchelina Quartzite, Willawalpa Fm, Top Mount Sandstone*
			?sequence boundary	
Willouran	CALLANNA	Curdimurka	Sandstone, siltstone, dolomite, limestone, evaporites, minor volcanics	*Boorloo Siltstone, Coorawina Fm, Hogan Dolomite, Recovery Fm, Rook Tuff, Dome Sandstone*
			?sequence boundary	
		Arkaroola	Mafic volcanics, carbonate, basal clastics	*Beda Volcanics, Noranda Volcanics, ?Black Knob Marble Backy Point Formation*
			major unconformity	N.B. Arkaroola Subgroup is nowhere in contact with Pandurra
MESOPROTEROZOIC			Red sandstone	*Pandurra Formation, intruded by Gairdner Dyke swarm*

The first rift event, of early Willouran age, is recorded by the Arkaroola Subgroup of Callanna Group. The eastern Gawler Craton underwent NE-SW extension and intrusion of the NW-trending Gairdner Dyke Swarm. The Beda Volcanics (Stuart Shelf), Wooltana Volcanics (Flinders Ranges), Noranda Volcanics (Willouran Ranges), and Wilangee Volcanics (Barrier Ranges) are all extrusive equivalents. Intrusives have been dated at 827 Ma in both the Gawler Craton and Barrier Ranges (Wingate et al., 1998).

The second rift event, of late Willouran age, resulted in deposition in NW-trending rift basins of the Curdimurka Subgroup of the Callanna Group, comprising thick, evaporitic, mixed clastics and carbonates, and minor volcanism, such as the Rook Tuff, 802 Ma (Fanning et al., 1986).

During the third rift event, of Torrensian age, rifting with NE-SW extension continued. Thick successions of Burra Group accumulated, comprising basal fluvial sediments, followed by marginal to shallow-marine clastics and carbonates (including sedimentary magnesite, e.g., Belperio, 1990), and finer clastics of marine transgression in the upper part.

The fourth rift event, of Sturtian age, produced troughs surrounding the Curnamona Province, but there was no active rifting at the THZ, where thin glaciomarine shelf deposits (Yudnamutana Subgroup of Umberatana Group) unconformably overlap Willouran and Torrensian rifts in Willouran Ranges (Krieg et al., 1991). Rodinia breakup is favoured at end of this fourth rift event.

The onset of post-breakup, sag phase deposition is recorded by the late Sturtian Nepouie Subgroup; Tapley Hill Formation carbonaceous and calcareous siltstone records the first marine transgression onto the craton proper, and involved post-rift flexure of the craton margin. Subsidence continued in Marinoan times, with shallower-water Upalinna Subgroup, aeolian and glaciomarine Yerelina Subgroup, and post-glacial marine shelf sediments of the Sandison Subgroup and upper Wilpena Group.

Delamerian Orogeny

Delamerian deformation in the Middle to Late Cambrian commenced with cratonward thrusting in the Fleurieu Arc of the Mount Lofty Ranges, from where deformation then propagated northward into the Nackara Arc (Preiss, 1995). Open dome-and-basin folds of the central Flinders Zone separate the upright, arcuate folds of the Nackara Arc from those of the North Flinders Arc. These North Flinders Arc folds continue into the Willouran Ranges.

The Norwest Fault is a steep reverse fault with major SW-directed displacement (Burra Group over Cambrian) near Leigh Creek (Coats, 1973), but displacement decreases to the north into Willouran Ranges. It is uncertain whether the Norwest Fault is listric, perhaps soling northeastwards into Willouran evaporites, or is rooted in basement. A narrow, NW-trending gravity low adjacent to the Norwest Fault suggests a rifted trough perhaps filled with evaporitic sediments.

Solid Geology of ANDAMOOKA and CURDIMURKA 1:250 000 map sheet areas

A solid geology map was constructed from outcropping geology, drill-hole data, and interpretation of aeromagnetic and gravity data, and shows restricted remnants of flat-lying Cambrian redbed and carbonate sediments on the Stuart Shelf, underlain by very widespread lower Wilpena Group shelf sediments (Tent Hill Formation of Sandison Subgroup). In the central

part of the transect, Yarloo Shale of the upper Wilpena Group intervenes between Tent Hill Formation and Cambrian Andamooka Limestone.

The northern part of the line passes over the THZ, with its northeastward-thickening stratigraphy, faulting and gentle folding. The northern extremity of line crosses the northwesterly extension of the Norwest Fault; strongly folded lower Adelaidean (Callanna Group and Burra Group) are known in outcrop several kilometres to the southeast; steep dips are common in these beds.

THE SEISMIC RECORD

From south to north, 03GA-OD1 traverses the northeastern transition from the Gawler Craton, through the THZ, into the rift complex of the Adelaide Geosyncline. The seismic record shows evidence of several erosional surfaces, which can readily be related to the predicted sequence boundaries between subgroups. The southern part of the line shows unattenuated Precambrian crust of the Gawler Craton, unconformably overlain by a thin veneer of Pandurra Formation in the Cariewerloo Basin. The lateral boundaries of the Pandurra Formation are largely faulted; these faults are post-depositional, not original boundaries of Cariewerloo Basin (Cowley, 1993).

Shallow basement (~300 m) near Olympic Dam is clearly visible in the seismic section; Sandison Subgroup (Tent Hill Formation, with basal Nuccaleena Formation 'cap dolomite') directly overlies basement. Basement deepens to the north, with the incoming of the Nepouie, Upalinna and Yerelina Subgroups between basement and Sandison Subgroup.

Buried rift faults are clearly identified beneath upper Adelaidean sediments of the THZ. One major early graben is bounded in the southwest by a northeast-dipping extensional fault, and an inversion anticline formed during Delamerian contraction. Subtle variations in the magnetic character of near-surface Adelaidean sediments outlines the limbs and extent of this anticline on TMI images, hence the possible extent of the early graben. Within the zone of early rifting, an interpreted Torrensian-age rift (Burra Group) oversteps the earlier Willouran (Callanna Group) rift, accompanied by a switch in polarity of rifting to southwest-dipping faults.

The axial zone of the Willouran rift contains a unit with reflectivity suggestive of volcanics; this accords well with predicted early Willouran basalts of the Arkaroola Subgroup (Beda Volcanics on Stuart Shelf, Noranda Volcanics in Willouran Ranges). Overlying the interpreted volcanics is a bulge that may represent a salt pillow, in accord with predicted evaporites low in Curdimurka Subgroup, which facilitated diapirism in the Flinders Ranges. A slight, NW-elongated dip in the gravity data at this point may be related to such evaporites.

These first (southernmost) early Adelaidean rifts have a clearly defined northern limit, north of which basement again shallows. From there, basement gradually deepens again to the north into the zone affected by more significant Delamerian thrusting and folding. Delamerian deformation becomes evident in the Torrens Hinge Zone, firstly as thrusts with minor displacement and associated hanging-wall anticlines, then as larger displacements. At the northeastern boundary of the Torrens Hinge Zone, lower Adelaidean units are thrust over younger units. The style of thrusting is thin-skinned; there is no evidence of thrusts being rooted in the basement as is evident near Adelaide. This probably related to evaporitic decollement surfaces in the Callanna Group.

There is no evidence in the seismic for the postulated deep trough adjacent to the Norwest Fault, filled with light sediments such as evaporites, as was anticipated from the gravity; the gravity low remains unexplained. There is some discrepancy between very gently northeast-dipping segments

separated by reverse faults seen on the poor seismic record at this end of the line, and the southwest-dipping limb of Burra Group suggested by the outcropping geology south of the seismic line.

CONCLUSIONS

The seismic data show overall good agreement with predicted stratigraphy and structure in the transition from the platform cover of the Stuart Shelf to the thick successions of the Adelaide Geosyncline – a complex of rift and sag basins related to Rodinia breakup. Early extensional faults, sequence boundaries, thrusts, folds, and possible volcanics and evaporites, are all expected features that have been imaged on seismic. Unexpected are Willouran and Torrensian buried rifts in the THZ for which there is no indication in the surface geology.

REFERENCES

Belperio, A.P., 1990. Palaeoenvironmental interpretations of the Late Proterozoic Skillogalee Dolomite in the Willouran Ranges, South Australia. *In*: Jago, J.B. and Moore, P.S. (Eds.). The evolution of a late Precambrian-early Palaeozoic rift complex: the Adelaide Geosyncline. *Geological Society of Australia, Special Publication*, **16**, 85-104.

Coats, R.P., 1973. COPLEY, South Australia, sheet SH54-9. *South Australian Geological Survey*, 1:250 000 Series ─ Explanatory Notes.

Cowley, W.M., 1993. Cariewerloo Basin. In: Drexel, J.F., Preiss, W.V. and Parker, A.J. (Eds). The Geology of South Australia. Volume 1, The Precambrian. *South Australian Geological Survey. Bulletin*, **54**, 139-142.

Dalziel, I.W.D., 1991. Pacific margins of Laurentia and East Antarctica-Australia as a conjugate rift pair: evidence and implications for an Eocambrian supercontinent. *Geology*, **19**, 598-601.

Dyson, I.A., 1992. Stratigraphic nomenclature and sequence stratigraphy of the lower Wilpena Group, Adelaide Geosyncline: the Sandison Subgroup. *South Australian Geological Survey. Quarterly Geological Notes*, **122**, 2-13.

Krieg, G.W., Rogers, P.A., Callen, R.A., Freeman, P.J., Alley, N.F. and Forbes, B.G., 1991. CURDIMURKA, South Australia, sheet SH53-8. *South Australian Geological Survey*, 1:250 000 Series ─ Explanatory Notes.

Fanning, C.M., Ludwig, K.R., Forbes, B.G. and Preiss, W.V., 1986. Single and multiple grain U-Pb zircon analyses for the early Adelaidean Rook Tuff, Willouran Ranges, South Australia. *In*: 8th Australian Geological Convention, Adelaide 1986. *Geological Society of Australia. Abstracts*, **15**, 71-72.

Preiss, W.V. (compiler), 1987. The Adelaide Geosyncline - late Proterozoic stratigraphy, sedimentation, palaeontology and tectonics. *South Australian Geological Survey, Bulletin*, **53**.

Preiss, W.V., 1995. Delamerian Orogeny. *In*: Drexel, J.F. and Preiss, W.V. (Eds.). The Geology of South Australia. Volume 2, The Phanerozoic. *South Australian Geological Survey. Bulletin*, **54**, 45-57.

Preiss, W.V., 2000. The Adelaide Geosyncline of South Australia, and its significance in continental reconstruction. *Precambrian Research*, **100**, 21-63.

Preiss, W.V., Dyson, I.A., Reid, P.W. and Cowley, W.M., 1998. Revision of lithostratigraphic classification of the Umberatana Group. *MESA Journal*, **9**, 36-42.

Preiss, W.V. and Cowley, W.M., 1999. Genetic stratigraphy and revised lithostratigraphic classification of the Burra Group in the Adelaide Geosyncline. *MESA Journal*, **14**, 30-40.

Wingate, M.T.D., Campbell, I.H., Compston, W. and Gibson, G.M., 1998. Ion-probe U-Pb ages for Neoproterozoic basaltic magmatism in south-central Australia and implications for the breakup of Rodinia. *Precambrian Research*, **87**, 135-159.

CRUSTAL ARCHITECTURE BENEATH OLYMPIC DAM FROM MAGNETOTELLURIC SOUNDING

Rob Gill[1], Graham Heinson[1], Nick Direen[1], Peter Milligan[2] and Anthony White[3]

[1] University of Adelaide
[2] Geoscience Australia
[3] Flinders University

The magnetotelluric (MT) method involves measurement of natural-sources of time-varying magnetic fields that penetrate the earth, and induce electrical fields and secondary magnetic fields. Observations of such fluctuations in horizontal and vertical components of the magnetic fields and corresponding changes in horizontal and orthogonal electrical fields provide constraint on both lateral and vertical changes in electrical resistivity. By measuring MT signals over a range of periods of 101 s to 104 s, structural information on resistivity on length-scales of 5 km to 50 km are obtained.

We present results from 58 new MT sites collected during two field campaigns in October 2003 and April 2004. Most sites were located adjacent the Woomera – Roxby Downs road and the Borefield Road, with a site spacing between 5 km and 10 km over a total of 220 km. Additional sites were collected towards Andamooka. Impedance tensor data were rotated to orientation of dominant geoelectric strike, approximately 60º west of geomagnetic north, and were generally found to be predominantly 2D. Both the transverse electric (electric field parallel to strike) and transverse magnetic (electric field perpendicular to strike) modes of the MT responses were inverted using the 2D inversion approach of Rodi and Mackie (2001).

The inversion shows four notable features:

(1) Sedimentary cover sequences have low resistivity (< 20 Ωm) and show a thickening of Neoproterozoic successions to the north. Over Olympic Dam, the sedimentary sequences thin, in agreement with the seismic section.

(2) A north-dipping crustal-scale boundary separates a region of high resistivity of >1000 Ωm to the south from with the more conductive crust to the north, typically <500 Ωm.

(3) In a region north of Olympic Dam, the upper-middle crust to about 20 km depth is quite resistive (~1000 Ωm), but the lower crust is much more conductive (<100 Ωm). A region of low resistivity appears to extend upwards beneath Olympic Dam, possibly due to mineral phases (graphite?) along ductile zones and fluid pathways. To the north of Olympic Dam, the middle and lower crust appear uniform.

(4) In the upper few kilometres beneath Olympic Dam, we image a resistive region coincident with the Burgoyne batholith. The more conductive region in the mid-lower crust beneath the batholith is coincident with a region of less seismic reflectivity.

REFERENCE

Rodi, W. and Mackie, R.L., 2001. Nonlinear conjugate gradients algorithm for 2-D magnetotelluric inversion. *Geophysics*, **66**, 174-187.

CRUSTAL ARCHITECTURE OF THE CENTRAL OLYMPIC CU-AU PROVINCE: CONSTRAINTS FROM GRAVITY MAGNETIC AND MAGNETOTELLURIC DATA.

Nicholas G Direen[1], Patrick Lyons[2], Peter R Milligan[2], Graham S Heinson[1], Robert Gill[1]

[1] Continental Evolution Research Group, Geology & Geophysics, University of Adelaide
[2] Geoscience Australia, PO Box 378, Canberra, ACT, 2601, Australia.

Up to 1500 m of Late Proterozoic, Early Palaeozoic, and Mesozoic cover conceals the Proterozoic rocks forming the eastern margin of the Gawler Craton. Inferences about the overall regional geometry of the IOCG minerals system have to come either from expensive drilling, which may alias the true structure due to undersampling or nugget effects, or from geophysical methods, which have non-unique interpretations.

Acquisition of deep regional seismic reflection data by Geoscience Australia & PIRSA adds a new layer of geophysical information about the regional crustal architecture near Olympic Dam. To aid the interpretation of the seismic data, we can add a substantial body of interpretation and inference gleaned from carefully integrating potential-field analyses with deep drilling data. This work has previously been presented by Direen and Lyons (2000), Direen *et al*. (2000), Milligan *et al*. (2002, 2000 & in review), Bastrakov *et al*., 2004, and Williams *et al*. (2004a;b).
Datasets include new compilations of the regional gravity and magnetic grids, constrained depth-to-basement images, interpreted basement geology maps, gradient analysis maps, depth to magnetic source images (Euler solutions), deep crustal source filtered images, statistical analyses of basement structures, a set of interlocking 2.5D structural models, and constrained and unconstrained inversions of potential-field data. Direen and Lyons (in prep) summarise these results as follows:

- Basement lithology and structure are continuous with “outcropping” areas to the south
- Sheets of Gawler Range Volcanics & Hiltaba Suite “laccolithic” plutons are accommodated in local transient extensional compartments/basins
- Faults and shears show favourable 1590 Ma alteration patterns that are geophysically mappable
- Faulting and shearings provided fluid pathways and drivers
- Kimban-aged basement is probably thick-skinned and transpressive with possible duplexes, megaboudinage, positive flower structures, and imbricate thrust stacks.

These self-consistent observations and inferences can be combined with information from new deep magnetotelluric inversion models interpretations of the seismic data. The insistence that any proposed seismically-derived architecture must also be required to reproduce the 3D gravity and magnetic fields, within constraints from known rock properties from the area, can be used to sift competing preliminary interpretations of the seismic geometry. The additional constraint that a seismically derived interpretation also fit the geometry of the electrical structure of the crust is more demanding, and less straightforward to interpret.

REFERENCES

Bastrakov, E.N, Skirrow, R.G., Direen, N.G., Mernagh, T.P. and Wyborn, L.A.I. 2004. Coupling geochemical and geophysical modeling to detect mineral systems undercover: an example from the Gawler Craton. *Geol.Soc.Aust Abstracts*, **73**, 52.

Direen, N.G. and Lyons, P. 2002. Geophysical interpretation of the Olympic Cu-Au province, 1:250 000 scale map. *Geoscience Australia*, Canberra.

Direen, N.G. and Lyons, P. *in prep*. Crustal architecture of the central Olympic Cu-Au province of the Gawler Craton, South Australia. *Economic Geology*.

Direen, N.G., Lyons, P., Jagodzinski, E.A., Milligan, P.R., Skirrow, R.G., Lane, R. and Collins, D., 2002. Observable crustal controls on hydrothermal activity in the Olympic Cu-Au province, *Gawler State of Play Workshop CD*, Adelaide, December 2002.

Direen, N.G., Lyons, P., Milligan, P.R, Jagodzinski, E.A. and Skirrow, R.G. 2002. A first-generation 3D-model of the crustal architecture of the north-eastern Gawler Craton and implications for Olympic Dam-style mineral systems, and implications for Olympic Dam style mineral systems. *Geol.Soc.Aust Abstracts*, **67**, 61.

Milligan, P.R., Direen, N.G.,and Lyons, P. *in review*. Analysis and 3D visualisation of new compilations of potential field data to help constrain 3D geological models. *Exploration Geophysics*.

Milligan, P.R., Direen, N.G. and Lyons, P. 2000. Analysis and 3D visualisation of new compilations of potential field data to help constrain 3d geological models. *Geol.Soc.Aust Abstracts*, **67**, 68.

Milligan, P.R., Direen, N.G. and Lyons, P. 2002, Analysis and 3D visualisation of new compilations of potential field data to help constrain 3D geological models. *In* Greenhalgh S A (compiler). *ASEG 2003 Extended Abstracts CD*, 16th ASEG international conference and exhibition, Adelaide, Feb 2003.

Williams, N.C., Lane, R. and Lyons, P., Regional constrained 3D inversion of potential field data from the Olympic Cu-Au province, *South Australian Preview*, **109**, 30-33.

Williams, N.C., Lyons, P., Lane, R. and Peljo, M. 2004. Constrained three-dimensional inversion of potential field data and crustal architecture of the Olympic Cu-Au province, South Australia. *Geol.Soc.Aust Abstracts*, **73**, 137.

IRON OXIDE CU-AU SYSTEMS: MODELS FOR THE GAWLER CRATON

Roger Skirrow

Geoscience Australia, P.O. Box 378, Canberra, ACT, 2601, Australia

This section contains some of the various models of alteration and mineralisation in IOCG systems, presented as a series of figures. Common to these models is the interplay between the contributions from intrusions (either as sources of mineralising fluids, heat, or both) and non-magmatic fluids.

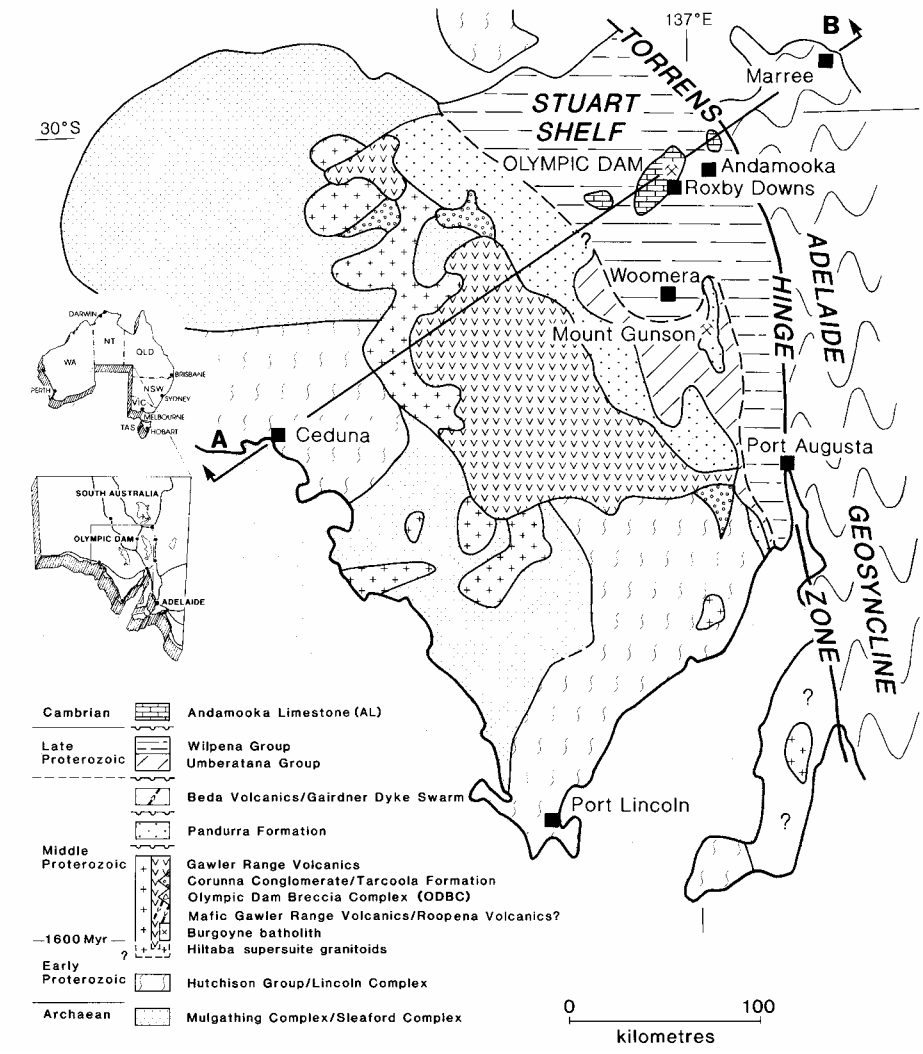

Figure 36: *Simplified regional geology from Reeve et al. (1990). A-B is the line of section presented in Figure 40.*

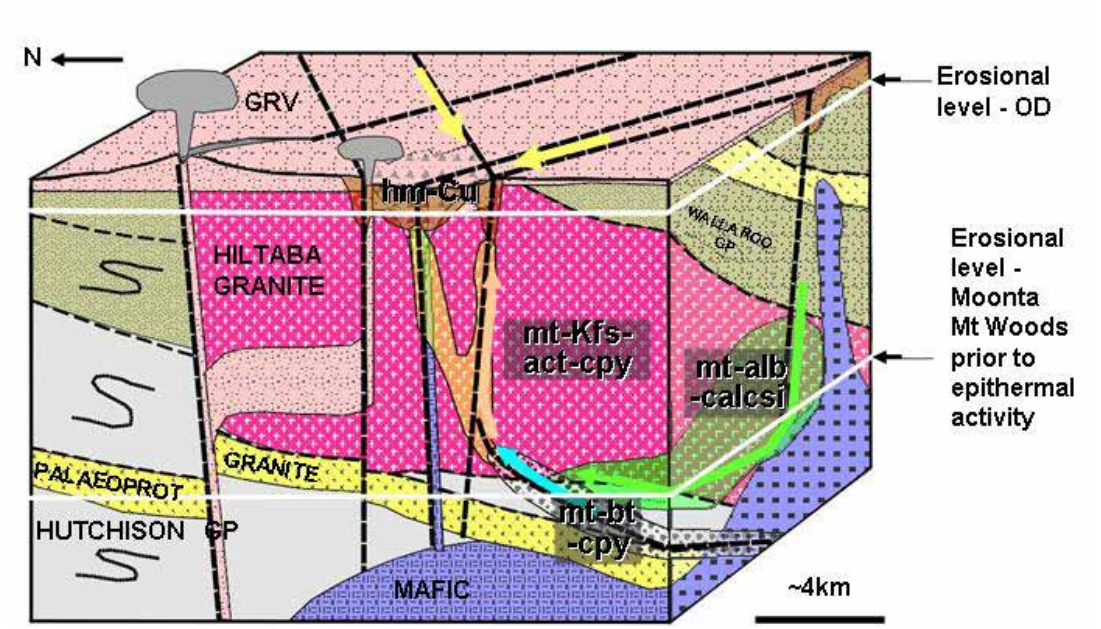

Figure 37: *Regional 3D model of an IOCG system in the Olympic Cu-Au province. From Skirrow et al., 2002 and www.ga.gov.au/map/web3d/gawler/.*

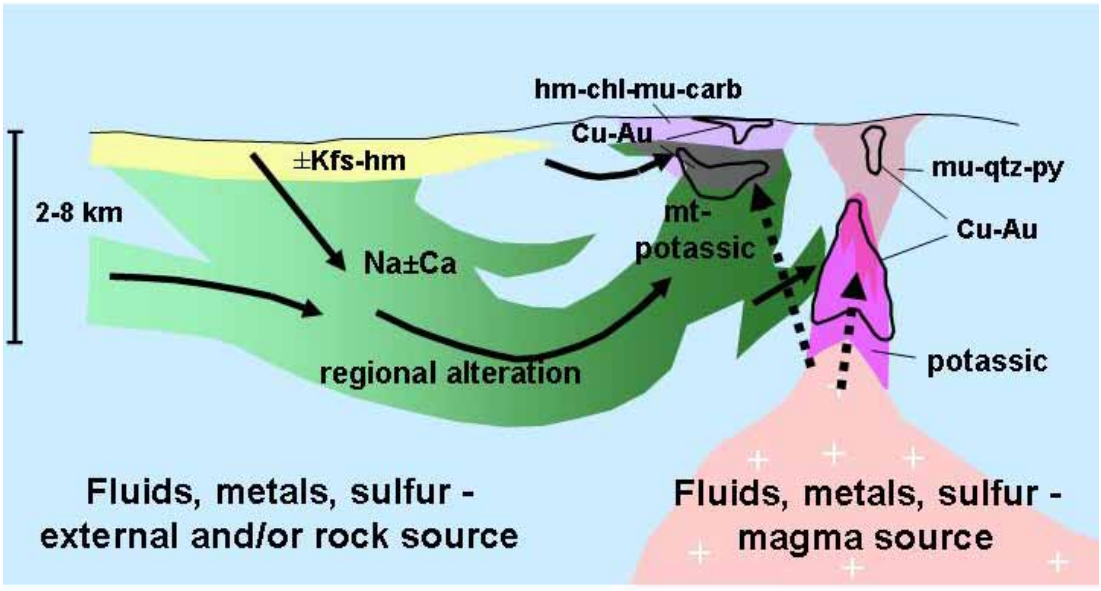

Figure 38: *Non-magmatic (left) vs. magmatic (right) IOCG fluid systems (Barton & Johnson, 2002)*

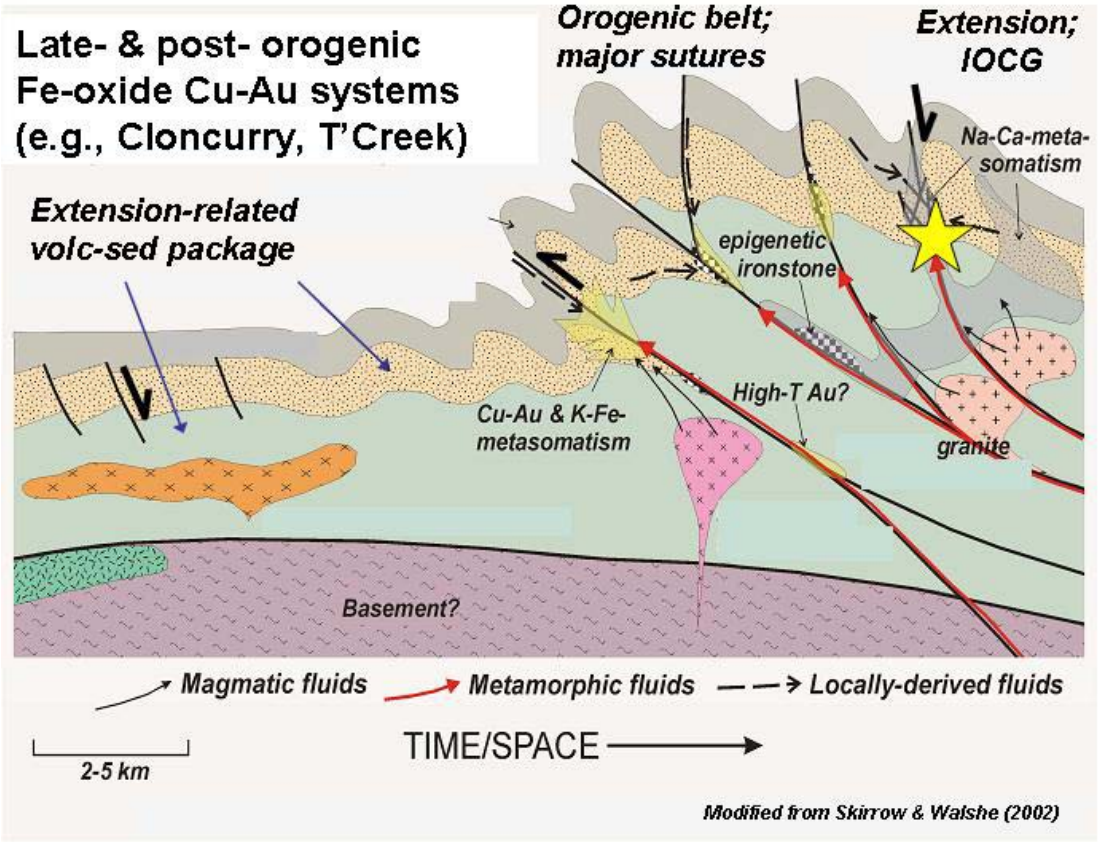

Figure 39: *Late- and post- orogenic Fe-oxide Cu-Au systems (eg Cloncurry, Tennant Creek). Modified from Skirrow and Walshe (2002).*

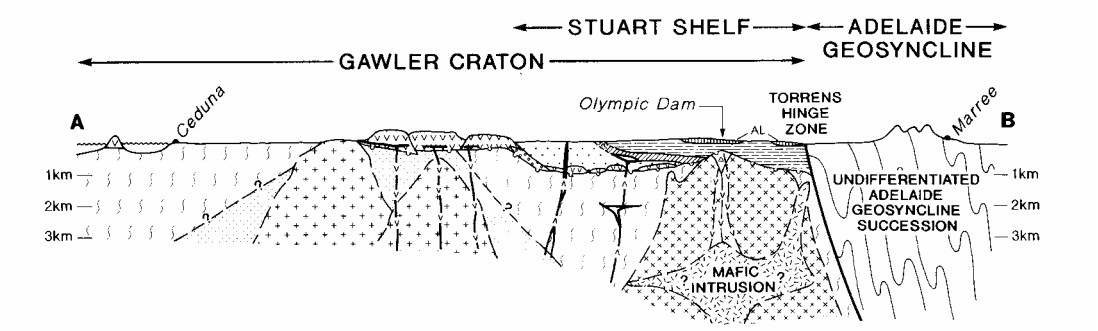

Figure 40: *Section from simplified regional geology given in Figure 36, from Reeve et al. (1990). Note the postulated mafic pluton, and its role in ore genesis, intruded into the Burgoyne batholith. Vertical exaggeration about 14:1.*

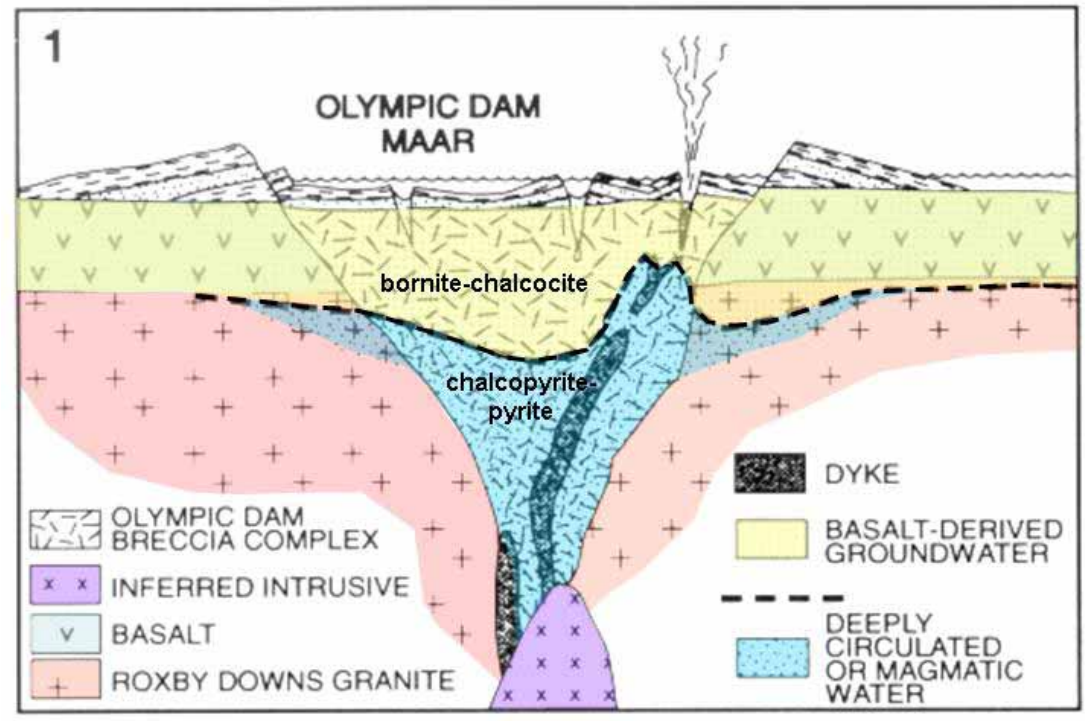

Figure 41: *Deposit-scale diagram showing the fluid mixing model of Haynes et al. (1995). Note the inferred intrusion below Olympic Dam. Dashed line shows schematic boundary between bornite-chalcocite zone and chalcopyrite-pyrite zone.*

REFERENCES

Barton, M.D. and Johnson, D.A. 2002. Alternative brine sources for Fe-oxide (-Cu-Au) systems; implications for hydrothermal alteration and metals. In: Porter, T.M (ed) Hydrothermal iron oxide copper-gold and related deposits; a global perspective, **1**, pp 43-60.

Haynes, D. W., Cross, K. C., Bills, R. T. and Reed, M. H. 1995. Olympic Dam ore genesis; a fluid-mixing model. *Economic Geology*, **90**, 281-307.

Reeve, J. S., Cross, K. C., Smith, R. N. and Oreskes, N. 1990. Olympic Dam copper-uranium-gold-silver deposit, *in* Hughes, F. E., ed., Geology of the mineral deposits of Australia and Papua New Guinea Australasian Institute of Mining and Metallurgy Monograph 14, **2**, pp 1009-1035.

Skirrow, R.G., Bastrakov, E., Davidson, G., Raymond, O. and Heithersay, P. 2002. Geological framework, distribution and controls of Fe-oxide Cu-Au deposits in the Gawler Craton. Part II. Alteration and mineralisation. *In:* Porter, T.M. (Ed.), Hydrothermal iron oxide copper-gold and related deposits, **2**, pp 33-47.

Skirrow RG and Walshe JL. 2002. Reduced and oxidised Au-Cu-Bi iron-oxide deposits of the Tennant Creek Inlier, Australia; an integrated geologic and chemical model. *Economic Geology*, **97,** 1167-1202.

CRUSTAL FLUID FLOW IN OROGENIC SYSTEMS AND IMPLICATIONS FOR THE OLYMPIC DAM DEPOSIT

B.J Drummond[1], B.E. Hobbs[2] and B.R. Goleby[1]

[1] Geoscience Australia, GPO Box 378, Canberra, ACT, 2601, Australia.
[2] CSIRO, 26 Dick Perry Avenue, Kensington, WA 6151, Australia.

Interpretation of the seismic reflection data indicates that the eastern Gawler Craton is a fold- and thrust-belt, provides a framework for understanding the regional fluid flow through the crust, and a possible first-order explanation of why the Olympic Dam deposit formed where it did.

In crust under compression, fluids migrating from deeper crust can concentrate in tabular zones at a number of levels, both below and above the plastic-viscous transition, commonly referred to as the brittle-ductile transition. Faults transecting the upper crust and the lower crust, through the plastic-viscous transition, provide pathways for fluids and their focussing in the upper crust.

In active orogens, fluids are observed in seismic images as “bright spots”; i.e., very high amplitude reflections, often with negative phase, together implying a drop in shear modulus at seismic strain rates. This is most likely caused by fluids at greater than lithostatic pressure. Bright spots have been observed in the Tibetan orogen, and in the accretionary orogens of western South America, western North America, adjacent to the San Andreas Fault, and in Japan. In South America, the bright spots are west-dipping and project to the surface in the core of the volcanic arc, which hosts a number of iron oxide-copper-gold type deposits. In Japan, they are found under volcanic centres, lying at, or close to, the base of the upper crustal seismogenic region. The bright spots in the upper crust in Japan are attributed to aqueous fluids, whereas the Tibetan bright spots are attributed by different researchers to both aqueous fluids and magmas.

Fluid-rich zones that once formed above the plastic-viscous transition would have been loci of great fluid flux. In ancient orogens, in which fluids are no longer present, old aqueous fluid pathways have a number of seismic signatures. As they would be characterised by chemical alteration, there is an effect on their seismic impedance (wave speed multiplied by density). They are, therefore, often imaged as efficient reflectors, with either positive or negative seismic polarity depending on whether the seismic impedance is greater or less than that of the surrounding rock. Fluid-rich zones that formed below the plastic-viscous transition would have been stagnant and, therefore, have less alteration. Such regions are unlikely to be strongly reflective today. Strong reflectors attributed to fluid-rich zones have been interpreted in the Yilgarn Craton, an Archaean accretionary orogen, and possibly in the middle to upper crust under the Eastern Succession of Mount Isa.

Likewise, ancient fault systems along which fluids migrated should also be reflective, due to both the chemical alteration within the fault-rock and in the adjacent rock of the hanging- and footwalls, and seismic anisotropy caused by the preferred orientation of phyllosilicate minerals parallel to the fault-plane. Reflections attributed to fluid migration along faults have been interpreted, and identified, in many parts of the world, including the Yilgarn Craton, Mount Isa Inlier, the Broken Hill region, and the Lachlan Fold Belt.

Computer modelling of crustal deformation and fluid flow in both young (Japan) and ancient orogens (Yilgarn Craton) produce a number of results that appear generic to orogens. This is so,

partly because the boundary conditions in the models, representing similar conditions within the crust at the time of orogeny, were similar. For that reason, to a first approximation the results are applicable in the Gawler Craton. The modelling assumed a crust 30 km thick (The present crustal thickness below the seismic traverses of the Gawler Craton is ~40 km, but may have been less before the crust was shortened.). The modelling assumed a fault penetrating at 45° to the plastic-viscous transition and the crust was assumed to be of granitic composition for the purpose of determining rheology, although in the Gawler Craton the crust may tend toward intermediate composition, on average.

The computer modelling predicts that a high strain shear zone will develop antithetic to the imposed fault. As the crust continues to shorten, fluids concentrate near the bottom of the imposed fault and migrate both up it and through a series of en-échelon, sub-horizontal, tabular regions with transitory, strain-induced porosity, and permeability, in the antithetic shear zone. These tabular regions would be reflective in seismic images.

The fault systems of the Gawler Craton imaged in the seismic data form a series of nested main and antithetic faults (thrust-wedges or pop-up structures). The largest (main) fault system consists of the north-dipping fold and thrust system in the upper crust in the south of the profile, which detaches on the ?mafic mid-crustal layer in several places where crustal shortening is accommodated by sub-horizontal movement (duplexing). Shortening on this main fault system focuses into a narrower high-strain zone in the lower crust at the southern end of the seismic profile. High amplitude sub-horizontal reflections occur at 9 km and 12 km depth along this its south-dipping antithetic shear zone. The higher reflections are more laterally extensive, extending over 8 km in the seismic profile, and are distinctive not just because of their amplitude but because the regional reflections above and below lie at an acute angle to them. These high amplitude reflections would be interpreted as evidence of fluid-rich zones during orogeny.

Nested main and antithetic fault systems are interpreted in the upper crust. Some extend through the Burgoyne batholith, evidenced by a series of relatively high amplitude, laterally short reflections in the migrated seismic data on the long regional profile. The line of reflections projects to the surface at the Jubilee Fault, which in 03GA-OD1 has high amplitude reflections that would be from the length of the fault trace rather than isolated zones within it. The seismic data would suggest, therefore, some of these fault systems and the Jubilee Fault provided fluid migration pathways from the lower and upper crust into the region of the Olympic Dam ore deposit. The presence of bright reflectors along the pathway would be indicative of fluid pressures exceeding lithostatic in places.

Other upper crustal antithetic fault systems developed during the orogeny. Examples would be at the Wirrda Fault Complex. We observe that the antithetic faults penetrate the Burgoyne batholith. The fault complexes (Wirrda and Elizabeth Creek Fault Complexes) formed above thrust breaks in the reflective mafic(?) layer in the mid-crustal layer which could have provided fluid migration pathways between the upper and lower crust.

APPENDIX 1: ACQUISITION INFORMATION

RECORDING EQUIPMENT

- **Aram 24 Seismic Data Acquisition and Processing System including**
- Real Time Parallel Processor Correlator.
- One (1) 10 metre Radio Mast on Recorder with High Gain Antenna.
- Forty Five (45) Remote Acquisition Modules (360 Channels).
- Forty Five (45) Telemetry Data Cables (360 Channels), 348 metres long with 8 Take-outs spaced at 43 metres apart.
- Geospace GS-32CT 10 Hz 395 ohm vertical geophones.
- Three Hundred and Sixty (360) geophone strings (360 Channels with 12 ph/group).
- Sensor SMT-200 Geophone Tester and QC system.

SOURCE EQUIPMENT

- **Four (4) IVI Hemi 60 4x4 Articulated Buggy mounted Vibrators**
- Peak Force is 62,031 lbs per Vibe.
- Hold Down Weight is 63,000 lbs per Vibe.
- One (1) Pelton Advance 2 Model 6 PC based VIBRASIG.
- Real Time Similarity System.
- Five (5) Pelton Advance 2 Model 6 VCE's plus various spare boards.
- One (1) Pelton Advance 2 Model ESG for Recording Truck plus various spare boards.
- Three (3) Vibrators operating Online (186,093 lbs Force) with one on standby (Figure 3XXX).
- Vibrators are equipped with Force Control and Ground Force Lock using M5 High Performance Accelerometers.
- Electronics are capable of correlating various individual sweep frequencies and compositing any range or variation of Up sweeps or Down sweeps within the same VP location. This process is Trade Marked as Varisweep.

RECORDING PARAMETERS – LINE 02GA-OD1

RECORDING PARAMETER SHEET

Client:	ANSIR	Crew:	401
Prospect Area:	Gawler Craton, SA	Line:	**02GA-OD1**
Survey:	2003 Gawler Craton Seismic Survey		
Instrument:	ARAM24 NT (Ver 1.309)	Direction of Rec:	North to South
Date Recorded:	22 July to 1 August 2003		

Recording Parameters

Traces per File	242
Record Length	18 sec
Sample Rate:	2 msec
Tape Format	SEG-Y
Shot Points	1000 to 5834
Rec To Rec	1000 to 5834
Files	2446

Sweep Frequency

Sweep 1	7 to 56 Hz
Sweep 2	12 to 80 Hz
Sweep 3	8 to 72 Hz
Sweep 4	
Sweep 5	
Sweep 6	
Sweep 7	

Receiver Parameters

Station Interval	40 m
Geophone Array Length	40 m
Geophone Array Centre	Mid Station .5
Geophone Type	OYO GS32CT
Strings Per Station	1
Connection	Series/Parallel
Spread Geometry	Symmetrical
# of Station Gap at SP	0

Auxiliary Traces

Time Break	241
Time Reference	242

Source Parameters

No. of Sources on-Line	3
No. of Sweeps per VP	3
Sweep Length:	12 sec
Sweep Type	Linear
Geophones Per String	12
Sweep Type Mono / Vari	Varisweep
VP Interval	80 m
Source Array Length	60 m
Vibe Spacing Pad to Pad	15 m
Vibe Move Up	15 m
VP Source Centre	On Station
Vibe Electronics	Pelton Adv II Model 6
Vibrator QC	Vibra Sig
Force Control	Peak and Trough
Phase Lock	Ground Force
High Force Output	90%
Pelton Rev. Level	6E

RECORDING PARAMETERS – LINE 02GA-BT2

RECORDING PARAMETER SHEET

Client:	ANSIR	Crew:	401
Prospect Area:	Gawler Craton, SA	Line:	**02GA-OD2**
Survey:	2003 Gawler Craton Seismic Survey		
Instrument:	ARAM24 NT (Ver 1.309)	Direction of Rec:	West to East
Date Recorded:	2 August to 5 August 2003		

Recording Parameters

Traces per File	242
Record Length	18 sec
Sample Rate:	2 msec
Tape Format	SEG-Y
Shot Points	1000 to 2436
Rec To Rec	1000 to 2436
Files	718

Sweep Frequency

Sweep 1	7 to 56 Hz
Sweep 2	12 to 80 Hz
Sweep 3	8 to 72 Hz
Sweep 4	
Sweep 5	
Sweep 6	
Sweep 7	

Receiver Parameters

Station Interval	40 m
Geophone Array Length	40 m
Geophone Array Centre	Mid Station .5
Geophone Type	OYO GS32CT
Strings Per Station	1
Connection	Series/Parallel
Spread Geometry	Symmetrical
# of Station Gap at SP	0

Auxiliary Traces

Time Break	241
Time Reference	242

Source Parameters

No. of Sources on-Line	3
No. of Sweeps per VP	3
Sweep Length:	12 sec
Sweep Type	Linear
Geophones Per String	12
Sweep Type Mono / Vari	Varisweep
VP Interval	80 m
Source Array Length	60 m
Vibe Spacing Pad to Pad	15 m
Vibe Move Up	15 m
VP Source Centre	On Station
Vibe Electronics	Pelton Adv II Model 6
Vibrator QC	Vibra Sig
Force Control	Peak and Trough
Phase Lock	Ground Force
High Force Output	90%
Pelton Rev. Level	6E

SOURCE AND RECORDING ARRAY DIAGRAMS – 02GA-BT1 AND 02GA-BT2

Source Array:
3 vibes over 60m, 15m pad to pad, centred on VP 15m moveups, 3 sweeps

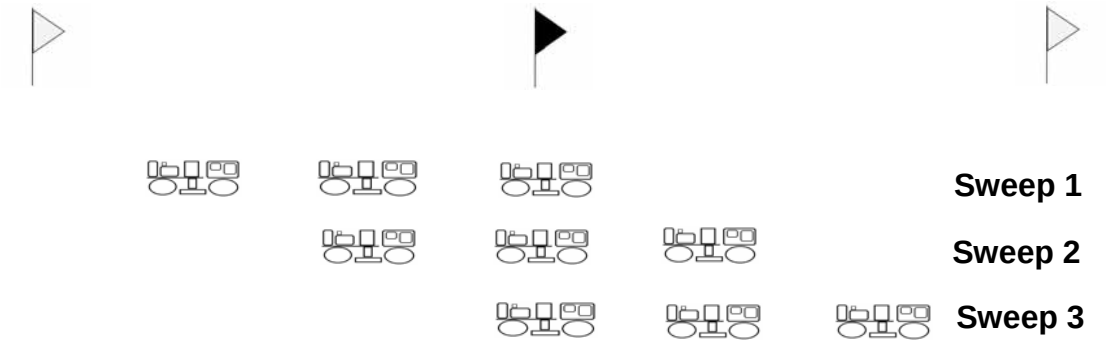

Receiver Array:
12 Phones over 40m, 3.33m between Phones, Centred between pegs